A FUNCTIONAL ANALYSIS OF THE ROLE OF SHP-2 IN VERTEBRATE HEART
DEVELOPMENT

Yvette Gabrielle Langdon

A dissertation submitted to the faculty of the University of North Carolina at Chapel Hill in
partial fulfillment of the requirements for the degree of Doctor of Philosophy in the
Department of Biology (Molecular Cellular and Developmental Biology).

Chapel Hill
2008

Approved by:

Frank L. Conlon

Keith Burridge

Robert J. Duronio

Sharon Milgram

Mark Peifer

ABSRTACT

YVETTE G. LANGDON: A Functional Analysis of the Role of SHP-2 in Vertebrate Heart
Development
(Under the direction of Frank Conlon)

SHP-2 is a protein tyrosine phosphatase that has been shown to be required for proper

vertebrate embryogenesis. Loss of function studies demonstrate roles for SHP-2 in

gastrulation, cell migration, and the maintenance of trophoblast stem cells and results in

lethality prior to or during gastrulation. In addition to the requirement for SHP-2 during

early vertebrate development, there is also a requirement for SHP-2 during heart

development which is supported by studies showing patients with Noonan syndrome often

having mis-sense mutations in *Shp-2*. To date the mechanism leading to abnormal cardiac

development in Noonan syndrome patients has not been determined. We have examined the

effects of SHP-2 inhibition and of human mis-sense mutations of *Shp-2* on early heart

development using *Xenopus*. We find that in the absence of SHP-2 signaling, cardiac

progenitor cells down-regulate genes associated with early heart development and fail to

initiate cardiac differentiation. We further show that this requirement for SHP-2 is restricted

to cardiac precursor cells undergoing active proliferation. By demonstrating that SHP-2 is

phosphorylated on Y542/Y580 and that it binds to FRS-2, an effector of FGF signaling, we

place SHP-2 in the FGF pathway during early embryonic heart development. Furthermore,

we demonstrate that inhibition of FGF signaling mimics the cellular and biochemical effects

of SHP-2 inhibition and that these effects can be rescued by constitutively active/Noonan

syndrome associated forms of SHP-2. We also find that N308D, a Shp-2 mutation associated with Noonan Syndrome, leads to cardiac abnormalities in *Xenopus*. Characterization of the phenotypic defects in these hearts show that they are reduced in size and display delayed morphological movements. These cardiac abnormalities appear to be associated with alterations in the actin cytoskeleton. In addition, we also observed a dramatic increase in the number of cells in M-phase of the cell cycle without an increase in cell number. These defects appear to reflect lengthening of the cardiac cell cycle. Collectively, these results show that SHP-2 functions within the FGF/MAPK pathway to maintain survival of proliferating populations of cells and that *Shp-2* N308D function primarily to alter actin muscle development which ultimately leads to defects in cardiac morphogenesis.

ACKNOWLEDGEMENTS

This dissertation is made possible through the help, love, and support of a number of individuals throughout the years. I would first like to thank members of the Conlon lab both past and present. I would like to thank Sarah Goetz, Kathleen Christine, Elizabeth Mandel, Erika Paden, Jackie Swanik, Elizabeth Jarvis, Jen Duddy, and Shauna Vasilatos for making lab a fun and exciting place to grow scientifically. I would like to thank the Conlon men, Chris Showell, Daniel Brown, and Stephen "Stevo" Sojka for bringing a little balance to a lab full of estrogen. Most importantly, I would like to thank my advisor Frank Conlon. Frank has gone above and beyond to help me make the most of my graduate school tenure- from extra help in the lab, kicks in the pants when needed, to personal conversations when I just needed to talk. I think that graduate school would have been ten times harder with a different advisor and I am grateful that Frank allowed me to be a part of the Conlon lab family.

I would like to thank my committee members for asking me the tough questions in order to help me evaluate my research project from multiple angles. I would especially like to acknowledge Sharon Milgram. It is hard not to do well when you know that you have someone in your corner that wants you to succeed and is willing to help in any way possible.

Throughout my graduate school career I have had the support of many friends and I would to thank those who undertook the graduate school journey with me (Tiana Garrett,

Julie Hall, and Mia Lowden) as well as those not in graduate school with me (Karmeshia Rice, Lia Sheppard, Debbie Owolabi, and the Omicron Gamma chapter of Zeta Phi Beta Sorority, Inc.) who helped to keep me sane. Of all of my friends I would like to thank Deyanna Boston the most because she has suffered through all the stages of the graduate school process with me by listening to my highs, my lows, and offering many words of encouragement.

Finally I would like to thank my family. My mother and stepfather, Joan and Larry Langdon provided years of encouragement and set shining examples of scholarly excellence that I have used as the framework for my academic career and I want them both to realize that this dissertation partly belongs to them. I would like to thank my sisters by blood (Tomaysa Sterling and Heather Langdon) and by my heart (Michelle "Chris" Francis Bell) for all of their love and support. But my biggest supporter throughout it all has always been my twin sister Yvonne Langdon. Yvonne and I share a bond that can withstand anything and we have tested it a time or two, but throughout this whole process she has been my rock so I thank her from the bottom of my heart.

TABLE OF CONTENTS

LIST OF FIGURES

ABBREVIATIONS

ALL	Acute lymphoblastic leukemia
AML	Acute myelogenous leukemia
Aph	Aphidicolin
BF	Brightfield
BMP	Bone morphogenic protein
Cdk	Cyclin-dependent kinase
DMSO	Dimethyl sulfoxide
Edd	Endodermin
EGF	Epidermal growth factor
FGF	Fibroblast growth factor
FGFR	Fibroblast growth factor receptor
G1	Gap phase 1
G2	Gap phase 2
HSPG	Heparin sulfate proteoglycan
Isl1	Islet 1
JMML	Juvenile myelomonocytic leukemia
MAPK	Mitogen-activated protein kinase
MHC	Myosin heavy chain
MLC	Myosin light chain
NKX	Homeodomain containing protein
PDGF	Platelet derived growth factor
pH3	Phospho-Histone H3

PLC-γ	phospholipase C gamma
PTP	Protein tyrosine phosphatase
RTK	Receptor tyrosine kinase
S	DNA synthesis phase
SH2	SRC-homology 2
SHP	SRC-homology 2 domain containing protein tyrosine phosphatase
TBX	T-box domain containing protein
TEM	Transmission electron microscopy
TMY	Tropomyosin

CHAPTER 1

Introduction

Currently, there are nearly one million adults in the United States living with congenital heart defects with new cases occurring in one of one hundred twenty live births (Pierpont et al., 2007). Advances in medicine, technology, and health care have increased life expectancy for individuals living with these defects. As the number of cases of congenital heart defects and cardiovascular disease rises, it becomes critical to understand the signals and mechanisms required for proper cardiac development. Scientists have made tremendous strides towards the understanding of a number of these critical developmental processes. However, despite numerous efforts, there is still much we do not understand about the complex mechanisms used to specify cardiac cells, to regulate cardiac proliferation and differentiation, and to promote cardiac cell survival.

Overview of Cardiac Development

The basic mechanisms of vertebrate cardiac development are conserved from fish and frogs through to humans. In *Xenopus* development, cardiac precursor cells reside in two bilateral populations located dorsally and equatorially in the early stage embryo. During gastrulation the cardiac precursor cells are specified and committed into the cardiac lineage in response to inductive signals from the Spemann organizer and the underlying endoderm (Harland and Gerhart, 1997; Nascone and Mercola, 1995; Sater and Jacobson, 1989). By early neurula

stage the cells begin to migrate anteriorly and ventrally towards the antero-ventral midline. Once the two populations of cells reach the midline the cells fuse to form a single population of cardiac progenitors (Fig. 1.1A). The sheet of cardiac progenitor cells then rounds up dorsally to form a bilaminar heart tube patterned along the anterior-posterior axis of the embryo with the inflow tract positioned posteriorly and the outflow tract positioned anteriorly (Fig. 1.1B). In mouse and chick, the linear heart tube is then extended by the addition of cardiac cells from extra-cardiac sources of the anterior and secondary heart fields. The anterior heart field is comprised of cephalic mesoderm located anteriorly to the heart. Cells within this region delaminate and migrate posteriorly to eventually give rise to the myocardium of the outflow tract (conus and truncus) and right ventricle of the heart (Cai et al., 2003; Mjaatvedt et al., 2001). Similarly, cells are added to the poles of the heart from the secondary heart field which is derived from pharyngeal mesoderm caudally adjacent to the distal end of the heart tube and eventually gives rise to the myocardium of the truncus and arterial pole (Kelly et al., 2001; Waldo et al., 2001). Concomitant with linear tube expansion, the heart begins a coordinated set of morphological movements resulting in rightward looping of the heart. Chamber morphogenesis is initiated following cardiac looping and infiltration of cardiac neural crest cells. Through further morphological movements the heart is septated into a three chambered heart in Xenopus, and a four chambered heart in chick, mice, and humans.

Fibroblast Growth Factor (FGF) Family

Studies have shown that the FGF family is highly conserved across species (Itoh, 2007; Ornitz and Itoh, 2001). In *Xenopus* and chick seven FGF ligands and four receptors have been identified (Itoh, 2007; Ornitz and Itoh, 2001). Orthologs of these FGF genes are

2

found among the twenty-two ligands and four receptors found in humans and mice (Ornitz and Itoh, 2001).

The majority of FGF signaling proceeds in a paracrine fashion with FGF ligands secreted from cells and interacting with their cognate receptors on adjacent cells or tissues. Ligand binding initiates receptor dimerization and autophosphorylation of the cytoplasmic tail of the receptor leading to activation of downstream signaling pathways which include the mitogen-activated protein kinase (MAPK) pathway, PI-3 kinase (PI3K) pathway, and phospholipase C gamma (PLC-γ) pathway (Fig 1.2).

Although FGFs are expressed in a number of embryonic and adult tissues, their signaling is tightly regulated both temporally and spatially with a subset of ligands expressed exclusively in embryonic tissues (FGF-8) and others expressed in both embryonic and adult tissues (FGF-2) (Kengaku and Okamoto, 1993; Meyers et al., 1998; Montero et al., 2000). Similar to FGF ligands, FGF receptors can be developmentally restricted to specific tissues (epithelial or mesenchymal) (Ornitz and Itoh, 2001; Peters et al., 1992). Moreover, the FGF receptors exist as splice variants, generating a spatially or a temporally restricted receptor signaling component (Ornitz and Itoh, 2001; Peters et al., 1992).

Within the heart, differential and overlapping domains of FGF expression mediate tissue specific effects necessary for proper cardiac development. For instance, FGF-9 signaling from the endocardium and epicardium to the myocardium is required to pattern the mouse ventricle (Lavine et al., 2005). Heparin sulfate proteoglycans which bind and stabilize FGF ligands add an additional level of regulation. For example, Allen et al. demonstrated FGF2 and FGF4 recognize and bind the same heparin sulfates in some tissues, however FGF4 can not bind heparin sulfate in the heart or vascular system (Allen et al., 2001).

FGFs and Vertebrate Heart Development

FGF signaling is critical for both early and late cardiac development and a large number of FGF ligands have been shown to be expressed in the vertebrate heart including FGF 1, 2, 4, 8-10, 16, 18, and 20 as well as the FGF receptors FGFR 1 and 2 (Franciosi et al., 2000; Lavine et al., 2005; Macatee et al., 2003; Mima et al., 1995; Reifers et al., 2000; Sugi et al., 2003; Sugi et al., 1995; Sugi et al., 1993; Zhu et al., 1996). However, only in a few cases has an endogenous role for any ligand been demonstrated.

Cardiac Specification and Maintenance

Specification of the cardiac fields at gastrulation, involves the complex coordination of a number of instructive cues to direct a small population of lateral plate mesodermal cells into the cardiac lineage. In *Ciona intestinalis*, a bHLH transcription factor Mesp, specifies a region of mesodermal cells competent to respond to FGF signals (Davidson et al., 2006; Davidson et al., 2005). In turn, FGF signaling, most likely FGF9 expressed in adjacent cells, leads to expression of Ets1/2 transcription factors which in turn regulates cardiac gene expression of *Gata4*, *Nkx2.5*, and *Hand-like* (Beh et al., 2007; Davidson et al., 2006). Like *Ciona*, FGF signaling is also required for the induction of cardiac gene expression in zebrafish myocardial precursors. Zebrafish FGF8 mutants (*acerebellar*) have reduced expression of molecular markers of early heart development including *Nkx2.5, Nkx2.7,* and *Gata4* (Reifers et al., 2000). In rescue experiments, Reifers et al. found that expression of *Nkx2.5* and *Gata4* can be restored in response to FGF signaling, but that *Nkx2.5* and *Gata4* expression was never observed outside of endogenous domains suggesting that only a subset of mesodermal cells are competent to respond to FGF signals (Reifers et al., 2000). FGF signals emanating directly from Henson's node and/or rostral endoderm are sufficient to

4

induce cardiogenesis in chick embryos, further suggesting a requirement for FGF signals in cardiac specification (Lopez-Sanchez et al., 2002).

FGF signaling has also been shown to be required for cardiac progenitor cell survival both prior to and during differentiation of the heart (Langdon et al., 2007). Langdon et al. determined that the non-receptor protein tyrosine phosphatase SHP-2 is required to maintain proliferating cardiac progenitor cells during early and late stages of cardiac development and in its absence the progenitor cells die (Langdon et al., 2007). They further determined that signaling is mediated through the FGF/SHP-2/MAPK pathway (Langdon et al., 2007).

FGF signaling is also required to maintain cardiac progenitor cells derived from the anterior heart field. The LIM homeobox transcription factor Islet 1 (Isl1) marks progenitor cells of the anterior heart field and Isl1 null mice lack an outflow tract and right ventricle (Cai et al., 2003) Recently, Cohen et al. determined that FGF signaling in the anterior heart field was required to maintain Isl1 progenitor cells (Cohen et al., 2007) and demonstrated that Wnt signaling was required upstream of FGFs to stimulate the maintenance of Isl1 positive cells. Interestingly, although a number of FGFs are expressed in the anterior heart field only FGF3, 10, and 16 are positively regulated in response to Wnt signals while others were repressed (FGF4) or unaffected (FGF8, 13, and 18) (Cohen et al., 2007). Although these studies appear to suggest that FGF3, 10, and 16 are required for survival of Isl1 positive cells, the observation that FGF4 was suppressed may indicate that FGFs also function to promote proliferation of cardiac progenitor cells. The FGF ligands un-responsive to Wnt signaling (FGF 8, 13 and 18) may be required for cell identity or required in conjunction with other signaling molecules such as BMPs to promote additional cardiac processes such as cell migration or actin rearrangement.

FGF8 plays a similar role for the maintenance of cardiac neural crest cell survival both pre- and post incorporation into the heart and is also required for survival of inflow tract cells (Abu-Issa et al., 2002). These studies would suggest that rather than altering the mechanisms of cardiac cell survival after the heart has begun to differentiate that these pathways are maintained. This suggests that elaborate signaling networks act to coordinate FGF mediated progenitor cell survival and proliferation with FGF mediated cardiac differentiation.

Cardiac Cell Migration

FGF signals also play a role during migration of mesodermal cells, which is also critical for proper cardiac development. In *Drosophila*, FGF receptor expression is essential for migration of the mesoderm and subsequent cardiac development. *Heartless* mutants lacking the FGF receptor (DFR1) in the mesoderm are unable to migrate and spread out to form the second germ layer over the ectoderm resulting in a reduction of visceral mesoderm leading to a failure in heart formation (Beiman et al., 1996; Shishido et al., 1997). Similarily, chimeric analysis of FGF receptor 1 (Fgfr1) in mouse found that FGF receptor 1 deficient cells were unable to contribute to the heart (Ciruna et al., 1997). Thus, there appears to be an evolutionarily conserved role for FGF signaling in mesoderm migration and cardiac specification.

The majority of studies have been unable to separate the requirement for FGF signaling for cardiac specification from the requirement for FGF signaling for early migration but the two processes have recently begun to be mechanistically separated. Davidson et al. found that cardiac specification occurs through the Mesp activation of FGF signals which act on Ets1/2 to initiate cardiac specification in *Ciona* (Davidson et al., 2006).

In a separate study they further demonstrated that a constitutively active form of Mesp resulted in ectopic formation of cardiac tissue in the tail. Thus at least in *Ciona* cardiac specification can be mechanistically separated from cardiac cell migration (Davidson et al., 2005). More recently in *Ciona*, Beh et al. determined that FoxF functions both downstream and in parallel to the FGF/MAPK/Ets1/2 pathway to promote migration, yet is dispensable for cardiac specification (Beh et al., 2007). Together, these studies suggest that although cardiac specification and migration are linked and utilize several of the same molecules these common pathways diverge to promote specific functions (Beh et al., 2007; Davidson et al., 2005).

FGF Signaling and Cardiac Proliferation and Differentiation

In addition to their role in migration, FGF receptors have additional requirements during cardiac development in the fly. To address the specific temporal requirements for the *Drosophila* FGF receptor (*heartless*) on cardiac development, Beiman et al. used an inducible dominant negative FGF receptor (DN-*htl*) to demonstrate that although the dorsal vessel undergoes proper vessel closure, there were fewer pericardial and cardial cells (Beiman et al., 1996). The reduction in cardiac cell numbers is consistent with a requirement for FGF signaling to promote proliferation and/or cardiac cell survival. This data also suggests that FGF receptor 1 may be the major receptor involved in cardiac proliferation and or survival.

In vertebrates, as the heart develops, cardiac cells undergo two phases of proliferation. The first phase is initiated prior to linear heart tube formation while the second phase is initiated following cardiac looping (Alsan and Schultheiss, 2002; Soufan et al., 2006; Thompson and Fitzharris, 1979). A number of studies are consistent with a role for

FGF signaling in regulating cardiac cell proliferation (Sheikh et al., 1999; Sheikh et al., 1997; Sugi et al., 1995; Thompson and Fitzharris, 1979). In chicks, FGF1, FGF2, and FGF4 lead to the proliferation of precardiac mesoderm, while blocking FGF signaling leads to the converse effect, a decrease in either cell proliferation or cell survival during the first phase of cardiac proliferation (Franciosi et al., 2000; Mima et al., 1995; Zhu et al., 1996). The majority of proliferation during the later stages occurs in the ventricles, outflow tract and cardiac cushions. The requirement for FGFs to regulate cardiac proliferation is supported by genetic studies in mice by Lavine et al. which show that both endocardial and epicardial derived FGF signals (Fgf9, Fgf16, and Fgf20) regulate myocardial proliferation (Lavine et al., 2005). Similarly, FGF4 has been shown to be required for the proliferation of cells in the cardiac cushions (Sugi et al., 2003). The role of FGFs is further emphasized by the observation that mutations in three of the four FGF receptors are associated with human congenital diseases (reviewed in Coumoul and Deng, 2003).

In general, growth factor signaling has been shown to regulate cell cycle progression at the G1/S transition (reviewed in Goetz and Conlon, 2007). These factors promote S phase entry through induction of cyclin expression and promotion of cyclin association with the respective cyclin dependent kinases (cdks) during G1. The cyclin/cdk complexes initiate a signaling cascade resulting in activation of the E2F transcription factor and subsequent activation of genes required for cell cycle progression. Frederick and Wood show that FGF2 induces the expression of Cyclin D in early G1 and Cyclin E in late G1 to promote cell cycle progression in oligodendrocyte progenitor cells (Frederick and Wood, 2004). It is possible that FGF regulation of cardiac cell proliferation results from a direct or indirect role in cell

cycle progression. However, at this time data demonstrating a direct role for FGF signaling in cardiac cell cycle progression has yet to be reported.

Cardiac Differentiation

Concurrent with a role for FGFs in cardiac proliferation FGF signaling has been implicated as a mediator of cardiac differentiation. *In vitro* studies with FGF1, 2, 4, or FGF receptor 1 demonstrate that these signaling molecules are required for cardiac differentiation and in their absence cardiomyocyte differentiation is reduced or absent (Dell'Era et al., 2003; Kawai et al., 2004; Rosenblatt-Velin et al., 2005; Sugi and Lough, 1995; Zhu et al., 1996). Consistent with these findings, FGF2 and 4 signaling *in vivo* is required to drive pericardial mesoderm into an epicardial cell lineage (Kruithof et al., 2006). Similarly, FGF4 drives valve precursor cells within the endocardial cushions toward differentiation into tendon cells and away from a cartilage cell lineage (Lincoln et al., 2006). These studies show that FGF signals are critical for cardiac differentiation as evident by the fact that expression of FGF4 and BMP2 are sufficient to induce non-precardiac mesoderm to form contractile differentiated cardiac tissue (Barron et al., 2000; Lough et al., 1996). Collectively these studies suggest FGF signaling is critical for cardiac differentiation, but that this process *in vivo* requires coordination between multiple growth factor signaling pathways. In spite of the suggestion of interplay between FGFs and other signaling pathways in the promotion of cardiac proliferation and/or differentiation the mechanisms required to initiate and/or switch from a cardiac proliferation program to a cardiac differentiation program remains elusive.

9

Modulation of FGF Signaling

Different mechanisms are used to modulate the length and strength of FGF signals including FGF inhibitors such as sproutys, spreds, XFLRT3, MAP kinase phosphatase 3 (MKP3), and ERM proteins (reviewed in Thisse and Thisse, 2005). However, the role for any of these molecules in heart development remains to be established.

Discussion

Heart development can be divided into 4 major processes- specification, proliferation, differentiation, and cardiac morphogenesis/remodeling. It is evident from numerous studies that FGF signaling has a defined temporal role in each of these processes. Alterations in FGF signaling leads to an assortment of cardiac abnormalities ranging from under/over proliferation of cardiac cells to premature differentiation of cardiomyocytes. Vertebrates have devised multiple mechanisms to tightly regulate the process of cardiac development and FGF signaling is one mechanism used to coordinate and promote the signals necessary for proper cardiac development.

FGF signaling appears to have opposing roles in heart development; in some instances promoting proliferation or cardiac cell survival and in other instances promoting differentiation or migration. This phenomenon can be partially explained through spatial and temporal expression of FGF ligands and receptors. FGF receptors 1and 2 are both expressed in a number of the same tissues in the heart. The expression level of the receptors in some instances appears to be altered with respect to each other in time and space. For example, between 9.5 to 12.5 days p.c. of mouse cardiac development, FGF receptor 2 is highly expressed in endocardial cushions and the overlying endothelium. Simultaneously, FGF receptor 1 is highly expressed in the myocardium and expressed to a lesser extent in

endocardial cushions (Peters et al., 1992). These FGF receptor expression patterns suggest both independent and overlapping domains of receptor expression and thus establishing a means to differentially regulate cellular output while utilizing the same signaling pathway. Further examination of a number of tissues suggests that when the two FGF receptors are expressed at the same time and place, within an organ, receptor expression may be restricted to specific cell types within the tissue, i.e. FGF receptor 2 expression restricted to epithelial tissue and FGF receptor 1 expression restricted to mesenchymal tissue (Peters et al., 1992). This data lend credence to the idea that a major means of cellular regulation is simply regulating the localization of critical signaling components. Through regulation of receptor or ligand expression, the organism can specify populations of cells within the same cardiac region to both proliferate and differentiate. Similarly, the organism expresses FGF ligands in independent and overlapping domains of expression to promote the maintenance and proliferation of cardiac progenitor cells and differentiation of cardiomyocytes (Cohen et al., 2007; Kruithof et al., 2006; Lincoln et al., 2006).

Little is known about what signals lie upstream of FGFs to regulate their expression during cardiac development and even less is known about what lies downstream of FGF/MAPK signaling to mediate the effects of FGF signaling. In a few instances portions of the pathway have been defined (Fig. 1.3). For example, in *Ciona* Beh et al determined that Ets1/2 and FoxF function downstream of FGF signaling to promote migration of cardiac progenitor cells and Cohen et al. determined that Wnt/β-catenin signaling functions upstream of FGF3, 10, 16, and 20 in the anterior heart field to promote Isl1 progenitor cell expansion (Beh et al., 2007; Cohen et al., 2007). However the majority of studies on the role of FGFs during cardiac development have not looked at specific FGFs and/or FGF receptors (Barron

et al., 2000; Kruithof et al., 2006; Lincoln et al., 2006; Lopez-Sanchez et al., 2002; Lunn et al., 2007; Macatee et al., 2003; Marguerie et al., 2006; Mima et al., 1995; Rosenblatt-Velin et al., 2005; Sugi et al., 2003; Zhu et al., 1996). Instead studies focused on the pathway as a whole and inhibited FGF signaling through inactivation of the FGF receptors by retroviruses or pharmacological inhibitors. Therefore, there is a large gap in our understanding of which ligand and receptors are required for which processes and tissues during cardiac development. However, as we complete more genetic analysis we are discovering greater roles for FGF signals in heart development through knock down of multiple FGFs in concert to generate a clearer understanding of the role of FGF signals in cardiac development. At this time, further research into FGF signaling and cardiac development needs to focus on determining what molecules and pathways lie up and downstream of FGFs in the heart.

Understanding the up and downstream modulators of the FGF/MAPK pathway will help to determine where the specificity for FGF ligands and receptors are in relationship to their role in cardiac development. In addition, future studies need to focus on determining which FGF inhibitors are expressed in the heart and by which mechanisms these inhibitors regulate FGF signaling. These studies are critical since much of FGF signaling in cardiac development occurs through the MAPK pathway resulting in either transient or prolonged ERK activation and it has been suggested that the strength and/or length of ERK activation is associated with alternate cellular responses i.e. proliferation versus differentiation (reviewed in Marshall, 1995). Sprouty proteins have been suggested to function at the level of ERK and thus to modulate the strength and length of FGF signals. Therefore if we can establish the requirement for each ligand and receptor in heart development and the FGF inhibitor

feedback loops we can create a signaling network that can be used towards the development

of new therapies to treat cardiovascular disease and congenital heart defects.
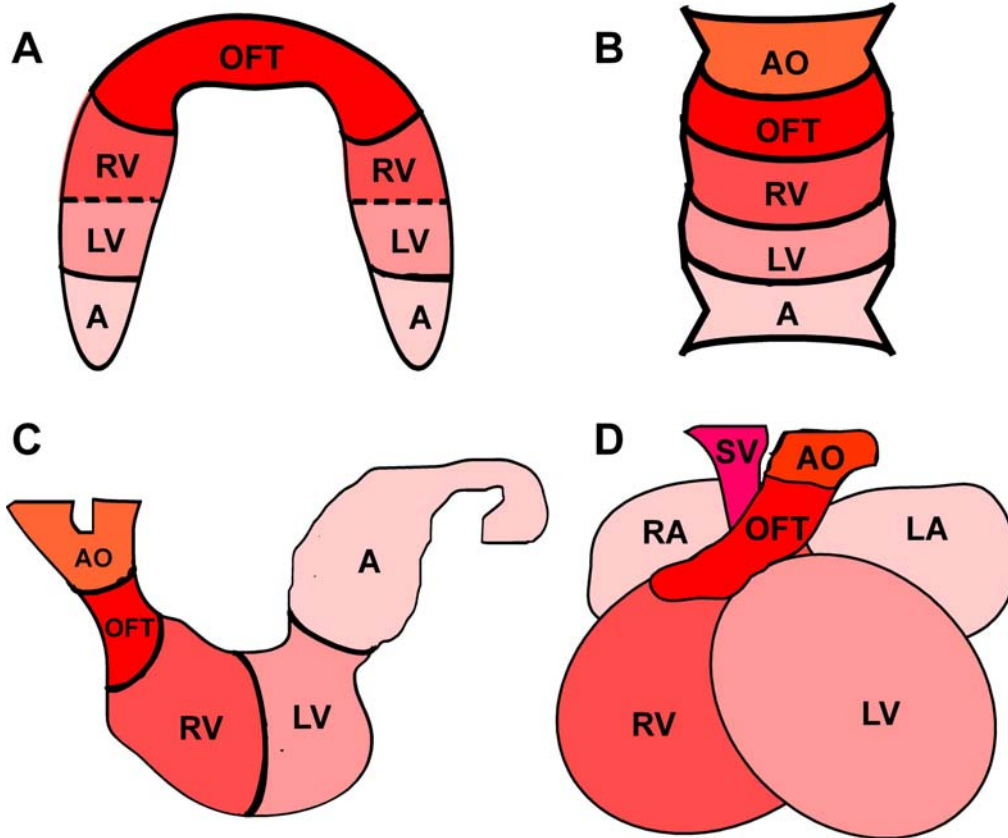
Figure 1.1. Vertebrate heart development.

Schematic of vertebrate heart development. (A) Cardiac crescent. (B) Linear heart tube. (C) The process of cardiac looping. (D) Mature four-chambered heart. RV, right ventricle; LV, left ventricle; RA, right atria; LA, left atria; OFT, outflow tract; AO, aorta; SV, sinus venosus.
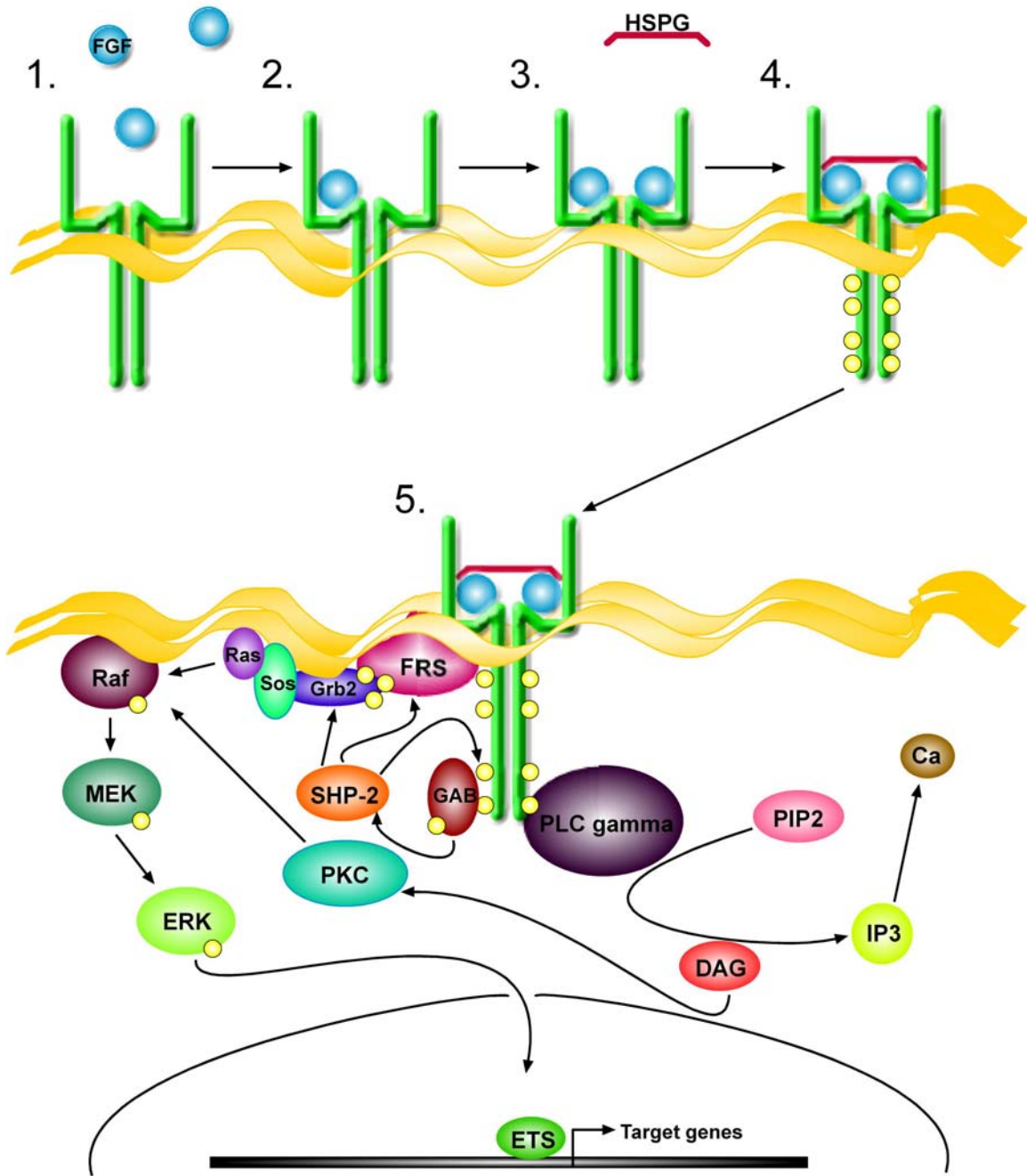
Figure 1.2. Activation of FGF receptors and downstream signaling pathways.

(1-4) Activation of FGF receptors- FGF ligands bind to FGF receptors and the complex is

stabilized with heparin sulfate proteoglycans (HSPG). These interactions result in

dimerization and autophosphorylation of tyrosine residues on the FGF receptors. (5) MAPK

signaling and PLCγ signaling are two major signal transduction pathways through which

FGFs signal. MAPK signaling is initiated in several different ways in response the FGF

receptor activation. FRS is directly activated through interaction with the FGF receptor and

subsequently activates the Grb2-Sos complex leading to activation of Ras and transduction of

MAPK signaling. Alternatively the MAPK pathway can be activated by SHP-2 which can

interact directly with the FGF receptor as well as GAB, FRS, and Grb2. PLCγ signaling is

initiated when PLCγ bind to the activated FGF receptor. Activated PLCγ hydrolyzes

phosphatidyl-inositol-4,5-diphosphate (PIP2) to diacylglycerol (DAG) and inositol-1,4,5-

triphophate (IP3). The IP3 releases Ca^{2+} while DAG activates protein kinase C-δ (PKCδ)

which in turn can activate Raf and signaling through the MAPK pathway.
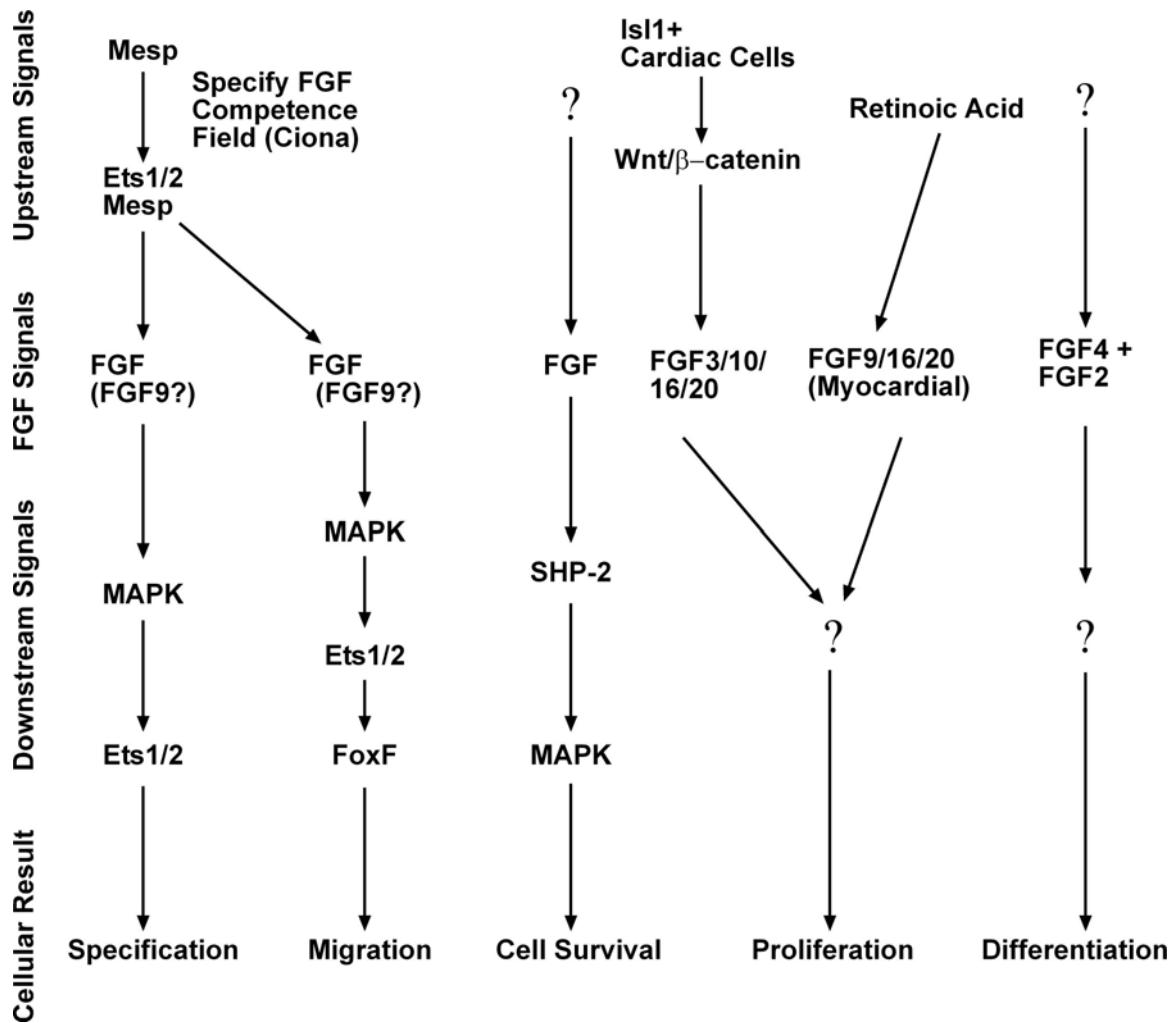
Figure 1.3. In vivo requirements for FGF signaling during Chordate cardiac development.

Schematic of upstream and downstream *in vivo* mediators of FGF signaling during cardiac development for the processes of cardiac specification, migration, proliferation and differentiation.

References

Abu-Issa, R., Smyth, G., Smoak, I., Yamamura, K. and Meyers, E. N. (2002). Fgf8 is required for pharyngeal arch and cardiovascular development in the mouse. *Development* **129**, 4613-25.

Allen, B. L., Filla, M. S. and Rapraeger, A. C. (2001). Role of heparan sulfate as a tissue-specific regulator of FGF-4 and FGF receptor recognition. *J Cell Biol* **155**, 845-58.

Alsan, B. H. and Schultheiss, T. M. (2002). Regulation of avian cardiogenesis by Fgf8 signaling. *Development* **129**, 1935-43.

Barron, M., Gao, M. and Lough, J. (2000). Requirement for BMP and FGF signaling during cardiogenic induction in non-precardiac mesoderm is specific, transient, and cooperative. *Dev Dyn* **218**, 383-93.

Beh, J., Shi, W., Levine, M., Davidson, B. and Christiaen, L. (2007). FoxF is essential for FGF-induced migration of heart progenitor cells in the ascidian Ciona intestinalis. *Development* **134**, 3297-305.

Beiman, M., Shilo, B. Z. and Volk, T. (1996). Heartless, a Drosophila FGF receptor homolog, is essential for cell migration and establishment of several mesodermal lineages. *Genes Dev* **10**, 2993-3002.

Cai, C. L., Liang, X., Shi, Y., Chu, P. H., Pfaff, S. L., Chen, J. and Evans, S. (2003). Isl1 identifies a cardiac progenitor population that proliferates prior to differentiation and contributes a majority of cells to the heart. *Dev Cell* **5**, 877-89.

Ciruna, B. G., Schwartz, L., Harpal, K., Yamaguchi, T. P. and Rossant, J. (1997). Chimeric analysis of fibroblast growth factor receptor-1 (Fgfr1) function: a role for FGFR1 in morphogenetic movement through the primitive streak. *Development* **124**, 2829-41.

Cohen, E. D., Wang, Z., Lepore, J. J., Lu, M. M., Taketo, M. M., Epstein, D. J. and Morrisey, E. E. (2007). Wnt/beta-catenin signaling promotes expansion of Isl-1-positive cardiac progenitor cells through regulation of FGF signaling. *J Clin Invest* **117**, 1794-804.

Coumoul, X. and Deng, C. X. (2003). Roles of FGF receptors in mammalian development and congenital diseases. *Birth Defects Res C Embryo Today* **69**, 286-304.

Davidson, B., Shi, W., Beh, J., Christiaen, L. and Levine, M. (2006). FGF signaling delineates the cardiac progenitor field in the simple chordate, Ciona intestinalis. *Genes Dev* **20**, 2728-38.

Davidson, B., Shi, W. and Levine, M. (2005). Uncoupling heart cell specification and migration in the simple chordate Ciona intestinalis. *Development* **132**, 4811-8.

Dell'Era, P., Ronca, R., Coco, L., Nicoli, S., Metra, M. and Presta, M. (2003). Fibroblast growth factor receptor-1 is essential for in vitro cardiomyocyte development. *Circ Res* **93**, 414-20.

Franciosi, J. P., Bolender, D. L., Lough, J. and Kolesari, G. L. (2000). FGF-2-induced imbalance in early embryonic heart cell proliferation: a potential cause of late cardiovascular anomalies. *Teratology* **62**, 189-94.

Frederick, T. J. and Wood, T. L. (2004). IGF-I and FGF-2 coordinately enhance cyclin D1 and cyclin E-cdk2 association and activity to promote G1 progression in oligodendrocyte progenitor cells. *Mol Cell Neurosci* **25**, 480-92.

Goetz, S. C. and Conlon, F. L. (2007). Cardiac progenitors and the embryonic cell cycle. *Cell Cycle* **6**, 1974-81.

Harland, R. and Gerhart, J. (1997). Formation and function of Spemann's organizer. *Annu Rev Cell Dev Biol* **13**, 611-67.

Itoh, N. (2007). The Fgf families in humans, mice, and zebrafish: their evolutional processes and roles in development, metabolism, and disease. *Biol Pharm Bull* **30**, 1819-25.

Kawai, T., Takahashi, T., Esaki, M., Ushikoshi, H., Nagano, S., Fujiwara, H. and Kosai, K. (2004). Efficient cardiomyogenic differentiation of embryonic stem cell by fibroblast growth factor 2 and bone morphogenetic protein 2. *Circ J* **68**, 691-702.

Kelly, R. G., Brown, N. A. and Buckingham, M. E. (2001). The arterial pole of the mouse heart forms from Fgf10-expressing cells in pharyngeal mesoderm. *Dev Cell* **1**, 435-40.

Kengaku, M. and Okamoto, H. (1993). Basic fibroblast growth factor induces differentiation of neural tube and neural crest lineages of cultured ectoderm cells from Xenopus gastrula. *Development* **119**, 1067-78.

Kruithof, B. P., van Wijk, B., Somi, S., Kruithof-de Julio, M., Perez Pomares, J. M., Weesie, F., Wessels, A., Moorman, A. F. and van den Hoff, M. J. (2006). BMP and FGF regulate the differentiation of multipotential pericardial mesoderm into the myocardial or epicardial lineage. *Dev Biol* **295**, 507-22.

Langdon, Y. G., Goetz, S. C., Berg, A. E., Swanik, J. T. and Conlon, F. L. (2007). SHP-2 is required for the maintenance of cardiac progenitors. *Development* **134**, 4119-30.

Lavine, K. J., Yu, K., White, A. C., Zhang, X., Smith, C., Partanen, J. and Ornitz, D. M. (2005). Endocardial and epicardial derived FGF signals regulate myocardial proliferation and differentiation in vivo. *Dev Cell* **8**, 85-95.

Lincoln, J., Alfieri, C. M. and Yutzey, K. E. (2006). BMP and FGF regulatory pathways control cell lineage diversification of heart valve precursor cells. *Dev Biol* **292**, 292-302.

Lopez-Sanchez, C., Climent, V., Schoenwolf, G. C., Alvarez, I. S. and Garcia-Martinez, V. (2002). Induction of cardiogenesis by Hensen's node and fibroblast growth factors. *Cell Tissue Res* **309**, 237-49.

Lough, J., Barron, M., Brogley, M., Sugi, Y., Bolender, D. L. and Zhu, X. (1996). Combined BMP-2 and FGF-4, but neither factor alone, induces cardiogenesis in non-precardiac embryonic mesoderm. *Dev Biol* **178**, 198-202.

Lunn, J. S., Fishwick, K. J., Halley, P. A. and Storey, K. G. (2007). A spatial and temporal map of FGF/Erk1/2 activity and response repertoires in the early chick embryo. *Dev Biol* **302**, 536-52.

Macatee, T. L., Hammond, B. P., Arenkiel, B. R., Francis, L., Frank, D. U. and Moon, A. M. (2003). Ablation of specific expression domains reveals discrete functions of ectoderm- and endoderm-derived FGF8 during cardiovascular and pharyngeal development. *Development* **130**, 6361-74.

Marguerie, A., Bajolle, F., Zaffran, S., Brown, N. A., Dickson, C., Buckingham, M. E. and Kelly, R. G. (2006). Congenital heart defects in Fgfr2-IIIb and Fgf10 mutant mice. *Cardiovasc Res* **71**, 50-60.

Marshall, C. J. (1995). Specificity of receptor tyrosine kinase signaling: transient versus sustained extracellular signal-regulated kinase activation. *Cell* **80**, 179-85.

Meyers, E. N., Lewandoski, M. and Martin, G. R. (1998). An Fgf8 mutant allelic series generated by Cre- and Flp-mediated recombination. *Nat Genet* **18**, 136-41.

Mima, T., Ueno, H., Fischman, D. A., Williams, L. T. and Mikawa, T. (1995). Fibroblast growth factor receptor is required for in vivo cardiac myocyte proliferation at early embryonic stages of heart development. *Proc Natl Acad Sci U S A* **92**, 467-71.

Mjaatvedt, C. H., Nakaoka, T., Moreno-Rodriguez, R., Norris, R. A., Kern, M. J., Eisenberg, C. A., Turner, D. and Markwald, R. R. (2001). The outflow tract of the heart is recruited from a novel heart-forming field. *Dev Biol* **238**, 97-109.

Montero, A., Okada, Y., Tomita, M., Ito, M., Tsurukami, H., Nakamura, T., Doetschman, T., Coffin, J. D. and Hurley, M. M. (2000). Disruption of the fibroblast growth factor-2 gene results in decreased bone mass and bone formation. *J Clin Invest* **105**, 1085-93.

Nascone, N. and Mercola, M. (1995). An inductive role for the endoderm in Xenopus cardiogenesis. *Development* **121**, 515-23.

Ornitz, D. M. and Itoh, N. (2001). Fibroblast growth factors. *Genome Biol* **2**, REVIEWS3005.

Peters, K. G., Werner, S., Chen, G. and Williams, L. T. (1992). Two FGF receptor genes are differentially expressed in epithelial and mesenchymal tissues during limb formation and organogenesis in the mouse. *Development* **114**, 233-43.

Pierpont, M. E., Basson, C. T., Benson, D. W., Jr., Gelb, B. D., Giglia, T. M., Goldmuntz, E., McGee, G., Sable, C. A., Srivastava, D. and Webb, C. L. (2007). Genetic basis for congenital heart defects: current knowledge: a scientific statement from the American Heart Association Congenital Cardiac Defects Committee, Council on Cardiovascular Disease in the Young: endorsed by the American Academy of Pediatrics. *Circulation* **115**, 3015-38.

Reifers, F., Walsh, E. C., Leger, S., Stainier, D. Y. and Brand, M. (2000). Induction and differentiation of the zebrafish heart requires fibroblast growth factor 8 (fgf8/acerebellar). *Development* **127**, 225-35.

Rosenblatt-Velin, N., Lepore, M. G., Cartoni, C., Beermann, F. and Pedrazzini, T. (2005). FGF-2 controls the differentiation of resident cardiac precursors into functional cardiomyocytes. *J Clin Invest* **115**, 1724-33.

Sater, A. K. and Jacobson, A. G. (1989). The specification of heart mesoderm occurs during gastrulation in Xenopus laevis. *Development* **105**, 821-30.

Sheikh, F., Fandrich, R. R., Kardami, E. and Cattini, P. A. (1999). Overexpression of long or short FGFR-1 results in FGF-2-mediated proliferation in neonatal cardiac myocyte cultures. *Cardiovasc Res* **42**, 696-705.

Sheikh, F., Jin, Y., Pasumarthi, K. B., Kardami, E. and Cattini, P. A. (1997). Expression of fibroblast growth factor receptor-1 in rat heart H9c2 myoblasts increases cell proliferation. *Mol Cell Biochem* **176**, 89-97.

Shishido, E., Ono, N., Kojima, T. and Saigo, K. (1997). Requirements of DFR1/Heartless, a mesoderm-specific Drosophila FGF-receptor, for the formation of heart, visceral and somatic muscles, and ensheathing of longitudinal axon tracts in CNS. *Development* **124**, 2119-28.

Soufan, A. T., van den Berg, G., Ruijter, J. M., de Boer, P. A., van den Hoff, M. J. and Moorman, A. F. (2006). Regionalized sequence of myocardial cell growth and proliferation characterizes early chamber formation. *Circ Res* **99**, 545-52.

Sugi, Y., Ito, N., Szebenyi, G., Myers, K., Fallon, J. F., Mikawa, T. and Markwald, R. R. (2003). Fibroblast growth factor (FGF)-4 can induce proliferation of cardiac cushion mesenchymal cells during early valve leaflet formation. *Dev Biol* **258**, 252-63.

Sugi, Y. and Lough, J. (1995). Activin-A and FGF-2 mimic the inductive effects of anterior endoderm on terminal cardiac myogenesis in vitro. *Dev Biol* **168**, 567-74.

Sugi, Y., Sasse, J., Barron, M. and Lough, J. (1995). Developmental expression of fibroblast growth factor receptor-1 (cek-1; flg) during heart development. *Dev Dyn* **202**, 115-25.

Sugi, Y., Sasse, J. and Lough, J. (1993). Inhibition of precardiac mesoderm cell proliferation by antisense oligodeoxynucleotide complementary to fibroblast growth factor-2 (FGF-2). *Dev Biol* **157**, 28-37.

Thisse, B. and Thisse, C. (2005). Functions and regulations of fibroblast growth factor signaling during embryonic development. *Dev Biol* **287**, 390-402.

Thompson, R. P. and Fitzharris, T. P. (1979). Morphogenesis of the truncus arteriosus of the chick embryo heart: the formation and migration of mesenchymal tissue. *Am J Anat* **154**, 545-56.

Waldo, K. L., Kumiski, D. H., Wallis, K. T., Stadt, H. A., Hutson, M. R., Platt, D. H. and Kirby, M. L. (2001). Conotruncal myocardium arises from a secondary heart field. *Development* **128**, 3179-88.

Zhu, X., Sasse, J., McAllister, D. and Lough, J. (1996). Evidence that fibroblast growth factors 1 and 4 participate in regulation of cardiogenesis. *Dev Dyn* **207**, 429-38.

CHAPTER 2

SHP-2 is Required for the Maintenance of Cardiac Progenitors

PREFACE TO CHAPTER 2

Although SHP-2 has previously been suggested to have a role in proper cardiac development as mutations in *Shp-2* are associated with the human congenital syndrome Noonan Syndrome (Noonan and O'Connor, 1996; Tartaglia et al., 2001), a direct role for SHP-2 in cardiac development has not been demonstrated. Chapter 2 describes the requirement for the protein tyrosine phosphatase SHP-2 to maintain cardiac progenitor cells during early vertebrate heart development as well as the role of the FGF growth factor signal pathway in this process.

This work was published in *Development* in 2007 and is a co-first author publication between myself and a former graduate student in the lab Dr. Sarah C. Goetz. Additional collaborators on the paper include Anna Berg and Dr. Jackie Thomas Swanik. I performed the SHP-2 inhibitor studies, the rescue experiments and the phosphorylation studies. In addition I assisted with the FGF inhibitor and cell cycle inhibitor experiments.

Summary

The isolation and culturing of cardiac progenitor cells has demonstrated that growth factor signaling is required to maintain cardiac cell survival and proliferation. In this study, we demonstrate that SHP-2 activity is required for the maintenance of cardiac precursors in vivo. In the absence of SHP-2 signaling, cardiac progenitor cells down-regulate genes associated with early heart development and fail to initiate cardiac differentiation. We further show that this requirement for SHP-2 is restricted to cardiac precursor cells undergoing active proliferation. By demonstrating that SHP-2 is phosphorylated on Y542/Y580 and that it binds to FRS-2, we place SHP-2 in the FGF pathway during early embryonic heart development. Furthermore, we demonstrate that inhibition of FGF signaling mimics the cellular and biochemical effects of SHP-2 inhibition and that these effects can be rescued by constitutively active/Noonan syndrome associated forms of SHP-2. Collectively, these results show that SHP-2 functions within the FGF/MAPK pathway to maintain survival of proliferating populations of cardiac progenitor cells.

Introduction

Cells of the cardiac lineage are amongst the first mesodermal cells to be allocated to a specific tissue type in vertebrates. By the onset of gastrulation, the cells which will give rise to cardiac tissue are located in two regions at the anterior edge of the mesoderm. Extirpation, explantation, and tissue isolation studies in amphibian and avian embryos are all consistent with the cells of the cardiac lineage being specified and committed to the heart lineage during these early stages of development (Dehaan, 1963; Sater and Jacobson, 1989; Warkman and

24

Krieg, 2006). Once cells are committed to the cardiac lineage, the cells migrate laterally and anteriorly, and subsequently fuse at the ventral anterior midline to form the bilaminar heart tube comprised of an outer myocardial and an inner endocardial layer (van den Hoff et al., 2004). It is during this period that the vertebrate heart expresses the first molecular markers of cardiac development *Tbx5*, *Gata4*, *Tbx20* and *Nkx2.5*, the homologue of the *Drosophila* gene *tinman* (Fishman and Chien, 1997; Harvey et al., 2002)**.** It is also during this time that the cardiac precursors begin a period of rapid proliferation (Goetz and Conlon, 2007; Pasumarthi and Field, 2002).

The isolation and culturing of cardiac progenitor cells has strongly implied the requirement for growth factor function to maintain cardiac cell survival. Collectively these studies have shown that survival and proliferation of cardiac progenitor populations requires either the aggregation of clonal colonies, that the cells be co-cultured with heart tissue, or that the cultures be supplemented with a mixture of growth factors and cytokines (Goetz and Conlon, 2007; Kouskoff et al., 2005; Moretti et al., 2006; Parmacek and Epstein, 2005; Srivastava, 2006; Wu et al., 2006). However the precise nature of the endogenous growth factors and the downstream signaling pathways required for cardiac survival or proliferation remain unidentified.

SHP-2, also known as SH-PTP2, Ptpn11, PTP1D, or PTP2C, is the vertebrate homologue of the Drosophila gene *corkscrew* (*Csw*), a widely expressed non-receptor protein tyrosine phosphatase (PTP) known to function genetically and biochemically downstream of a number of growth factors including epidermal growth factors (EGFs), platelet derived growth factor (PDGF), insulin and fibroblast growth factors (FGFs) (Delahaye et al., 2000; Feng, 1999; Pawson, 1994; Qu, 2000; Van Vactor et al., 1998; Zhang et al., 2000). The

sequence, expression pattern and function of SHP-2 are highly conserved throughout evolution with genetic studies in a number of animal models all suggestive of a critical role for SHP-2 in early development. For example, mice homozygous for a null mutation in *Shp-2* die at implantation, due to a failure in the development of the extra-embryonic trophectodermal lineage, while introduction of a dominant negative form of SHP-2 in *Xenopus* can completely block mesoderm formation in response to the FGF/MAPK pathway and leads to gastrulation arrest (Tang et al., 1995; Yang et al., 2006).

Studies have also suggested a role for SHP-2 in heart development. Noonan syndrome, a relatively common autosomal dominant disorder that leads to a number of cardiac abnormalities including atrial septal defects, ventricular septal defects, pulmonary stenosus and hypertrophic cardiomyopathy, is associated with mutations in *Shp-2* in approximately half of affected individuals (Noonan and O'Connor, 1996; Tartaglia et al., 2001). All SHP-2 associated Noonan syndrome mutations are mis-sense mutations and occur within one of the two SRC-homology 2 (SH2) domains, regions required for protein-protein interactions, or within the phosphatase domain. These mutations are thought to be involved in switching SHP-2 between its inactive and active states, and to act in a constitutively active fashion (Allanson, 2002; Maheshwari et al., 2002; Schollen et al., 2003; Tartaglia et al., 2002; Tartaglia et al., 2001). However, the precise requirement for SHP-2 in heart development remains to be established.

In this study, we have bypassed the early embryonic requirements for SHP-2 by means of a cardiac explant assay. Using this assay, we define a requirement for SHP-2 in maintaining cardiac precursor populations in vivo. In the absence of SHP-2 signaling all early cardiac makers are down regulated and cardiac cells fail to initiate cardiac

differentiation. We further show that SHP-2 is required for cardiac progenitor populations that are actively proliferating but not those that have exited the cell cycle. We show that SHP-2 functions directly downstream of FGF in this process and that inhibiting FGF phenocopies SHP-2 inhibition. Furthermore, SHP-2 is directly phosphorylated on specific residues in vivo in response to FGF signaling, and co-immunoprecipitates with FRS, a component of the FGF pathway. Most critically, we can rescue the cardiac lineage and the downstream signaling pathways in FGF inhibited tissues by the expression of a constitutively active/Noonan syndrome version of SHP-2.

Materials and Methods

DNA Constructs

FL-SHP-2 was generously provided by Nikola Pavletich (Georgescu et al., 2000). *Shp-2* N308D and N308D-PTP were generated by site-directed mutagenesis (Stratagene) according to the manufacturer's protocol. Primer sequences available upon request. For epitope labeling, each construct was subcloned into a HA modified pcDNA3.1(+) vector kindly provided by Da-Zhi Wang.

Embryo Injections

Xenopus embryos were obtained by in vitro fertilization (Smith and Slack, 1983), cultured in 0.1X Modified Barth's Saline (MBS) and staged according to the Normal Table of *Xenopus laevis* (Nieuwkoop and Faber, 1975). RNA for injection was synthesized using the mMessage in vitro transcription kit (Ambion) according to manufacturer's instructions.

Embryos were injected at the one-cell stage with 2ng RNA dissolved in 10nl water unless otherwise stated.

Cardiac Explants

Tissue posterior to the cement gland and including the heart field was excised at stage 22 in a manner similar to that described by Raffin et al. (Raffin et al., 2000). The explants include overlying pharyngeal endoderm and some foregut endoderm. Explants were cultured at 23 °C in either 2.5mM DMSO, 500μM NSC-87877 (Sigma), 50μM SU5402 (Pfizer), 150μM aphidicolin (Sigma), 20mM hydroxyurea (Sigma), or 50μM colchicine (Sigma) in 1X MBS (Chemicon) (Chen et al., 2006; Dasso and Newport, 1990; Harris and Hartenstein, 1991; Mason et al., 2002). Explants were cultured until specified stages and fixed for 2 hours in MEMFA at room temperature.

Immunoblotting

To detect endogenous SHP-2, five embryos per condition were homogenized in lysis buffer (100 mM NaCl, 20 mM NaF, 50 mM Tris pH 7.5, 10 mM Sodium Pyrophosphate, 5 mM EDTA, 1% NP40 and 1% Sodium Deoxycholate) with the addition of complete protease inhibitor cocktail (Roche) and PMSF (Sigma) and processed according to standard protocols. In vitro translation of SHP-2 was performed using wheatgerm TNT coupled transcription/translation (Promega) according to manufacturer's instructions.

Western blots were probed with anti-mouse total SHP-2 antibody PTP1D/SHP-2 (BD Transductions Laboratories) at 1:2500. Heart explant western blots were probed with antibodies against phospho-ERK1/2 and total ERK1/2, each used at 1:1000 (Cell Signaling).

Whole heart immunoblots were prepared from seventy dissected hearts as described and probed with antibodies against total SHP-2. Calf intestinal phosphatase (CIP) treatment was carried out by incubating whole embryo lysate or heart lysate with 5U of CIP, CIP buffer, and EDTA-free complete protease inhibitors at 37°C for 1.5 hr prior to western blot analysis. Loading levels of tissue were standardized in pilot runs of western blots assayed by densitometry.

Whole Mount Antibody Staining and in situ hybridization

Whole-mount antibody staining of whole embryos and explants were performed as described (Kolker et al., 2000) with anti-tropomyosin (1:50; Developmental Studies Hybridoma Bank), anti-Myosin Heavy Chain (1:500 Abcam), and phospho-histone H3 (1:200 Upstate) to mark cells in M phase (Goetz et al., 2006) and visualized on a Leica MZFLIII microscope. Immunostaining of histological sections was performed according to protocols and procedures described previously (Goetz et al., 2006). For these studies, phospho-SHP-2 (Tyr542; Cell Signaling) and phospho-SHP-2 (Tyr580; Cell Signaling) were used at 1:1000. Whole-mount in situ hybridizations were performed with *Nkx2.5* (Tonissen et al., 1994), *Tbx5* (Brown et al., 2003; Horb and Thomsen, 1999), *Tbx20* (Brown et al., 2003), *Gata4* (Jiang and Evans, 1996), *Gata5* (Jiang and Evans, 1996), *Gata6* (Gove et al., 1997), *MLC1v'* (IMAGE clone 4408657, GenBank Accession No.: **BG884964**) , *Sox2* (Lu et al., 2004), *Endocut* (Costa et al., 2003), *Ami* (Inui and Asashima, 2006), *Xmsr* (*Xenopus* EST clone XL327k24ex (Mills et al., 1999)), and Shp1 (IMAGE clone 5513271, GenBank Accession No.: **BC09538**), using protocols as previously described (Harland, 1991). In situ hybridization of sectioned *Xenopus* hearts was performed on 14μm cryostat sections using

DIG-labeled antisense RNA probes followed by enzymatic detection according to manufactures protocols (Roche). The following probes were used *Shp-2* (cloned from stage 19-26 *X. laevis* pCS2+ cDNA library) using a forward *Shp-2* primer sequence of CGCCCTAAAGAATCGCAC and a reverse *Shp-2* primer sequence of ACACTGTAGAGATGAAGATGCCTC resulting in a 1.8kb insert, *Shp-1* (IMAGE clone 5513271, GenBank Accession No.: **BC09538**), and *Tbx20* (Brown et al., 2003). Embryos were cleared using 2:1 benzyl benzoate/benzyl alcohol.

Whole Mount TUNEL Staining

Apoptotic cells were detected by TUNEL staining as previously described (Hensey and Gautier, 1998) with the chromogenic detection of DIG-dUTP incorporation carried out with BCIP (175 ug/mL, Roche) and nitro blue tetrazolium (337 ug/mL, Roche).

Immunoprecipitation

For immunoprecipitations from hearts, embryos were injected, as described above, with 2ng of HA-tagged full length *Shp-2* RNA. 1400 hearts were dissected at stage 35 and homogenized in lysis buffer (50 mM Tris 7.6, 150 mM NaCl, 10 mM EDTA, 1 % Surfact-Amps Triton-100, 25 mM PMSF supplemented with complete protease inhibitor mini tablet (Roche)). Supernatants were precleared with protein A/G beads for two hours at 4°C. 20μl of HA beads (Covance) or 30μl of *Shp-2* agarose beads (Santa Cruz Biotechnology) was added to the supernatant and rotated overnight at 4°C. Immunoblotting was performed using anti-HA (Covance) at 1:1000, anti-FRS-2 (Santa Cruz) at 1:200, anti-SHP-2 (BD Transduction Labs) at 1:2500, and anti-phospho Y-542 SHP-2 (Cell Signaling) at 1:1000.

For immunoprecipitations from explants, endogenous SHP-2 was immunoprecipitated from 100 explants per condition, and immunoprecipitations carried out as described above.

Results

SHP-2 is required for MHC expression in cardiac tissue

To begin to elucidate the molecular pathways involved in cardiac cell survival, we have focused on the role of SHP-2 during the early stages of heart development. Clinical studies in humans and genetic studies in mice are all consistent with a role for SHP-2 in early heart development. However it remains unclear if SHP-2 acts directly or indirectly in the cardiac lineage. Western blot analysis with an antibody specific for total SHP-2 as well as section in situs shows SHP-2 to be present throughout stages of early *Xenopus* embryogenesis including in embryonic heart tissue (Fig. S2.1A-C, S2.2B).

Having established that SHP-2 is expressed in early embryos, we next tested the requirement for SHP-2 in early heart development. To bypass the early embryonic requirement for SHP-2, we have used a cardiac explant assay. Based on anatomical and gene expression studies in *Xenopus*, at late neurulation (stage 22) the cardiac precursors exist in two cell populations which lie directly posterior to the cement gland along the anterior-ventral aspects of the embryo (Dale and Slack, 1987; Moody, 1987; Raffin et al., 2000; Sater and Jacobson, 1989). When dissected and cultured in isolation this tissue forms a ridge of cardiac tissue on top of developing endoderm (stages 22-33) and will eventually form a beating heart (stage 38/40) while the donor embryo completely lacks any cardiac tissue (*Xenopus* can develop to late tadpole stage in the absence of a functioning heart or circulation). We have carried out an extensive analysis of these explants using early, mid and

late molecular markers of heart tissue and show that the explants display a temporal and spatial expression of cardiac genes that faithfully recapitulates that of control (unmanipulated) embryos (Fig. 2.1A-B). Therefore, the use of explants for studying the requirement for SHP-2 allows us to bypass secondary morphogenesis and tissue interactions that may complicate the analysis of the role of SHP-2 in early heart development. To determine the requirement for SHP-2 in developing heart tissue, explants were treated with DMSO or the SHP-2 specific inhibitor NSC-87877 (Chen et al., 2006). We observe a dramatic downregulation of myosin heavy chain (MHC) expression in NSC-87877 treated explants compared to controls suggesting that SHP-2 is required for the maintenance of MHC expression (Fig. 2.1C).

Previous studies have shown that NSC-87877 can also inhibit SHP-1 activity. To ensure the downregulation of MHC is not due to interference with SHP-1, we identified a full length *Xenopus Shp-1* EST (Image Clone 5513271, GenBank Accession No. BC097538) and performed in situ analysis on early stage *Xenopus* embryos. Consistent with work in mouse, we never detected the presence of *Shp-1* in developing *Xenopus* heart tissue between stages 22-37 (Fig. S2.2), therefore the defects we observe are most likely due to the inhibition of SHP-2. To confirm the specificity of NSC-87877, we show that its effect on MHC can be rescued by injection of the Noonan syndrome-associated constitutively active form of human SHP-2, N308D (*Shp-2* N308D) but not a phosphatase dead version of N308D (Fig. 2.1C, 2.S3; data not shown). To ensure that N308D is not inducing ectopic cardiac tissue in explants, we further tested the effects of *Shp-2* N308D on heart development by injecting mRNA encoding *Shp-2* N308D and performing whole mount in situ hybridization with markers of early heart development including *Nkx2.5* (Tonissen et al., 1994), *Tbx5* (Brown et

32

al., 2003; Horb and Thomsen, 1999), and *Tbx20* (Brown et al., 2003). Consistent with the

results shown in Fig. 2.1 there are no alterations in the expression of any of these markers

between control and N308D derived embryos (Fig. S2.4). Taken together, these data indicate

that SHP-2 signaling is required to induce or maintain expression of MHC.

SHP-2 signaling is required for the maintenance of cardiac progenitors

Since we observed that the SHP-2 is required for MHC expression in cardiac tissue, we

addressed whether this effect is specific for MHC or reflects a general requirement for SHP-2

signaling in heart development. To establish the role of SHP-2 in heart development and to

determine how rapidly SHP-2 inhibition effects cardiac gene expression, we assayed cardiac

explants for expression of *Nkx2.5*, *Tbx5*, *Tbx20* and the cardiac differentiation marker

MLC1v′ at time points corresponding to stage 22, the stage when the cardiac precursors are

two distinct lateral populations of cells; stage 26, the period when the two cardiac precursors

populations are positioned at the anterior, ventral region of embryo flanking the midline;

stage 29 when the cardiac fields fuse across the ventral midline and stage 33 when the

bilaminar heart tube initiates cardiac looping. These studies show that there is a progressive

loss of all three early markers with increasing length of SHP-2 inhibition. We observe that

controls and tissue treated for one hour are indistinguishable at stage 22 (Fig. 2.2A-C)

however by early tailbud stage (St. 26) cardiac precursors in treated explants remain in two

bilateral populations while the cardiac precursors in controls have migrated toward the

midline (Fig. 2.2A-C). At stage 29, when the hearts in control explants have formed a linear

heart tube, the cardiac fields in SHP-2 inhibited explants remain unfused and display reduced

expression of *Nkx2.5*, *Tbx5*, and *Tbx20*. Similarly, at stage 33, *Nkx2.5*, *Tbx5*, and *Tbx20*

expression appears to continue to be restricted to a subset of tissue at the leading edge of the

cardiac field or is absent entirely. The expression of the cardiac differentiation marker

MLC1v' is never initiated in SHP-2 inhibited explants (Fig. 2.2D). Thus overall there

appears to be a progressive and rapid loss of early cardiac marker expression in SHP-2

inhibited explants and markers of cardiac differentiation fail to be expressed (Fig. 2.2A-D).

We do note however, that cardiac cells at the leading edge continue to express *Tbx5* until at

least stage 33 (Fig. 2.2B, arrows) suggesting that in these cells *Tbx5* expression is regulated

in a SHP-2-independent fashion.

To confirm and extend these findings we tested explants for expression of the early

cardiac/endoderm markers *Gata4*, *Gata5*, and *Gata6*. Similar to *Nkx2.5*, *Tbx5*, and *Tbx20*, we

detect a dramatic down-regulation of *Gata4, Gata5* and *Gata6* (Fig. S2.5). The loss of

cardiac markers is not due to dedifferentiation since the explants do not express markers of

undifferentiated mesoderm (data not shown). Moreover, the effects of SHP-2 are dose

dependent with the dose of NSC-87877 that affects early cardiac marker expression being the

same dose that in cardiac explants blocks MAPK signaling, a downstream mediator of SHP-2

signaling (Fig. S2.6). However, we cannot formally exclude the possibility that other SHP-2

like molecules may also be involved in the same signaling process. Consistent with published

reports showing that NSC-87877 affects SHP-2's phosphatase activity, we are able to rescue

the expression of molecular markers of early cardiac development in SHP-2 inhibited

explants by the expression of a constitutively active SHP-2 N308D and to a lesser extent

wildtype SHP-2 (Fig. 2.2E, S2.3, S2.6, data not shown).

Since NSC-87877 cannot be absorbed by whole *Xenopus* embryos, to determine if the

effects we observe with our tissue culture explants is reflective of a requirement for SHP-2 in

developing embryos we cultured the anterior third of stage 22 embryos in media containing

NSC-87877 at the same dose used in our explant studies. Identical to the cardiac explants, treatment with NSC-87877 specifically inhibits expression of *Nkx2.5* in the developing heart while having no effects on its expression in the developing pharyngeal endoderm (Fig. 2.2F). Collectively, these results suggest that SHP-2 is required to maintain the expression of early cardiac markers in most of the cardiac field and for the onset of cardiac differentiation.

SHP-2 signaling is required for pharyngeal mesoderm but is not required for the induction and/or maintenance of endodermal or endothelial tissue types

To determine whether the requirements for SHP-2 are cardiac-specific, we assayed the effects of SHP-2 inhibition on the additional cell types present in tissue explants; endoderm, endothelial cells, and overlying pharyngeal mesoderm (Fig. 2.3A). Similar to our findings with cardiac-specific markers, SHP-2 signaling is required for the maintenance of the pharyngeal mesoderm-associated genes *Fgf8*, *Tbx1*, and *Isl1* as inhibition of SHP-2 signaling results in loss of expression of these genes in explanted tissue (Fig. 2.3B and data not shown). In contrast, results show that SHP-2 signaling is not required for the expression of genes associated with the deep endoderm (*Edd* and *Endocut* positive tissue) or pharyngeal endoderm (*Sox2* positive; Fig. 2.3C). Similarly, we observe that SHP-2 signaling is not required for the onset of expression of the endothelial cell markers *Xmsr* and *Ami* (Fig. 2.3C). We note however, that *Xmsr* and *Ami* are expressed in SHP-2 inhibited tissue in coherent un-branched patterns verses control explants suggesting that SHP-2 is required either directly or indirectly for the proper development and growth of endothelial tissues. Collectively, these results show SHP-2 is required for the maintenance of early markers of cardiac and pharyngeal mesoderm but is not required for the maintenance of endodermal or endothelial

cell types, and further imply that the requirement for SHP-2 in cardiac tissue is not an indirect effect of alterations in endodermal induction or patterning.

Inhibition of SHP-2 results in a progressive increase in cardiac cell death

To determine if the loss of cardiac tissue in response to SHP-2 inhibition is due to defects in cardiac cell survival or proliferation, we repeated our analysis examining programmed cell death in control explants and explants in which SHP-2 signaling was inhibited. Explants were again treated with the SHP-2 inhibitor beginning at stage 22, and then analyzed at stages 22, 26, 29, and 33. TUNEL staining of cardiac explants reveals that at stage 22 there is no apparent difference in cardiac cell death in the ridge of mesodermal tissue which contains the cardiac tissue in either control or SHP-2 inhibited explants (Fig. 2.4) however, by stage 26 we begin to detect an increase in TUNEL positive cells in SHP-2 inhibited in cardiac tissue (Fig. 2.4). By stages 29 and 33, the number of apoptotic cells in the SHP-2 inhibited explants has further expanded in the more lateral regions of the cardiac ridge (Fig. 2.4). To further ensure that the cells undergoing programmed cell death are cardiac cells, we performed double in situ-TUNEL staining on cardiac explants in which SHP-2 was inhibited. Results from these studies show that the cells undergoing programmed cell death are adjacent with those expressing TBX5, which is only expressed in the cardiac tissue in the explants (Fig. 2.4). Therefore, in the absence of SHP-2 signaling, cardiac cells cease development and undergo programmed cell death initiated by stage 26.

SHP-2 is required in proliferating cardiomyocytes

Since studies have implied a role for SHP-2 in cell cycle progression (Guillemot et al., 2000; Yuan et al., 2005; Yuan et al., 2003), we tested if withdrawal from the cell cycle could

account for the observed loss of cardiac marker expression and programmed cell death in SHP-2 inhibited explants. Therefore, we treated explants with cell cycle inhibitors and determined the effects on the expression of early and late heart markers. As expected, the explants cultured in media containing aphidicolin (Aph) which blocks S-phase progression, leads to a dramatic reduction in the number of mitotic cells (Fig. 2.5A). Surprisingly, results show Aph leads to a loss of the early cardiac markers *Nkx2.5*, *Tbx5*, *Tbx20,* and *Gata6* (Fig. 2.5B,C) however, G1/S interphase arrest by Aph has no effect on the expression of the expression of other early heart markers including *Gata4* and *Gata5* (Fig. 2.5C), and in contrast to SHP-2 inhibition, has no effect on markers of cardiac differentiation including *Hsp27* (Brown et al., 2007), *MLC1v'*, MHC, and tropomyosin (Fig. 2.5D,E). However, as predicted from cell cycle arrest, we observed a reduction in the size of the hearts in the Aph-treated explants. These results are not due to treatment with Aph per se since identical results were obtained with M-phase arrest by treatment with colchicine (Fig. 2.5F). Thus, these findings suggest that the lack of cardiac differentiation in SHP-2 inhibited tissue is not the result of cell cycle arrest. Moreover, these observations are consistent with studies demonstrating that genetic mutations or protein depletion of *Nkx2.5*, *Tbx5*, and/or *Tbx20* has no effect on cardiac differentiation and further implies that cell cycle arrest and cardiac differentiation are independently regulated in vivo (Brown et al., 2005; Bruneau et al., 2001; Cai et al., 2005; Goetz et al., 2006; Lyons, 1995; Singh et al., 2005; Stennard et al., 2005; Takeuchi et al., 2005).

To determine the developmental period at which SHP-2 functions to maintain survival of cardiomyocytes, SHP-2 signaling was blocked in cardiac explants beginning at a series of developmental stages: late neurula (St. 22 and 24), early tailbud (St. 26), and late

tailbud (St. 29); and cultured to tadpole stage (St. 37; Fig. 2.6A). Results from these studies show a decreasing requirement for SHP-2 between stages 22 and 33; treatment at stage 22 shows no MHC expression, starting at stages 24 and 26 show a marked reduction in MHC expression by stage 37, while treatment beginning from stage 29 results in hearts with high levels of MHC expression, but that are reduced in size by stage 37 (Fig. 2.6A).

Our results demonstrate that SHP-2 signaling is required during late neurula stages a period when increasing numbers of cardiomyocytes begin to exit the cell cycle and undergo terminal differentiation (Goetz et al., 2006). To further examine the correlation between the requirement for SHP-2 and cell cycle exit, we analyzed cardiac cell proliferation and terminal differentiation between stages 33 and adult. Taken together with our past studies (Goetz et al., 2006), these results demonstrate that there is a gradual reduction in cycling cardiomyocytes during early and mid-tadpole stages and a proliferation persists in terminally differentiated cardiomyocytes until late tadpole stage (Fig. 2.6B).

To directly determine if SHP-2 signaling is required for the maintenance of proliferating cardiac cells, we inhibited SHP-2 signaling beginning at a stage when there are two populations of cardiomyocytes: one that is undergoing active division and a second that is exited the cycle and undergone terminal differentiation (stage 29) and allowed the explants to mature to stage 37. Results from these studies show that SHP-2 is required at this later stage, inhibited explants have a mitotic index that is approximately half that of control explants (Fig. 2.6C,D), suggesting that SHP-2 signaling is required for the maintenance and survival of proliferating cardiac cells.

SHP-2 functions downstream of the FGF pathway to regulate cardiac cell survival

The phosphorylation state of SHP-2 has been demonstrated to be reflective of its function within a specific receptor tyrosine kinase (RTK) pathway (e.g. (Bjorbaek et al., 2001)). For example, SHP-2 has been shown to be phosphorylated on tyrosine residues 542 and 580 in response to FGF or PDGF stimulation but not EGF stimulation (Araki et al., 2004). To determine the phosphorylation state of SHP-2 in heart tissue in vivo, we immunprecipitated SHP-2 from embryonic and adult hearts and conducted western blots with a phospho-Y542 SHP-2 antibody. Results show that SHP-2 is phosphorylated at residue Y542 in cardiac tissue during the same period when SHP-2 functions to maintain cardiac cell survival (Fig. 2.7B; Fig. 2.6). Consistent with these results, immunohistochemistry shows that both phospho-Y542 SHP-2 and phospho-Y580 SHP-2 are expressed in the developing myocardium (Fig. 2.7A). Collectively these results demonstrate that SHP-2 is present in its phosphorylated state in developing myocardial tissue, and therefore most likely acting within the FGF and/or PDGF pathways.

In tissue culture, SHP-2 interacts with the docking protein FRS within the FGF but not PDGF signaling pathway (Kouhara et al., 1997). To test if SHP-2 is functioning downstream of FGF in embryonic heart tissue in vivo, we carried out co-immunoprecipitation experiments from isolated embryonic heart tissue. Results show that in isolated embryonic heart tissue SHP-2 directly interacts with FRS (Fig. 2.7B). This is the first demonstration that SHP-2 interacts with FRS in vivo.

Since the decrease in *Nkx2.5* expression in SHP-2-inhibited explants is similar to that reported in embryos which genetically lack *Fgf8* (Ilagan et al., 2006) or those in which the endoderm adjacent to the cardiac mesoderm has been surgically removed (Alsan and

Schultheiss, 2002), and since we observe phosphorylation of SHP-2 on tyrosine residues 542 and 580 and direct association of SHP-2 with FRS in embryonic heart tissue, we reasoned that FGF acts through SHP-2 to maintain the cardiac lineage. To investigate this possibility, we tested the effects of inhibiting FGF signaling in cardiac explants. Results from these assays show that similar to SHP-2 inhibition, treatment of cardiac explants with the FGFR inhibitor SU5402 leads to a decrease in expression of early and late cardiac markers (Fig. 2.8A). However, we note that in contrast to SHP-2 inhibition, FGF inhibition leads to a reduction but not loss of *Tbx5* (Fig. 2.8A,B). Consistent with the weaker *Tbx5* phenotype, we observe the persistence of the SHP-2-FRS interaction and a reduction but not loss of phospho-Y542 SHP-2 in FGF inhibited explants (Fig. 2.8E). Taken together, these results imply that SHP-2 functions in both the FGF pathway and an additional unidentified SHP-2-FRS pathway in the developing heart.

To determine if SHP-2 functions within the FGF pathway to maintain survival of proliferating cardiomyocytes, we first determined if the alteration in cardiac gene in response to FGF inhibition expression temporally mimics that seen with SHP-2 inhibition. As observed with SHP-2 inhibition, the cardiac explants respond to FGF inhibition between stages 22 and 26 (data not shown) and western blots of cardiac explants lacking SHP-2 activity or FGF signaling show a dramatic decrease in phospho-ERK (3 fold or more in response to inhibition as assayed by densitometry; Fig. 2.8C-D). Consistent with SHP-2 acting downstream of FGF, injection of a constitutively active SHP-2 (N308D) in FGFR inhibited explants rescues expression of the early heart markers *Nkx2.5* and results in full expression of *Tbx5* (Fig. 2.8B). Taken together these studies demonstrate that SHP-2 functions in the FGF pathway to regulate cardiac progenitor survival.

Discussion

In recent years, there has been great clinical interest in identifying cardiac progenitor cells from various sources, however, little effort has been expended to understand the precise nature of the endogenous growth factor signaling pathways required for survival or proliferation of cardiac cells (Goetz and Conlon, 2007; Kattman et al., 2006; Kouskoff et al., 2005; Moretti et al., 2006; Parmacek and Epstein, 2005; Srivastava, 2006; Wu et al., 2006). To date, studies of early cardiac tissue have implied a requirement for growth factors to maintain cardiac cell survival, with survival and proliferation of cardiac progenitor populations requiring either the aggregation of clonal colonies, that cardiac progenitors be co-cultured with heart tissue, or that the cultures be supplemented with a mixture of growth factors and cytokines. However, neither the endogenous growth factor nor the signaling cascade required for cardiac progenitor survival has been identified (Parmacek and Epstein, 2005; Srivastava, 2006). To address these issues, we have characterized the endogenous role for SHP-2, a non-receptor protein phosphatase disrupted in the congenital heart disease Noonan syndrome, and have demonstrated that SHP-2 functions in the FGF pathway to maintain the survival of proliferating cardiomyocytes in vivo.

SHP-2 and cardiac cell cycle

The time at which SHP-2 is required for the maintenance of cardiac progenitor cells corresponds with a period of rapid cardiac proliferation (Fishman and Chien, 1997; Goetz and Conlon, 2007; Goetz et al., 2006; Pasumarthi and Field, 2002). In many tissues, such as muscle and the nervous system, the withdrawal of cells from the cell cycle is tightly associated with the onset of terminal differentiation (Alexiades and Cepko, 1996; Dyer and

Cepko, 2001; Lathrop et al., 1985; Li and Vaessin, 2000; Walsh and Perlman, 1997). In contrast, relatively little is known about the relationship between the cell cycle progression and terminal differentiation in the heart.

Our previous work has demonstrated that cardiac cells which initiate terminal differentiation retain the ability to divide (Goetz and Conlon, 2007; Goetz et al., 2006). In the current study, we have extended these findings to demonstrate that while cardiomyocytes of the adult frog ultimately exit the cell cycle, cells expressing markers of terminal differentiation are still undergoing cell division at stage 42. By this stage, cardiac morphogenesis is largely complete and all cardiac cells, including those still dividing, possess the anatomical and molecular hallmarks of differentiation suggesting that in the heart, the onset of terminal differentiation does not require cell cycle exit. Our findings are broadly consistent with recent work showing that cell cycle exit and terminal differentiation are mechanistically separable processes (Goetz and Conlon, 2007; Grossel and Hinds, 2006; Nguyen et al., 2006; Vernon and Philpott, 2003). As a corollary to these experiments, we have also examined here the consequences of induced cell cycle arrest on cardiac differentiation and found that blocking the cell cycle in S-phase with aphidicolin, or in M-phase with colchicine does not result in a block in cardiac differentiation. Interestingly, however, we have found that cell cycle arrest results in reduced expression of the early cardiac markers *Tbx5*, *Tbx20*, and *Nkx2.5*. Thus, these findings are consistent with the observation that none of these early cardiac proteins are required for cardiac differentiation, and further imply that the expression of these early cardiac transcription factors may be cell cycle-dependent.

Coinciding with program cell death, we also observe that blocking SHP-2 activity leads to a failure of early cardiac cells to fuse at the ventral midline. At present we can not distinguish between a role for SHP-2 mediating a trophic factor response and/or a role for SHP-2 in cell adhesion. However, genetic studies in zebrafish and mouse strongly imply that the inability of the cardiac fields to fuse is not the primary cause of the downregulation of early cardiac markers or the failure of SHP-2 inhibited explants to initiate cardiac differentiation. For example, genetic mutations resulting in cardiac bifidia, such as *Gata5*, *hand2*, *Casanova*, and *Bonnie and clyde* and *miles apart* in zebrafish (Alexander et al., 1999; Kupperman et al., 2000; Reiter et al., 1999) or *Gata4* and *MesP1* (Molkentin et al., 1997; Saga et al., 1999) in mouse, as well as genetic mutations in cardiac cell adhesion proteins (Trinh and Stainier, 2004), show no alteration in the expression of early cardiac markers such as *Nkx2.5* or of markers associated with terminal differentiation. Therefore, it is most likely that the failure of cardiac cells to migrate is a secondary consequence of cell survival or it maybe that SHP-2 has two temporally distinct roles in heart development one, regulating cell adhesion and a second in cell survival.

SHP-2 and the FGF pathway

In this study we show SHP-2 to be phosphorylated on tyrosines 542 and 580 in the embryonic heart and that it co-immunoprecipitates with FRS-2, demonstrating an in vivo interaction between SHP-2 and FRS-2 for the first time. Given that we have shown inhibitors of both SHP-2 and FGFR to cause comparable cardiac phenotypes, and that a constitutively active form of SHP-2 can rescue formation of cardiac tissue in FGF inhibited

explants, we conclude that SHP-2 participates in the FGF signal transduction pathway in *Xenopus* embryonic hearts.

Recent work examining the role of FGFs in response to cardiac damage or injury lends further support for the direct role of SHP-2 in cardiac cell survival. The over-expression of both FGF-1 and FGF-2 have been shown to promote the survival of adult cardiomyocytes in response to ischemic injury in vivo (House et al., 2005; Jiang et al., 2002; Jiang et al., 2004; Palmen et al., 2004) and the cardioprotective effects of FGF-2 in the adult myocardium are mediated through the MAPK pathway (House et al., 2005); the same branch of the FGFR signaling cascade which we have shown in cardiac tissue functions through SHP-2. Interestingly, the specific function of FGF-2 in preventing programmed cell death in response to ischemic insult was shown to be independent of its mitogenic or angiogenic functions, suggesting that FGF-2 is functioning specifically to promote cardiomyocyte cell survival (Jiang et al., 2004). Together with our data showing that SHP-2 activity downstream of FGFR is required for the maintenance of proliferating cardiac progenitor cells, these data suggest that the FGF/MAPK pathway functions in promoting cardiac progenitor cell survival during development and further suggests that the FGF/SHP-2/MAPK pathway must be maintained to promote survival of cardiac progenitor cells in vitro. Intriguingly, the FGF/SHP-2 has also recently been shown to be required for the survival of trophectoderm stem cells and for the ability of hematopoietic stem cells to self-renew (Chan et al., 2006; Yang et al., 2006) thus, raising the possibility that the FGF/SHP-2 pathway is a common pathway for progenitor cell survival.

What are the mechanisms by which SHP-2 acts to activate the MAPK pathway and promote cell survival? Studies have shown that SHP-2 acts as a positive regulator in the FGF

pathway in at least two ways, the first is by acting as a scaffold to recruit GRB2 which in turn recruits SOS, the guanine nucleotide exchange factor for RAS which leads to the activation of the ERK cascade potentially leading to the destabilization of the pro-apoptotic protein BIM (Yang et al., 2006). Alternatively or concomitantly, SHP-2 may act as a positive regulator in RAS signaling by inhibiting Sprouty, a key FGF/RTK inhibitor (Christofori, 2003; Kim et al., 2004; Tsang and Dawid, 2004). Consistent with the later possibility, Sprouty has recently been shown to be a direct substrate of SHP-2 and studies have shown that one of the four mammalian sproutys, Sprouty 1, is expressed in the heart and upregulated upon cardiac insult (Hanafusa et al., 2004; Huebert et al., 2004; Jarvis et al., 2006). However, it remains unknown if any of the Sprouty family have an endogenous role in early heart development or if like Drosophila, Sprouty acts as an endogenous substrate of SHP-2 in vivo (Jarvis et al., 2006).

Figure 2.1. Inhibition of SHP-2 activity results in loss of MHC expression.

Tissue explants show identical cardiac expression profiles as intact embryos. (A) Whole mount antibody staining of cardiac differentiation with tropomyosin (Tmy; red) or myosin heavy chain (MHC; red) antibodies as indicated, in whole embryos and cardiac explants at stages 22 (neurula), 29 (tailbud), and 37 (tadpole; scale bar=0.5 mm). (B) Whole mount in situ hybridization for early heart markers *Tbx5*, *Tbx20*, *Nkx2.5* in whole embryos and cardiac explants at stage 22, 29 and 37, as indicated (Scale bar = 1 mm).

(C) MHC expression is dependent on SHP-2 activity. Whole mount antibody staining for MHC (red) in cardiac explants taken from uninjected (Control) embryos or embryos injected with *Shp-2* N308D and treated with either buffer or DMSO carrier as controls or with NSC-87877 as indicated. BF= bright field (scale bar=0.5 mm).
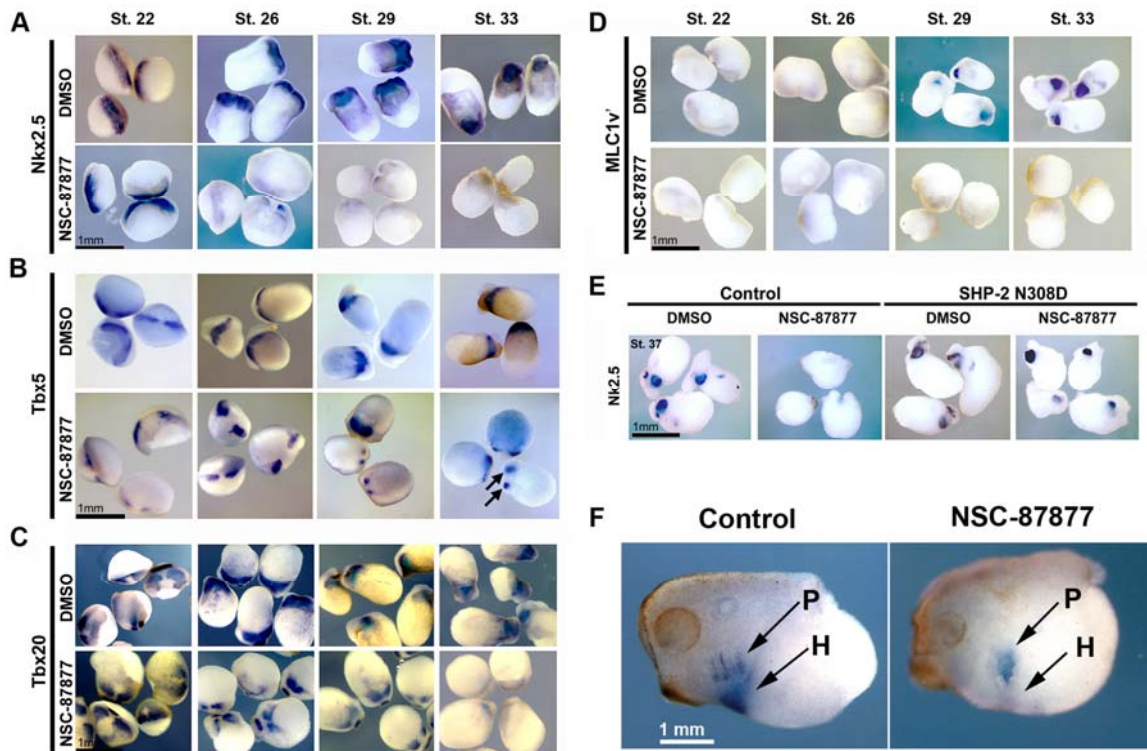
Figure 2.2. SHP-2 is required for the maintenance and the expression of cardiac markers.

(A-D) Cardiac explants isolated and cultured in DMSO or NSC-87877 beginning at stage 22. In situ hybridization performed on explants with *Nkx2.5* (A), *Tbx5* (B), *Tbx20* (C), and *MLC1v'* specific probes (D) at stages 22, 26, 29, and 33, as indicated. Black arrows denote *Tbx5* expression at the leading edge of the cardiac ridge at stage 33 (scale bar=1.0 mm). (E) In situ hybridization of *Nkx2.5* in uninjected (control) or *Shp-2* N308D injected explants treated with DMSO or NSC-87877 beginning at stage 22, and assessed at stage 37 (scale bar=1.0 mm). (F) In situ with *Nkx2.5* of anterior region of whole embryos cultured in DMSO (Control) or NSC-87877 P= pharyngeal arches. H= heart. (Scale bar=1.0 mm).
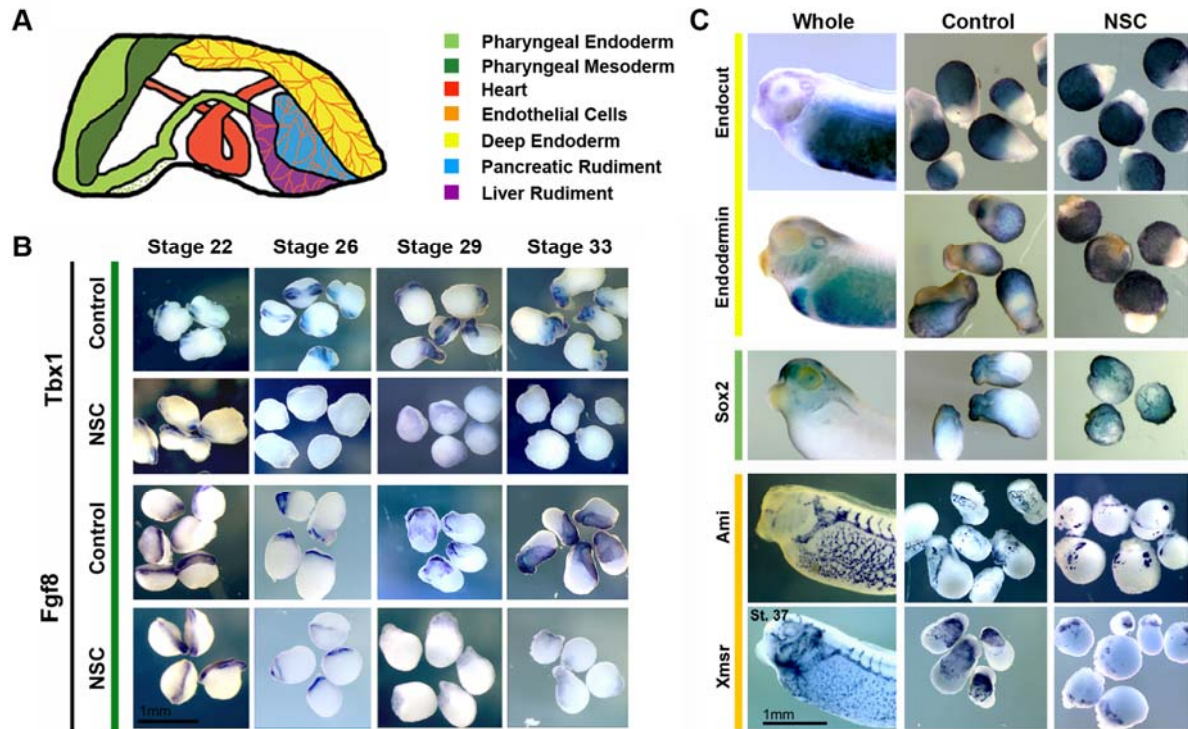
Figure 2.3. SHP-2 activity is required for pharyngeal mesoderm.

(A) Schematic of tissues and rudimentary organ structures in tissue explants. (B) Cardiac explants isolated and cultured in DMSO or NSC-87877 (NSC) beginning at stage 22. In situ hybridization performed on explants with *Tbx1*, *Fgf8*, at stages 22, 26, 29, and 33. (Scale bar = 1 mm). (C) Whole mount in situ hybridization of *Endocut*, *Endodermin*, *Sox2*, *Ami*, and *Xmsr* at stage 37; whole embryos and cardiac explants treated with DMSO (Control) or NSC-87877 (NSC), as indicated (scale bar=1.0 mm).
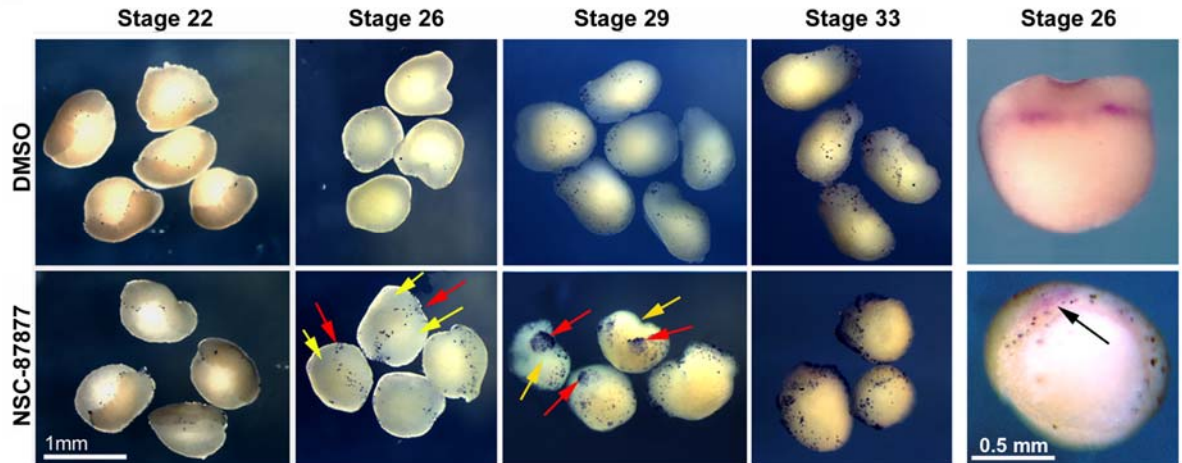
Figure 2.4. SHP-2 is required for cardiac cell survival.

TUNEL staining of control cardiac explants (DMSO) and explants treated with NSC-87877.

Cell death examined in explants at stages 22, 26, 29, and 33, as indicated. Red arrows denote

cardiac cells, yellow arrows denote endodermal cells (Scale bar = 1 mm). Double in situ

(red)/TUNEL (dark blue) using a *Tbx5* specific probe on stage 26 explants that were cultures

in DMSO or NSC-87877 from stage 22-26. Black arrow points to *Tbx5* expressing cells in

NSC-87877 treated explants (Scale bar = 0.5 mm).
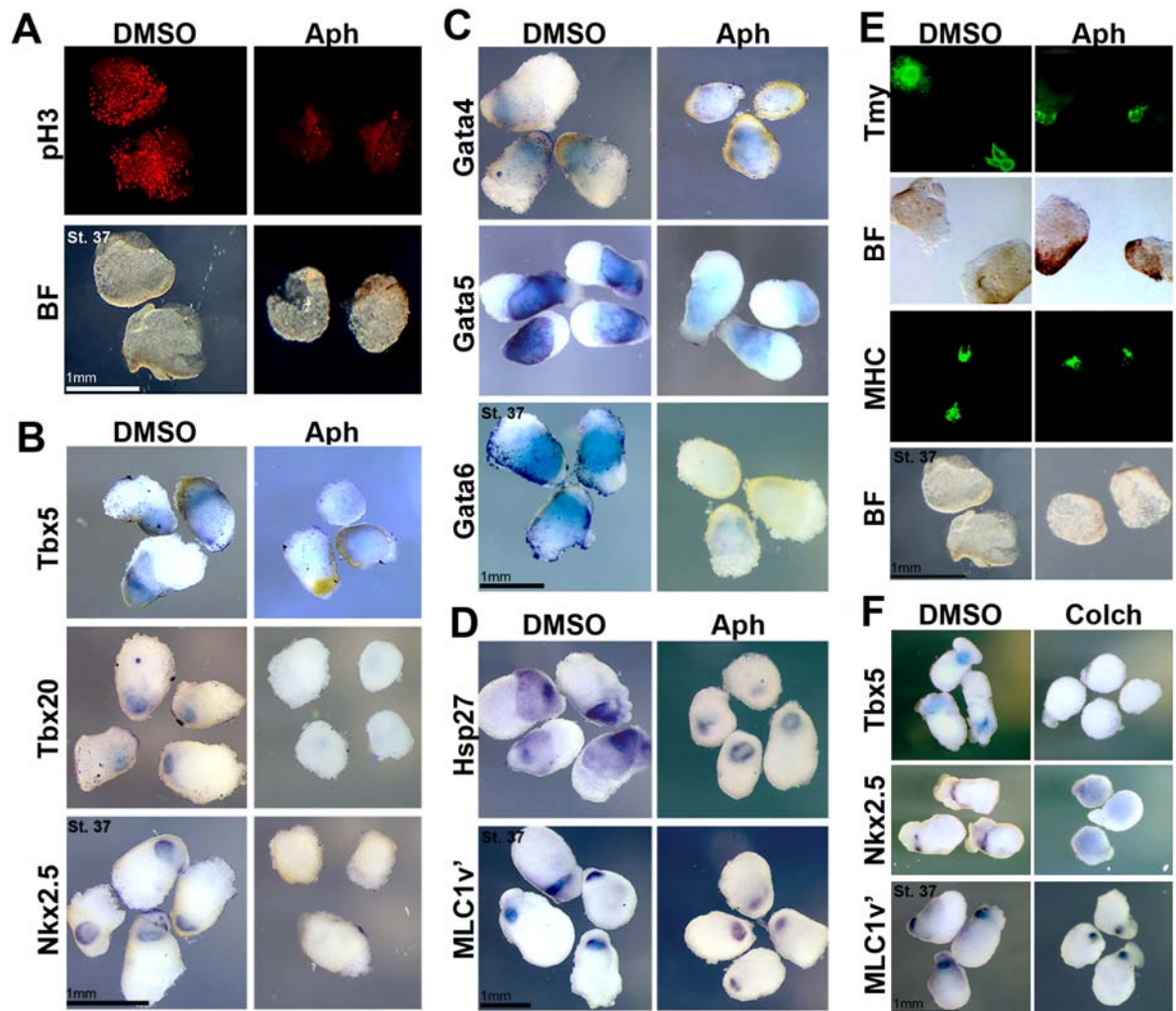
Figure 2.5. Blocking the cardiac cell cycle results in loss of early, but not late, cardiac markers.

(A) Cardiac explants isolated and cultured in DMSO or Aphidicolin (Aph) to block cell s in S-phase beginning at stage 22 and fixed at stage 37. Whole mount immunostaining of explants with phospho-histone H3 specific antibody (pH3; red; scale bar=1.0 mm). In situ hybridization on explants with early the cardiac markers (B) *Tbx5*, *Tbx20*, *Nkx2.5*, (C) *Gata4*, *Gata5*, and *Gata6* (scale bar=1.0 mm); (D) with the cardiac differentiation markers *Hsp27* and *MLC1v'* and (E) by whole mount immunostaining with the cardiac differentiation markers Tmy and MHC (BF- bright field, scale bar=1.0 mm). (F) Explants were treated with

DMSO or colchicine (Colch) to block cells in M-phase of the cell cycle. In situ hybridization

was performed to examine expression of *Tbx5*, *Nkx2.5*, and *MLC1V'*, as indicated (scale

bar=1.0 mm)
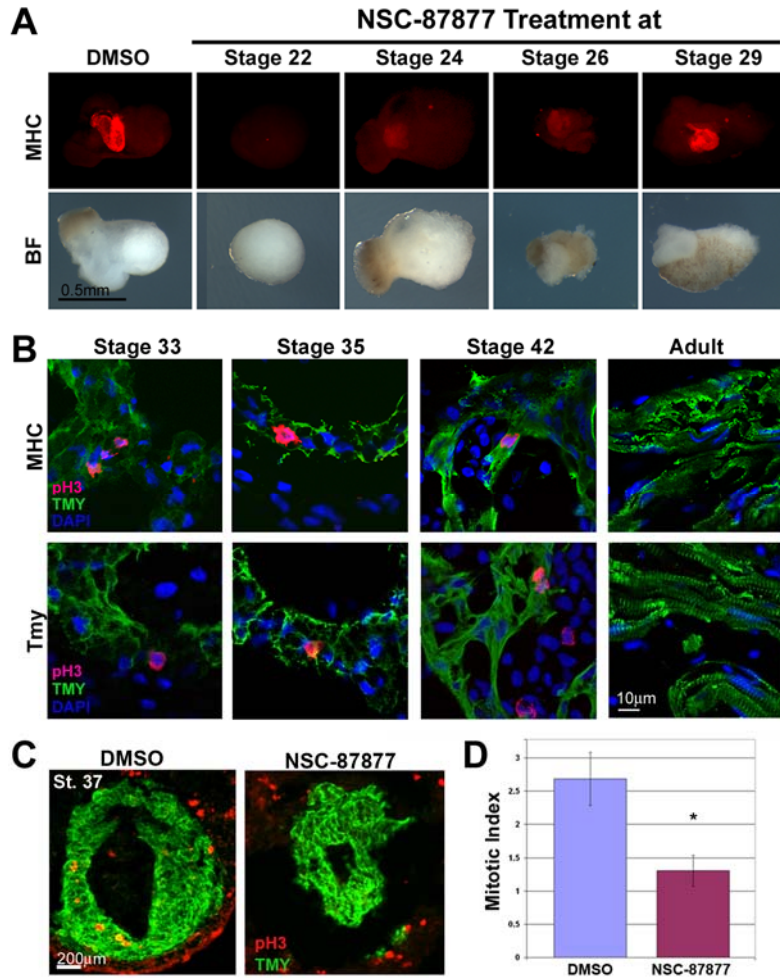
Figure 2.6. SHP-2 is required for the survival of proliferating cardiac cells.

(A) Cardiac explants were treated with the SHP-2 inhibitor NSC-87877 beginning at stage 22, 24, 26, or 29 as indicated, cultured to stage 37 and stained with an MHC antibody (red); (BF= bright field, scale bars=0.5 mm). (B) Representative transverse sections through stage 33, 35, 42 and adult *Xenopus* hearts with antibodies against MHC (green) or Tmy (green), phospho histone H3 (pH3; red) and DAPI (blue) (Scale bar = 10 µm). (C) Representative transverse sections through the cardiac tissue of a DMSO-treated and an explant treated with NSC-87877 beginning at stage 29, and stained with antibodies against phospho-histone H3 (pH3, red), and Tmy (green), as assessed at stage 37 (Scale bar = 200 µm). (D) Cardiac

mitotic index of explants treated beginning at stage 29 with DMSO (blue bar) or NSC-87877 (magenta bar) and assessed at stage 37. Bars represent the mean mitotic index of 4 explants per condition. Error bars denote the standard deviation. * denotes a statistically significant reduction in mitotic index of NSC-87877 treated explants (P = 0.0021).
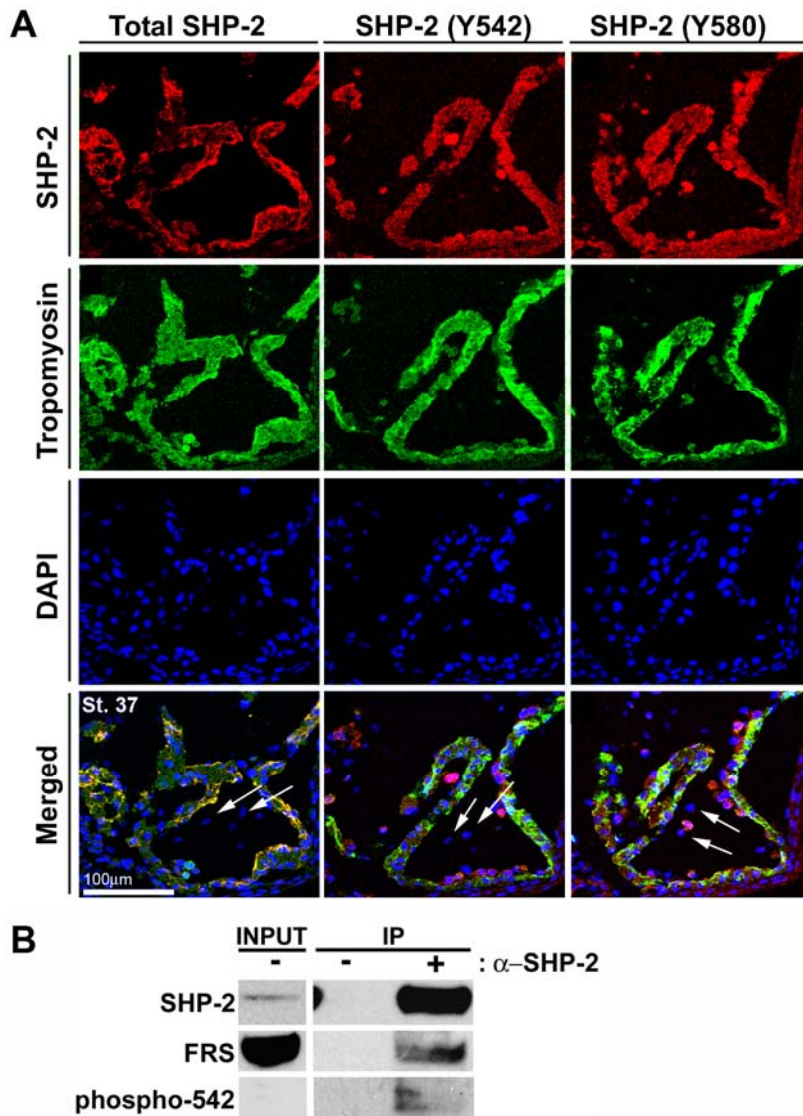
Figure 2.7. SHP-2 is phosphorylated and interacts with FRS in vivo.

(A) Transverse cryosections through the heart of control embryos stained with tropomyosin to mark cardiac tissue (Tmy; green), DAPI, to mark cell nuclei (blue), and anti-total SHP-2, anti-phospho-542 SHP-2 or anti-phospho-580 SHP-2 (all shown in red). Arrows denote endocardial cells that are negative for SHP-2. (All samples from stage 37, scale bars=100 μm). (B) SHP-2 interacts with FRS in vivo. Hearts from FL-HA-SHP-2 derived embryos were dissected at stage 35 and immunoprecipitated with an anti-SHP-2 antibody (+) or beads

with no antibody (-).Western analysis was then performed using antibodies specific for total

SHP-2, phospho-542 SHP-2 and FRS-2. Note the level of SHP-2 phopho-542 in input was

below levels of detection.

A

	Tbx5	Tbx20	Nkx2.5	MHC	BF
Control			St. 37		St. 37
SU5402					

B

Nkx2.5 | Tbx5

	DMSO	SU5402	DMSO	SU5402
Control				
SHP-2 N308D	St. 37			

C

	DMSO		NSC	
	Cont.	N308D	Cont.	N308D
pERK				
Total ERK				
α Tubulin				

D

	DMSO	SU5402
pERK		
Total ERK		
α Tubulin		

E

IP | IB

	MBS	SU5402		MBS	SU5402
SHP-2			SHP-2		
FRS			pERK		
P-542					

57
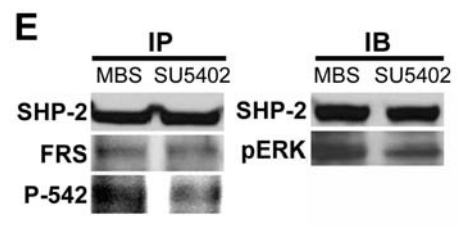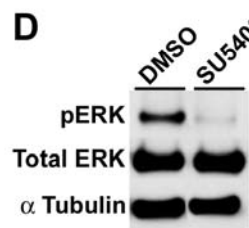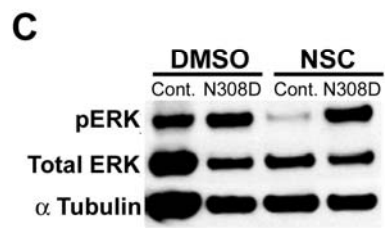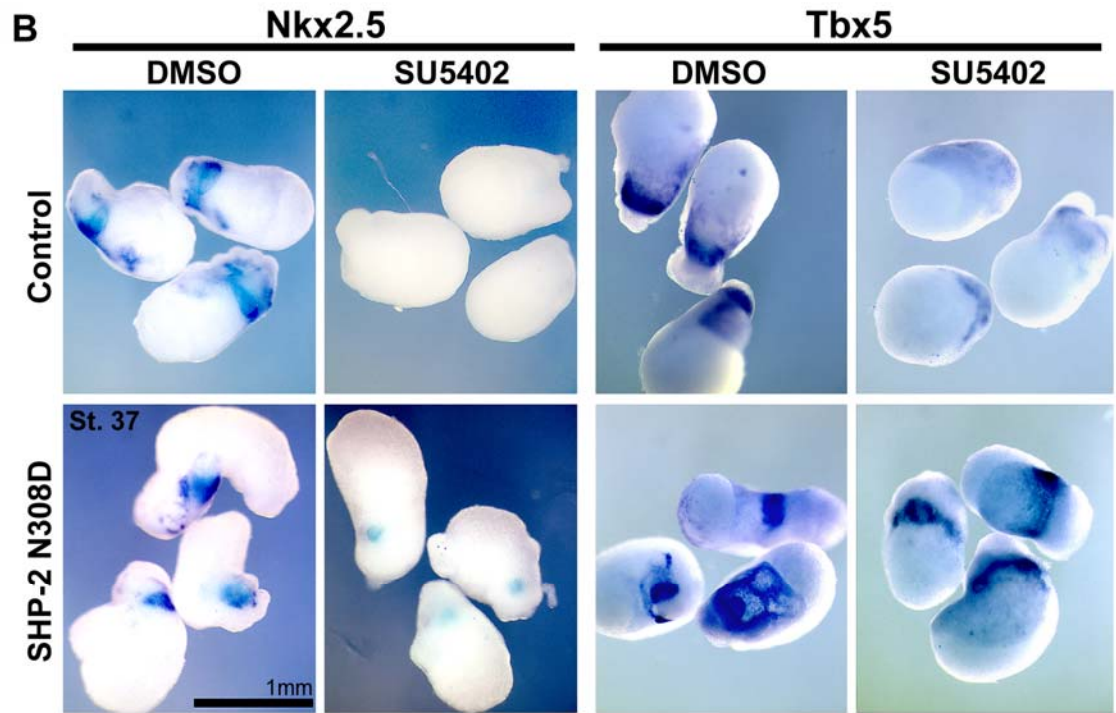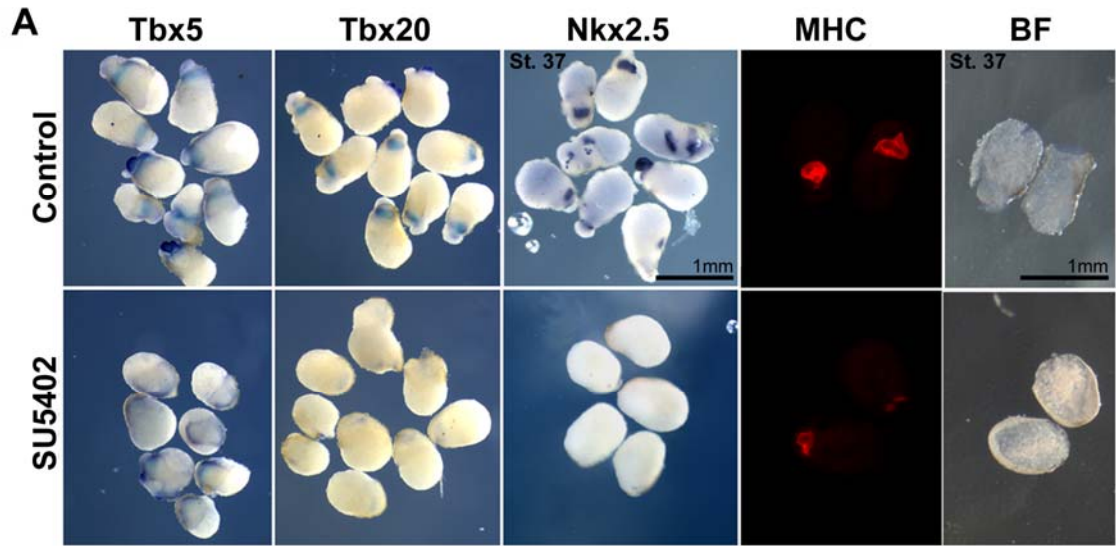
Figure 2.8. FGF functions through SHP-2 to maintain the cardiac lineage.

(A) Whole mount in situ hybridization for *Tbx5*, *Tbx20,* and *Nkx2.5* or whole mount

immunostaining for MHC (red) performed on explants treated with DMSO or the FGFR1

inhibitor SU5402 (Scale bars = 1 mm). (B) Explants isolated from uninjected (Control) or

SHP-2 N308D injected embryos cultured in DMSO or SU5402 and analyzed by in situ

hybridization for the cardiac markers *Nkx2.5* and *Tbx5* (Scale bar = 1 mm). (C, D) Western

blot analysis of DMSO, NSC-87877 (C) or SU5402 (D) treated explants for phosphorylated

and total ERK; α-tubulin is used as a loading control. (E) Explants were cut at stage 22 and

then incubated in either modified Barth's solution (MBS) or SU5402 until stage 35. Either

endogenous SHP-2 was immunoprecipitated (IP) or explants were lysed (IB) and western

analysis performed as in (Fig. 2.7B).
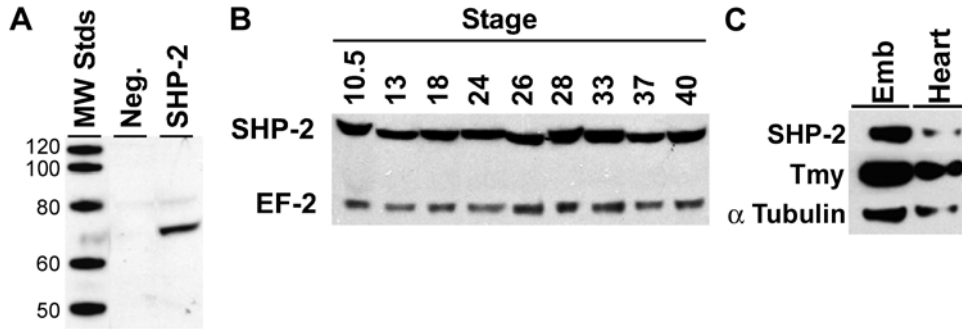
Supplemental Figure 2.1. SHP-2 is expressed in during early *Xenopus* development.

(A) Western blot of *in vitro* translated *Xenopus* SHP-2 in the sense orientation or anti-sense

orientation (Neg.) probed with an anti-SHP-2 antibody. (B) Western blot analysis of early

Xenopus embryogenesis at stages 10.5 (gastrula) through stage 40 (late tadpole) with a SHP-

2 specific antibody. Anti-EF-2 was used as a loading control. (C) Western blot analysis of

SHP-2 and Tmy in whole embryos and isolated heart tissue from stage 37 embryos with α-

tubulin as the loading control.
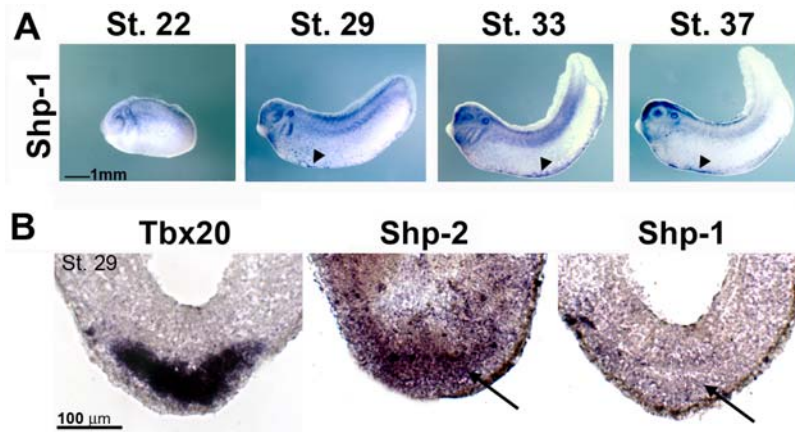
Supplemental Figure 2.2. *Shp-1* **expression in the** *Xenopus***.**

(A) Whole mount in situ hybridization of uninjected embryos at stages 22-37 with a *Shp-1* specific probe (Scale bars= 1mm; anterior is positioned to the left, posterior to the right). We observe that similar to studies of *Shp-1* expression in mice, *Xenopus Shp-1* expression is observed in the developing hematopoetic lineage; arrowheads in panels of stage 29, 33 and 37 embryos. (B) In situ hybridization of transverse serial sections through a stage 29 *Xenopus* heart with probes against *Tbx20*, *Shp-2*, and *Shp-1* with *Shp-1* being the most anterior section followed by *Tbx20* and *Shp-2* with arrow pointing to corresponding *Tbx20* positive tissue in adjacent sections (Scale bar=100μm).
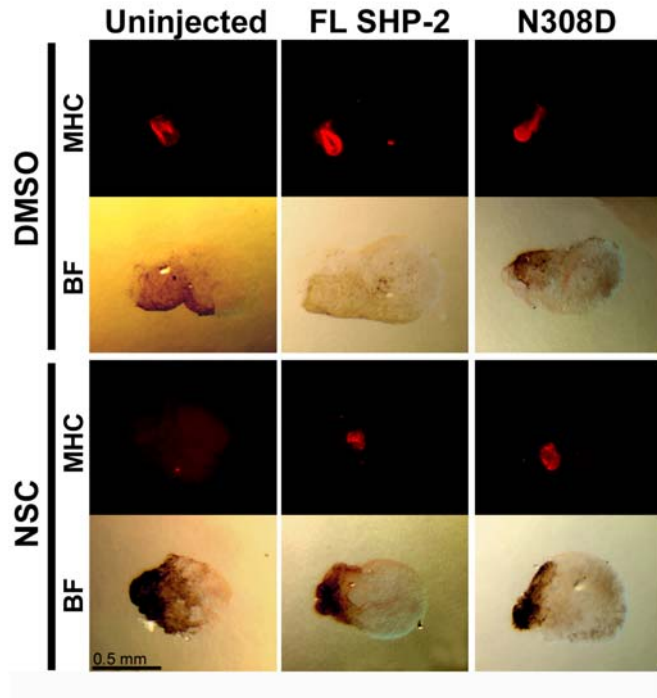
Supplemental Figure 2.3. *Shp-2* **rescues expression of cardiac tissue in a dose dependent manner.**

Whole mount antibody staining of cardiac explants derived from either uninjected embryos or embryos injected with 1ng of FL-*Shp2* or *Shp-2* N308D. Embryos shown at stage 37 stained with an antibody against myosin heavy chain (MHC; shown in red; anterior positioned to the left and dorsal to the top, scale bar=0.5mm).
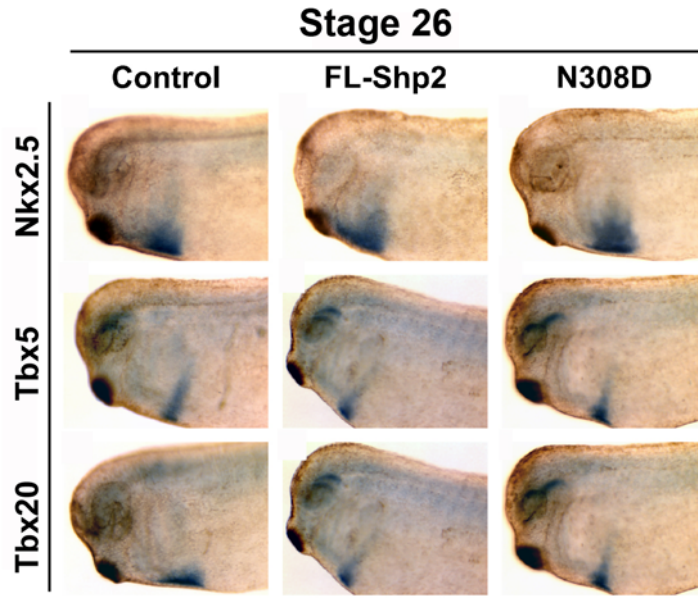
Supplemental Figure 2.4. *Shp-2* **N308D does not block cardiac commitment, migration or fusion.**

Whole mount in situ hybridization of control, full length *Shp-2* injected, or *Shp-2 N308D* injected embryos at stage 26 with cardiac specific probes *Nkx2.5*, *Tbx5*, or *Tbx20*.
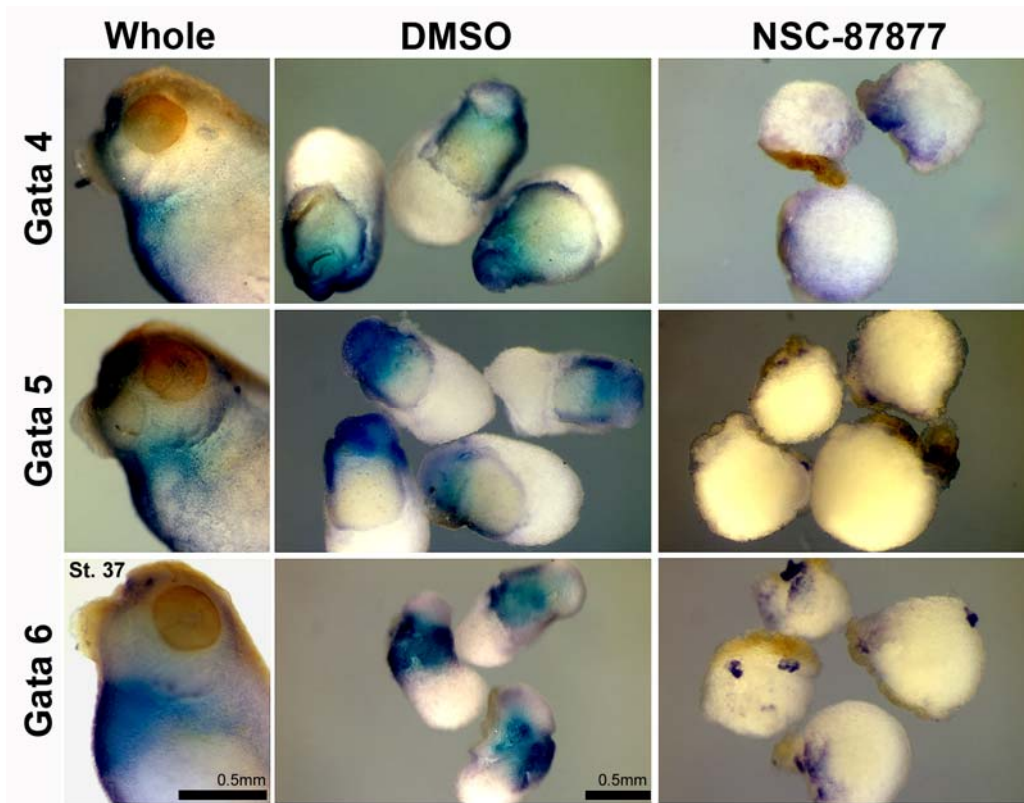
Supplemental Figure 2.5. *Gata 4*, *5*, and *6* expression in SHP-2 inhibited explants.

Whole embryo controls (whole) and cardiac explants were isolated at stage 22 and cultured until stage 37 in DMSO or NSC-87877. In situ hybridization was performed on explants with *Gata4, Gata5* and *Gata6* (Scale bars=0.5mm).
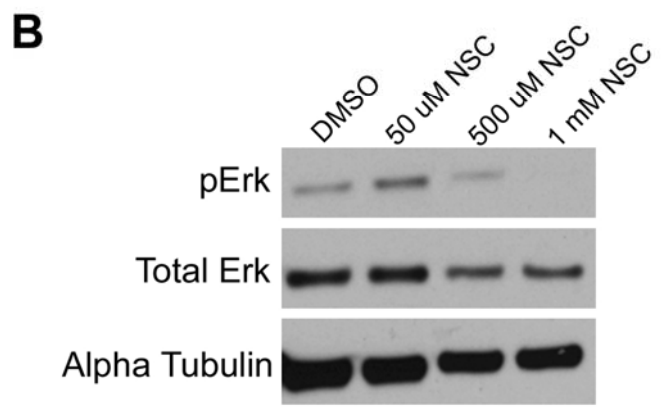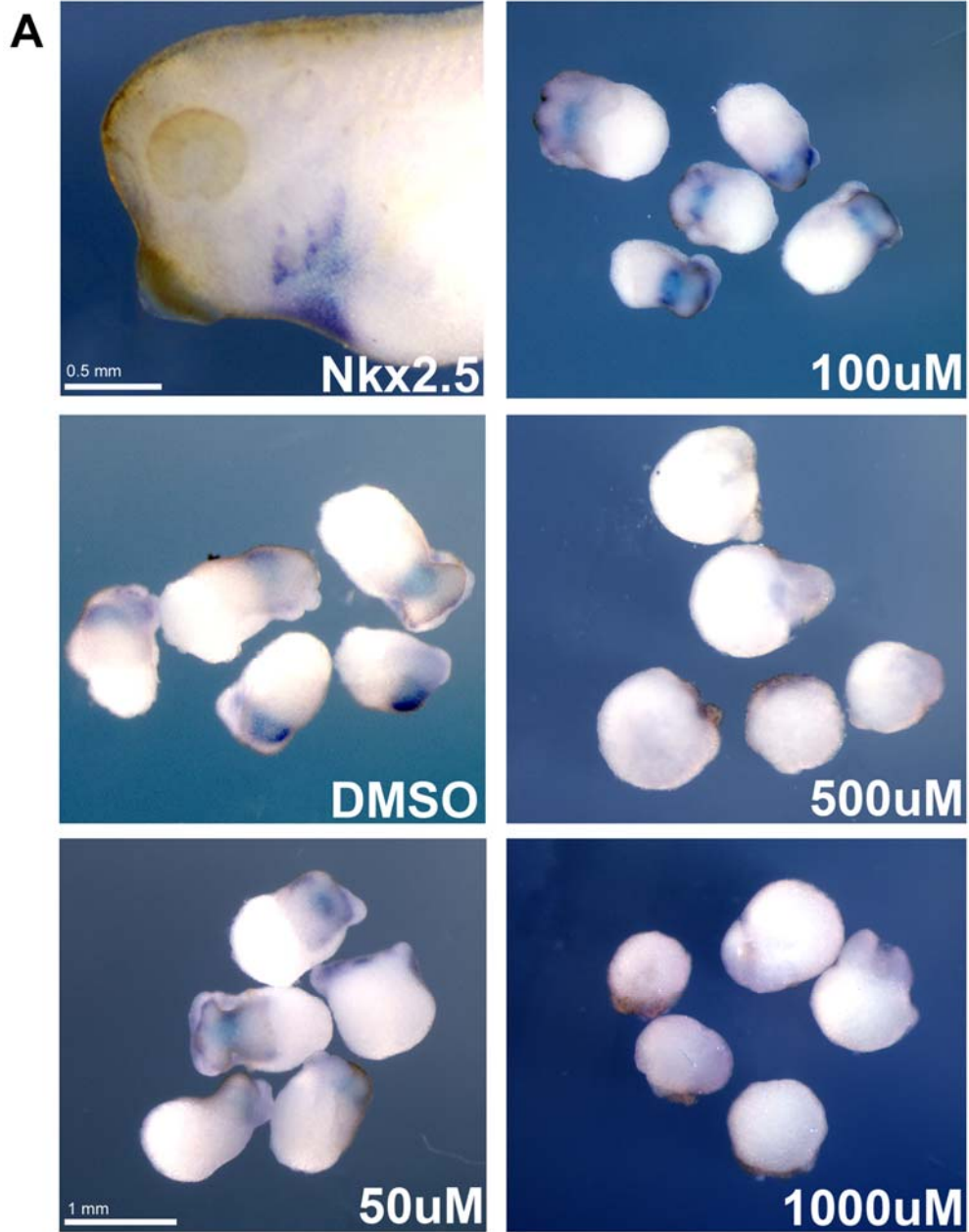
Supplemental Figure 2.6. Dose response of the SHP-2 inhibitor NSC-87877.

(A) Whole mount in situ analysis of whole embryo and cardiac explants with a *Nkx2.5* specific probe. All explants were removed and treated at stage 22 and cultured in either carrier (DMSO) with the respective dose of NSC-87877 until stage 37. Upper left-hand panel shows a representative *Nkx2.5* in situ of a stage 37 embryo (Scale bars=0.5mm for whole embryo and 1mm for explants). (B) Western blot analysis of active and total ERK in cardiac explants cultured in DMSO or increasing doses of NSC-87877 until stage 37 with alpha actin used as a loading control.

References

Alexander, J., Rothenberg, M., Henry, G. L. and Stainier, D. Y. (1999). casanova plays an early and essential role in endoderm formation in zebrafish. *Dev Biol* **215**, 343-57.

Alexiades, M. R. and Cepko, C. (1996). Quantitative analysis of proliferation and cell cycle length during development of the rat retina. *Dev Dyn* **205**, 293-307.

Allanson, J. (2002). The first Noonan syndrome gene: PTPN11, which encodes the protein tyrosine phosphatase SHP-2. *Pediatr Res* **52**, 471.

Alsan, B. H. and Schultheiss, T. M. (2002). Regulation of avian cardiogenesis by Fgf8 signaling. *Development* **129**, 1935-43.

Araki, T., Mohi, M. G., Ismat, F. A., Bronson, R. T., Williams, I. R., Kutok, J. L., Yang, W., Pao, L. I., Gilliland, D. G., Epstein, J. A. et al. (2004). Mouse model of Noonan syndrome reveals cell type- and gene dosage-dependent effects of Ptpn11 mutation. *Nat Med* **10**, 849-57.

Bjorbaek, C., Buchholz, R. M., Davis, S. M., Bates, S. H., Pierroz, D. D., Gu, H., Neel, B. G., Myers, M. G., Jr. and Flier, J. S. (2001). Divergent roles of SHP-2 in ERK activation by leptin receptors. *J Biol Chem* **276**, 4747-55.

Brown, D. D., Binder, O., Pagratis, M., Parr, B. A. and Conlon, F. L. (2003). Developmental expression of the Xenopus laevis Tbx20 orthologue. *Dev Genes Evol* **212**, 604-7.

Brown, D. D., Martz, S. N., Binder, O., Goetz, S. C., Price, B. M. J., Smith, J. C. and Conlon, F. L. (2005). Tbx5 and Tbx20 act synergistically to control vertebrate heart morphogenesis. *Development* **132**, 553-563.

Brown, D. D., S., C. K., Showell, C. and Conlon, F. L. (2007). The small heat shock protein Hsp27 is required for proper heart tube formation. *Genesis* **In Press**.

Bruneau, B. G., Nemer, G., Schmitt, J. P., Charron, F., Robitaille, L., Caron, S., Conner, D. A., Gessler, M., Nemer, M., Seidman, C. E. et al. (2001). A Murine Model of Holt-Oram Syndrome Defines Roles of the T-Box Transcription Factor Tbx5 in Cardiogenesis and Disease. *Cell* **106**, 709-721.

Cai, C. L., Zhou, W., Yang, L., Bu, L., Qyang, Y., Zhang, X., Li, X., Rosenfeld, M. G., Chen, J. and Evans, S. (2005). T-box genes coordinate regional rates of proliferation and regional specification during cardiogenesis. *Development* **132**, 2475-87.

Chan, R. J., Li, Y., Hass, M. N., Walter, A., Voorhorst, C. S., Shelley, W. C., Yang, Z., Orschell, C. M. and Yoder, M. C. (2006). Shp-2 heterozygous hematopoietic stem cells have deficient repopulating ability due to diminished self-renewal. *Exp Hematol* **34**, 1230-9.

Chen, L., Sung, S. S., Yip, M. L., Lawrence, H. R., Ren, Y., Guida, W. C., Sebti, S. M., Lawrence, N. J. and Wu, J. (2006). Discovery of a novel shp2 protein tyrosine phosphatase inhibitor. *Mol Pharmacol* **70**, 562-70.

Christofori, G. (2003). Split personalities: the agonistic antagonist Sprouty. *Nat Cell Biol* **5**, 377-9.

Costa, R. M., Mason, J., Lee, M., Amaya, E. and Zorn, A. M. (2003). Novel gene expression domains reveal early patterning of the Xenopus endoderm. *Gene Expr Patterns* **3**, 509-19.

Dale, L. and Slack, J. M. (1987). Fate map for the 32-cell stage of Xenopus laevis. *Development* **99**, 527-51.

Dasso, M. and Newport, J. W. (1990). Completion of DNA replication is monitored by a feedback system that controls the initiation of mitosis in vitro: studies in Xenopus. *Cell* **61**, 811-23.

Dehaan, R. L. (1963). Migration patterns of the precardiac mesoderm in the early chick embrvo. *Exp Cell Res* **29**, 544-60.

Delahaye, L., Rocchi, S. and Van Obberghen, E. (2000). Potential involvement of FRS2 in insulin signaling. *Endocrinology* **141**, 621-8.

Dyer, M. A. and Cepko, C. L. (2001). Regulating proliferation during retinal development. *Nat Rev Neurosci* **2**, 333-42.

Feng, G. S. (1999). Shp-2 tyrosine phosphatase: signaling one cell or many. *Exp Cell Res* **253**, 47-54.

Fishman, M. C. and Chien, K. R. (1997). Fashioning the vertebrate heart: earliest embryonic decisions. *Development* **124**, 2099-2117.

Georgescu, M. M., Kirsch, K. H., Kaloudis, P., Yang, H., Pavletich, N. P. and Hanafusa, H. (2000). Stabilization and productive positioning roles of the C2 domain of PTEN tumor suppressor. *Cancer Res* **60**, 7033-8.

Goetz, S. and Conlon, F. L. (2007). Cardiac Progenitors and the Embryonic Cell Cycle. *Cell Cycle* **In Press**.

Goetz, S. C., Brown, D. D. and Conlon, F. L. (2006). TBX5 is required for embryonic cardiac cell cycle progression. *Development* **133**, 2575-84.

Gove, C., Walmsley, M., Nijjar, S., Bertwistle, D., Guille, M., Partington, G., Bomford, A. and Patient, R. (1997). Over-expression of GATA-6 in Xenopus embryos blocks differentiation of heart precursors. *Embo J* **16**, 355-68.

Grossel, M. J. and Hinds, P. W. (2006). From cell cycle to differentiation: an expanding role for cdk6. *Cell Cycle* **5**, 266-70.

Guillemot, L., Levy, A., Zhao, Z. J., Bereziat, G. and Rothhut, B. (2000). The protein-tyrosine phosphatase SHP-2 is required during angiotensin II-mediated activation of cyclin D1 promoter in CHO-AT1A cells. *J Biol Chem* **275**, 26349-58.

Hanafusa, H., Torii, S., Yasunaga, T., Matsumoto, K. and Nishida, E. (2004). Shp2, an SH2-containing protein-tyrosine phosphatase, positively regulates receptor tyrosine kinase signaling by dephosphorylating and inactivating the inhibitor Sprouty. *J Biol Chem* **279**, 22992-5.

Harland, R. M. (1991). In situ hybridization: an improved whole mount method for Xenopus embryos. *Meth. Cell Biol.* **36**, 675-685.

Harris, W. A. and Hartenstein, V. (1991). Neuronal determination without cell division in Xenopus embryos. *Neuron* **6**, 499-515.

Harvey, R. P., Lai, D., Elliott, D., Biben, C., Solloway, M., Prall, O., Stennard, F., Schindeler, A., Groves, N., Lavulo, L. et al. (2002). Homeodomain factor Nkx2-5 in heart development and disease. *Cold Spring Harb Symp Quant Biol* **67**, 107-14.

Hensey, C. and Gautier, J. (1998). Programmed cell death during Xenopus development: a spatio-temporal analysis. *Dev Biol* **203**, 36-48.

Horb, M. E. and Thomsen, G. H. (1999). Tbx5 is essential for heart development. *Development* **126**, 1739-1751.

House, S. L., Branch, K., Newman, G., Doetschman, T. and Schultz Jel, J. (2005). Cardioprotection induced by cardiac-specific overexpression of fibroblast growth factor-2 is mediated by the MAPK cascade. *Am J Physiol Heart Circ Physiol* **289**, H2167-75.

Huebert, R. C., Li, Q., Adhikari, N., Charles, N. J., Han, X., Ezzat, M. K., Grindle, S., Park, S., Ormaza, S., Fermin, D. et al. (2004). Identification and regulation of Sprouty1, a negative inhibitor of the ERK cascade, in the human heart. *Physiol Genomics* **18**, 284-9.

Ilagan, R., Abu-Issa, R., Brown, D., Yang, Y. P., Jiao, K., Schwartz, R. J., Klingensmith, J. and Meyers, E. N. (2006). Fgf8 is required for anterior heart field development. *Development* **133**, 2435-45.

Inui, M. and Asashima, M. (2006). A novel gene, Ami is expressed in vascular tissue in Xenopus laevis. *Gene Expr Patterns* **6**, 613-9.

Jarvis, L. A., Toering, S. J., Simon, M. A., Krasnow, M. A. and Smith-Bolton, R. K. (2006). Sprouty proteins are in vivo targets of Corkscrew/SHP-2 tyrosine phosphatases. *Development* **133**, 1133-42.

Jiang, Y. and Evans, T. (1996). The Xenopus GATA-4/5/6 genes are associated with cardiac specification and can regulate cardiac-specific transcription during embryogenesis. *Dev Biol* **174**, 258-70.

Jiang, Z. S., Padua, R. R., Ju, H., Doble, B. W., Jin, Y., Hao, J., Cattini, P. A., Dixon, I. M. and Kardami, E. (2002). Acute protection of ischemic heart by FGF-2: involvement of FGF-2 receptors and protein kinase C. *Am J Physiol Heart Circ Physiol* **282**, H1071-80.

Jiang, Z. S., Srisakuldee, W., Soulet, F., Bouche, G. and Kardami, E. (2004). Non-angiogenic FGF-2 protects the ischemic heart from injury, in the presence or absence of reperfusion. *Cardiovasc Res* **62**, 154-66.

Kattman, S. J., Huber, T. L. and Keller, G. M. (2006). Multipotent flk-1+ cardiovascular progenitor cells give rise to the cardiomyocyte, endothelial, and vascular smooth muscle lineages. *Dev Cell* **11**, 723-32.

Kim, T. G., Chen, J., Sadoshima, J. and Lee, Y. (2004). Jumonji represses atrial natriuretic factor gene expression by inhibiting transcriptional activities of cardiac transcription factors. *Mol Cell Biol* **24**, 10151-60.

Kolker, S., Tajchman, U. and Weeks, D. L. (2000). Confocal Imaging of early heat development in Xenopus laevis. *Dev. Biol.* **218**, 64-73.

Kouhara, H., Hadari, Y. R., Spivak-Kroizman, T., Schilling, J., Bar-Sagi, D., Lax, I. and Schlessinger, J. (1997). A lipid-anchored Grb2-binding protein that links FGF-receptor activation to the Ras/MAPK signaling pathway. *Cell* **89**, 693-702.

Kouskoff, V., Lacaud, G., Schwantz, S., Fehling, H. J. and Keller, G. (2005). Sequential development of hematopoietic and cardiac mesoderm during embryonic stem cell differentiation. *Proc Natl Acad Sci U S A* **102**, 13170-5.

Kupperman, E., An, S., Osborne, N., Waldron, S. and Stainier, D. Y. (2000). A sphingosine-1-phosphate receptor regulates cell migration during vertebrate heart development. *Nature* **406**, 192-5.

Lathrop, B., Thomas, K. and Glaser, L. (1985). Control of myogenic differentiation by fibroblast growth factor is mediated by position in the G1 phase of the cell cycle. *J Cell Biol* **101**, 2194-8.

Li, L. and Vaessin, H. (2000). Pan-neural Prospero terminates cell proliferation during Drosophila neurogenesis. *Genes Dev* **14**, 147-51.

Lu, X., Borchers, A. G., Jolicoeur, C., Rayburn, H., Baker, J. C. and Tessier-Lavigne, M. (2004). PTK7/CCK-4 is a novel regulator of planar cell polarity in vertebrates. *Nature* **430**, 93-8.

Lyons, I., et al. (1995). Myogenic and morphogenic defects in the heart tubes of murine embrryos lacking the homeobox gene Nkx-2.5. *Genes Dev.* **9**, 1654-1666.

Maheshwari, M., Belmont, J., Fernbach, S., Ho, T., Molinari, L., Yakub, I., Yu, F., Combes, A., Towbin, J., Craigen, W. J. et al. (2002). PTPN11 mutations in Noonan syndrome type I: detection of recurrent mutations in exons 3 and 13. *Hum Mutat* **20**, 298-304.

Mason, H. S., Latten, M. J., Godoy, L. D., Horowitz, B. and Kenyon, J. L. (2002). Modulation of Kv1.5 currents by protein kinase A, tyrosine kinase, and protein tyrosine phosphatase requires an intact cytoskeleton. *Mol Pharmacol* **61**, 285-93.

Mills, K. R., Kruep, D. and Saha, M. S. (1999). Elucidating the origins of the vascular system: a fate map of the vascular endothelial and red blood cell lineages in Xenopus laevis. *Dev Biol* **209**, 352-68.

Molkentin, J. D., Lin, Q., Duncan, S. A. and Olson, E. N. (1997). Requirement of the transcription factor GATA4 for heart tube formation and ventral morphogenesis. *Genes Dev* **11**, 1061-72.

Moody, S. A. (1987). Fates of the blastomeres of the 32 cell *Xenopus* embryo. *Dev. Biol.* **122**, 300-319.

Moretti, A., Caron, L., Nakano, A., Lam, J. T., Bernshausen, A., Chen, Y., Qyang, Y., Bu, L., Sasaki, M., Martin-Puig, S. et al. (2006). Multipotent embryonic isl1+ progenitor cells lead to cardiac, smooth muscle, and endothelial cell diversification. *Cell* **127**, 1151-65.

Nguyen, L., Besson, A., Roberts, J. M. and Guillemot, F. (2006). Coupling cell cycle exit, neuronal differentiation and migration in cortical neurogenesis. *Cell Cycle* **5**, 2314-8.

Nieuwkoop, P. D. and Faber, J. (1975). Normal Table of *Xenopus laevis* (Daudin). Amsterdam: North Holland.

Noonan, J. and O'Connor, W. (1996). Noonan syndrome: a clinical description emphasizing the cardiac findings. *Acta Paediatr Jpn* **38**, 76-83.

Palmen, M., Daemen, M. J., De Windt, L. J., Willems, J., Dassen, W. R., Heeneman, S., Zimmermann, R., Van Bilsen, M. and Doevendans, P. A. (2004). Fibroblast growth factor-1 improves cardiac functional recovery and enhances cell survival after ischemia and reperfusion: a fibroblast growth factor receptor, protein kinase C, and tyrosine kinase-dependent mechanism. *J Am Coll Cardiol* **44**, 1113-23.

Parmacek, M. S. and Epstein, J. A. (2005). Pursuing cardiac progenitors: regeneration redux. *Cell* **120**, 295-8.

Pasumarthi, K. B. and Field, L. J. (2002). Cardiomyocyte cell cycle regulation. *Circ Res* **90**, 1044-54.

Pawson, T. (1994). Tyrosine kinase signalling pathways. *Princess Takamatsu Symp* **24**, 303-22.

Qu, C. K. (2000). The SHP-2 tyrosine phosphatase: signaling mechanisms and biological functions. *Cell Res* **10**, 279-88.

Raffin, M., Leong, L. M., Rones, M. S., Sparrow, D., Mohun, T. and Mercola, M. (2000). Subdivision of the cardiac Nkx2.5 expression domain into myogenic and nonmyogenic compartments. *Dev Biol* **218**, 326-40.

Reiter, J. F., Alexander, J., Rodaway, A., Yelon, D., Patient, R., Holder, N. and Stainier, D. Y. (1999). Gata5 is required for the development of the heart and endoderm in zebrafish. *Genes Dev* **13**, 2983-95.

Saga, Y., Miyagawa-Tomita, S., Takagi, A., Kitajima, S., Miyazaki, J. and Inoue, T. (1999). MesP1 is expressed in the heart precursor cells and required for the formation of a single heart tube. *Development* **126**, 3437-47.

Sater, A. K. and Jacobson, A. G. (1989). The specification of heart mesoderm occurs during gastrulation in Xenopus laevis. *Development* **105**, 821-30.

Schollen, E., Matthijs, G., Gewillig, M., Fryns, J. P. and Legius, E. (2003). PTPN11 mutation in a large family with Noonan syndrome and dizygous twinning. *Eur J Hum Genet* **11**, 85-8.

Singh, M. K., Christoffels, V. M., Dias, J. M., Trowe, M. O., Petry, M., Schuster-Gossler, K., Burger, A., Ericson, J. and Kispert, A. (2005). Tbx20 is essential for cardiac chamber differentiation and repression of Tbx2. *Development* **132**, 2697-707.

Smith, J. C. and Slack, J. M. W. (1983). Dorsalization and neural induction: properties of the organizer in *Xenopus laevis*. *J. Embryol. Exp. Morph.* **78**, 299-317.

Srivastava, D. (2006). Making or breaking the heart: from lineage determination to morphogenesis. *Cell* **126**, 1037-48.

Stennard, F. A., Costa, M. W., Lai, D., Biben, C., Furtado, M. B., Solloway, M. J., McCulley, D. J., Leimena, C., Preis, J. I., Dunwoodie, S. L. et al. (2005). Murine T-box transcription factor Tbx20 acts as a repressor during heart development, and is essential for adult heart integrity, function and adaptation. *Development* **132**, 2451-62.

Takeuchi, J. K., Mileikovskaia, M., Koshiba-Takeuchi, K., Heidt, A. B., Mori, A. D., Arruda, E. P., Gertsenstein, M., Georges, R., Davidson, L., Mo, R. et al. (2005). Tbx20 dose-dependently regulates transcription factor networks required for mouse heart and motoneuron development. *Development* **132**, 2463-74.

Tang, T. L., Freeman, R. M., Jr., O'Reilly, A. M., Neel, B. G. and Sokol, S. Y. (1995). The SH2-containing protein-tyrosine phosphatase SH-PTP2 is required upstream of MAP kinase for early Xenopus development. *Cell* **80**, 473-83.

Tartaglia, M., Kalidas, K., Shaw, A., Song, X., Musat, D. L., van der Burgt, I., Brunner, H. G., Bertola, D. R., Crosby, A., Ion, A. et al. (2002). PTPN11 mutations in Noonan

syndrome: molecular spectrum, genotype-phenotype correlation, and phenotypic heterogeneity. *Am J Hum Genet* **70**, 1555-63.

Tartaglia, M., Mehler, E. L., Goldberg, R., Zampino, G., Brunner, H. G., Kremer, H., van der Burgt, I., Crosby, A. H., Ion, A., Jeffery, S. et al. (2001). Mutations in PTPN11, encoding the protein tyrosine phosphatase SHP-2, cause Noonan syndrome. *Nat Genet* **29**, 465-8.

Tonissen, K. F., Drysdale, T. A., Lints, T. J., Harvey, R. P. and Krieg, P. A. (1994). XNkx-2.5, a Xenopus gene related to Nkx-2.5 and tinman: evidence for a conserved role in cardiac development. *Dev. Biol.* **162**, 325-328.

Trinh, L. A. and Stainier, D. Y. (2004). Fibronectin regulates epithelial organization during myocardial migration in zebrafish. *Dev Cell* **6**, 371-82.

Tsang, M. and Dawid, I. B. (2004). Promotion and attenuation of FGF signaling through the Ras-MAPK pathway. *Sci STKE* **2004**, pe17.

van den Hoff, M. J., Kruithof, B. P. and Moorman, A. F. (2004). Making more heart muscle. *Bioessays* **26**, 248-61.

Van Vactor, D., O'Reilly, A. M. and Neel, B. G. (1998). Genetic analysis of protein tyrosine phosphatases. *Curr Opin Genet Dev* **8**, 112-26.

Vernon, A. E. and Philpott, A. (2003). A single cdk inhibitor, p27Xic1, functions beyond cell cycle regulation to promote muscle differentiation in Xenopus. *Development* **130**, 71-83.

Walsh, K. and Perlman, H. (1997). Cell cycle exit upon myogenic differentiation. *Curr Opin Genet Dev* **7**, 597-602.

Warkman, A. S. and Krieg, P. A. (2006). Xenopus as a model system for vertebrate heart development. *Semin Cell Dev Biol*.

Wu, S. M., Fujiwara, Y., Cibulsky, S. M., Clapham, D. E., Lien, C. L., Schultheiss, T. M. and Orkin, S. H. (2006). Developmental origin of a bipotential myocardial and smooth muscle cell precursor in the mammalian heart. *Cell* **127**, 1137-50.

Yang, W., Klaman, L. D., Chen, B., Araki, T., Harada, H., Thomas, S. M., George, E. L. and Neel, B. G. (2006). An Shp2/SFK/Ras/Erk signaling pathway controls trophoblast stem cell survival. *Dev Cell* **10**, 317-27.

Yuan, L., Yu, W. M., Xu, M. and Qu, C. K. (2005). SHP-2 phosphatase regulates DNA damage-induced apoptosis and G2/M arrest in catalytically dependent and independent manners, respectively. *J Biol Chem* **280**, 42701-6.

Yuan, L., Yu, W. M., Yuan, Z., Haudenschild, C. C. and Qu, C. K. (2003). Role of SHP-2 tyrosine phosphatase in the DNA damage-induced cell death response. *J Biol Chem* **278**, 15208-16.

Zhang, J., Somani, A. K. and Siminovitch, K. A. (2000). Roles of the SHP-1 tyrosine phosphatase in the negative regulation of cell signalling. *Semin Immunol* **12**, 361-78.

CHAPTER 3

An Evolutionarily Conserved Role for SHP-2 Signaling in Early Heart Development

PREFACE TO CHAPTER 3

Chapter 3 describes the effects of the Noonan associated mutation *Shp-2* N308D on cardiac development. Previously, it has been shown that patients with Noonan syndrome have mutations in the protein phosphatase SHP-2 (Tartaglia et al., 2001). The most prevalent mutation of the Noonan associated mutations is *Shp-2* N308D with this mutation accounting for one third of all affected individuals (Musante et al., 2003). In this chapter we test the hypothesis that *Shp-2* N308D has a direct effect on heart development. This work was performed in collaboration with a former undergraduate in the lab, Jennifer Duddy.

Summary

Noonan syndrome is one of the most common causes of human congenital heart disease and is frequently associated with mis-sense mutations in the protein phosphatase *Shp-2*. A second subset of mis-sense mutations in *Shp-2* is associated with leukemia, thus suggesting a genotype-phenotype relationship between *Shp-2* mis-sense mutations and disease states. To establish the relationship between *Shp-2* mis-sense mutations and phenotypic abnormalities, and to identify the cellular and molecular pathways through which Noonan syndrome associated *Shp-2* mutations act, we introduced mRNAs encoding the most prevalent Noonan syndrome and leukemia associated *Shp-2* mutations into *Xenopus* embryos. The resulting embryos show a direct relationship between a Noonan *Shp-2* mutation and its ability to cause cardiac defects in *Xenopus*; the Noonan mutation leads to a morphologically abnormal heart whereas the leukemic associated mutation does not. Using this animal model, we have conducted a detailed phenotypic analysis and generated a 3D molecular model of the *Xenopus* hearts derived from the introduction of the Noonan mutation. Our findings strongly suggest that heart defects associated with Noonan mutations are associated with transient lengthening of the cardiac cell cycle and are associated with an increase in the mitotic index and an increase in S-phase associated proteins. In addition, we observe alterations in heart morphology. We further show that SHP-2 enzymatic activity is required for these cardiac defects, and that the abnormalities are associated with an elevation in both active ERK and active MEK, known mediators of SHP-2 signaling. Collectively these studies suggest that SHP-2 Noonan mutations lead to a MAPK-associated mis-regulation of embryonic cardiac cell cycle progression.

75

Introduction

Noonan syndrome is one of the most common causes of congenital heart disease. The disorder leads to a number of cardiac developmental abnormalities including atrial septal defects, ventricular septal defects, pulmonary stenosis and hypertrophic cardiomyopathy (Noonan, 1968; Noonan, 1994). It was recently shown that Noonan syndrome is associated with mis-sense mutations in *Shp-2* in approximately half of affected individuals (Kosaki et al., 2002; Maheshwari et al., 2002; Tartaglia et al., 2002; Tartaglia et al., 2001). *Shp-2* mis-sense mutations are associated with a gain of function and are thought to result in prolonged activation of downstream signaling pathways (Tartaglia et al., 2001). Interestingly, people with acute myelogenous leukemia (AML), acute lymphoblastic leukemia (ALL) and juvenile myelomonocytic leukemia (JMML) carry a second, mostly mutually exclusive, somatically introduced subset of mis-sense mutations in *Shp-2*, strongly suggesting a genotype-phenotype relationship between *Shp-2* mis-sense mutations and a disease state (Bentires-Alj et al., 2004; Kratz et al., 2005; Loh et al., 2004; Musante et al., 2003; Tartaglia et al., 2003). However, the cellular and biochemical basis for the role of SHP-2 in Noonan syndrome, AML, ALL, and JMML is unknown.

SHP-2 is a widely expressed non-receptor tyrosine phosphatase comprised of two tandemly arranged SH2 domains and a protein tyrosine phosphatase (PTP) domain. SHP-2 also known as SH-PTP2, Ptpn11, PTP1D, or PTP2C, is the vertebrate homologue of the Drosophila gene *corkscrew* (*Csw*). This protein is known to function genetically and biochemically downstream of a number of growth factors including epidermal growth factors (EGFs), fibroblast growth factors (FGFs), and platelet derived growth factor (PDGF) (Feng, 1999; Pawson, 1994; Qu, 2000; Van Vactor et al., 1998; Zhang et al., 2000). The sequence,

76

expression pattern and function of SHP-2 are highly conserved throughout evolution. For example, *Xenopus* and human orthologues display 94% sequence identity and, as in fly and mouse, *Xenopus Shp-2* is believed to be ubiquitously expressed (Tang et al., 1995). Moreover, a number of animal models have suggested a critical role for *Shp-2* in vertebrate development. For example, mice mutant for an internal deletion of the amino-terminal (N-SH2) domain of SHP-2 die at late gastrulation and display several mesodermal abnormalities including heart and vascular defects (Saxton et al., 1997; Saxton and Pawson, 1999; Yang et al., 2006). In addition SHP-2 mutant cells derived from homozygous mutant embryos, show SHP-2 to be required for full and sustained activation of the MAPK pathway in response to FGF, thus demonstrating SHP-2 functions downstream of the fibroblast growth factor (FGF)/MAPK pathway *in vivo* (Barford and Neel, 1998; Feng, 1999; Feng et al., 1993; Herbst et al., 1999; Saxton et al., 1997; Tang et al., 1995; Van Vactor et al., 1998; Vogel et al., 1993). Consistent with these findings, studies in *Xenopus* have shown a dominant negative form of *Xenopus Shp-2* can completely block mesoderm formation in response to both MAPK and FGF (Tang et al., 1995). Furthermore, recent reports have shown that in vitro and in tissue culture *Csw/Shp-2* can interact directly with the FGF inhibitor *sprouty* leading to *sprouty* phosphorylation and hence, rendering it inactive (Hanafusa et al., 2004; Jarvis et al., 2006). Finally, it appears that in addition to early requirements for SHP-2 signaling during development that SHP-2 is required downstream of FGF to promote cardiac cell survival (Langdon et al., 2007).

Recently it has been demonstrated in the mouse and chick that SHP-2 is required in the EGF pathway for formation of cardiac valves. However, since approximately one-third of patients with Noonan associated heart defects appear to undergo normal valvulogenesis

(Chen et al., 2000; Krenz et al., 2005), it remains unclear if SHP-2 is required downstream of other receptor tyrosine kinase receptors (RTK) for other aspects of heart development. To address if SHP-2 functions in cardiac pathways in addition to EGF and valvulogenesis, and to further characterize the evolutionarily conserved cellular and cardiac defects associated with *Shp-2* mis-sense mutations, we introduced the most prevalent human Noonan and JMML mutations into the human form of *Shp-2* (Kosaki et al., 2002; Maheshwari et al., 2002; Tartaglia et al., 2002; Tartaglia et al., 2001) and introduced these into *Xenopus*. This revealed a direct relationship between a Noonan mutation and the ability of SHP-2 to cause heart defects in *Xenopus*; the Noonan mutation leads to a morphologically abnormal heart whereas the JMML-associated mutation does not, thus demonstrating evolutionarily conserved tissue-specific effects of Noonan mutations.

Using this model, we have conducted a detailed marker analysis and molecular 3D modeling of the *Xenopus* hearts derived from the introduction of Noonan mutations versus those derived from injection of full-length SHP-2, a JMML associated mutation or control embryos. Results from these studies show that the Noonan mutation does not alter cardiac commitment or terminal differentiation but rather suggest that the mutation disrupts cell cycle progression and heart morphology. Consistent with this proposal, we observe a stage-specific increase in the cardiac mitotic index and a concomitant increase in S-phase associated proteins without an increase in programmed cell death. We further show, by mutating the SHP-2 catalytic site in the Noonan construct, that SHP-2 phosphatase activity is required *in vivo* for the effect of *Shp-2* N308D on heart tissue. In addition, we show that the cardiac defects caused by the Noonan associated mutation *Shp-2* N308D leads to an increase in levels of MEK and ERK, known signal transduction downstream mediators of SHP-2

78

activity. Collectively, these studies argue that Noonan associated mutations in *Shp-2* lead to a transient lengthening of the cell cycle and provide insights into the cellular and molecular mechanisms by which a Noonan associated *Shp-2* mutation affects cardiac tissue.

Materials and Methods

DNA Constructs

FL-SHP-2 and E76A were kindly provided by Nikola Pavletich (Georgescu et al., 2000). FL-PTP, N308D, and N308D-PTP were generated by site-directed mutagenesis (Stratagene) according to manufacturer's protocol. Primer sequences available upon request. Each construct was subcloned into an HA modified pcDNA3.1(+) vector kindly provided by Da-Zhi Wang.

Embryo Injections

Xenopus laevis embryos were fertilized in vitro and injected as previously described (Smith and Slack, 1983; Wilson and Hemmati-Brivanlou, 1995). Embryos were maintained in 0.1X Modified Barth's Serum and staged according to Nieuwkoop and Faber (Nieuwkoop and Faber, 1975). 2ng of RNA dissolved in 10nl water was injected into the one cell stage embryo unless otherwise stated.

Immunoblotting

For assays of endogenous levels of SHP-2, five whole embryos were homogenized in lysis buffer (100 mM NaCl, 20 mM NaF, 50 mM Tris pH 7.5, 10 mM Na Pyrophosphate, 5 mM EDTA, 1% NP40 and 1% Na Deoxycholate) with the addition of complete protease inhibitor cocktail (Roche) and PMSF (Sigma) and processed according to standard protocols. Anti-

mouse total SHP-2 antibody PTP1D/SHP-2 (BD Transductions Laboratories) was used to probe Western blots at 1:2500. Whole heart immunoblots were prepared from seventy dissected hearts as described above and probed with antibodies against phospho-MEK1/2 (1:1000), MEK1/2 (1:1000), p44/42 MAPK (1:1000), phospho-p44/42 MAPK (1:1000), (Cell Signaling), SLBP, (generous gift from W. Marzluff, 1:1000) (Wang et al., 1999) and PCNA (Zymed, 1:1000). Densitometry was used to standardize loading levels in western blot analysis.

Antibody Staining

Whole-mount antibody staining was performed as described (Kolker et al., 2000; Langdon et al., 2007) with anti-tropomyosin (1:50; Developmental Studies Hybridoma Bank) (Kolker et al., 2000), anti-fibrillin (1:50 Developmental Studies Hybridoma Bank) and phalloidin conjugated to Alexa 488 flourophore (1:500 Molecular Probes) and visualized on a Zeiss LSM410 confocal microscope. For immunostaining of histological sections, embryos were collected at indicated stages, fixed for 2 hours in 4% paraformaldehyde, and embedded in OCT cryosectioning medium (Tissue Tek). Cryostat sections (14um) were rinsed with wash buffer and incubated with corresponding antibodies according to (Goetz et al., 2006; Langdon et al., 2007). To calculate the mitotic index and index for program cell death, embryos at each stage were serial-sectioned through the cardiac regions and triple immuno-stained with anti-tropomyosin (Tmy) to mark cardiomyocytes, DAPI to mark cell nuclei, and either anti-phospho histone H3 (pH3) (1:200 Upstate) to mark cells in M phase or anti-caspase 3 (1:50 Pharmigen) to mark cells undergoing mitosis. All studies were carried out with a minimum of three embryos and repeated a minimum of two independent times (i.e. two independent rounds of injections).

3D Modeling

Global software a 3D reconstruction program was adapted from a program by Stephen Aylward, Remi Charrier, and Cedric Caron at the University of North Carolina. All data was collected and 3D models were created as described in Langdon, et al. (Submitted).

Microarray Analysis

Total RNA was isolated from hearts of embryos either injected with *Shp-2* N308D or FL-SHP-2 using Ambion's RiboPure kit. Isolated RNA was converted to cDNA and run on *Xenopus tropicalis* Affymetrix arrays according to standard protocols. The data was analyzed by GeneSpring GX 7.3.1.

Histology

Embryos were fixed in 2% paraformaldehyde/2.5% gluteraldehyde overnight. Embryos were then post-fixed in ferrocyanide-reduced osmium and embedded in Spurr's epoxy resin. Transverse thick (1 μm) sections were mounted on slides and stained with 1% toluidine blue in 1% sodium borate. Sections were imaged on Leica DMIRB inverted scope.

Transmission Electron Microscopy

Embryos were fixed in 2% paraformaldehyde/2.5% gluteraldehyde overnight and post-fixed in ferrocyanide-reduced osmium prior to embedding in Spurr's epoxy resin. Transverse ultrathin sections (70 μm) sections were placed on copper grids and stained first with 4% aqueous uranyl acetate followed by Reynolds' lead citrate. Sections were imaged on LEO EM-910 transmission electron microscope.

Mass Spectroscopy of *Xenopus tropicalis*

Xenopus tropicalis were anaesthetized with .025% tricane (Sigma) for 30 minutes and pre-primed with 10 units of human chorionic gonadotropin (hCG). Twenty hours later the tropicalis were anaesthetized as previously described and primed with 200 units of hCG. *Tropicalis* were place in water for one hour prior to being switched to 1X MMR. The eggs were *in vitro* fertilized according to standard protocols and 0.5ng of FL-SHP-2 RNA was dissolved in 3nl of water and injected into embryos. Control and injected embryos were collected at stage 16 and immuno-precipitation performed according to standard procedures using mouse total SHP-2 antibody PTP1D/SHP-2 (BD Transductions Laboratories) (Langdon et al., 2007). Samples were run on NuPage 4-12% Bis-tris gels (Invitrogen) and silver stained with SiverQuest (Invitrogen) according to protocols. Six bands were excised from the gel and analyzed at the Riken institute by the mass spectroscopy core facility.

Results

Shp-2 N308D but not *Shp-2* E76A leads to abnormal heart development in *Xenopus*

Noonan syndrome associated mutations in *Shp-2* result in a gain of function and occur in about half of affected individuals. Interestingly, humans with juvenile myelomonocytic leukemia (JMML) carry a second and mostly mutually exclusive somatically introduced subset of mis-sense mutations in *Shp-2* suggesting a genotype-phenotype relationship between *Shp-2* mis-sense mutations and disease states (Kosaki et al., 2002; Maheshwari et al., 2002; Tartaglia et al., 2002; Tartaglia et al., 2001). To test the relationship between specific *Shp-2* mis-sense mutations and normal heart development, we engineered into human *Shp-2* the most prevalent Noonan and JMML mutations by site-directed mutagenesis, *Shp-2* N308D and *Shp-2* E76A, respectively (Kosaki et al., 2002; Maheshwari et al., 2002;

Tartaglia et al., 2002; Tartaglia et al., 2001) (Fig. 3.1A; Note constructs used in this experiment were not epitope tagged with HA). Corresponding mRNAs were then introduced into *Xenopus* at the one cell stage. Tropomyosin staining of the resultant embryos at late tadpole stages clearly shows a direct relationship between Noonan mutations and the ability of *Shp-2* mutations to cause heart defects in *Xenopus*; Noonan mutation *Shp-2* N308D leads to a smaller heart that fails to complete looping or undergo chamber formation by stage 37 while the JMML mutation does not (Fig. 3.1C-L). These defects are confined to the cardiac tissue and we could detect no other developmental abnormalities at concentrations up to 4ng (data not shown). However, when RNA concentrations were increased to 5ng we began to observe anterior defects. Specifically we observed reduced heads and abnormal eyes (data not shown).

One explanation for the failure of the JMML mutation to result in cardiac defects could be a decrease in the efficiency of RNA translation or in RNA/protein stability. To test these possibilities, we epitope tagged all constructs with hemagglutinin (HA; Fig. 3.1A). Corresponding RNAs were injected and total protein was isolated from embryos at defined time-points during early heart development (stages 10, 16, 26). Western blot analysis of embryo extracts probed with an anti-HA or total SHP-2 antibody show no differences in protein levels between controls, Noonan or JMML constructs at any stage (Fig. 3.1B), demonstrating that neither Noonan- nor JMML-associated *Shp-2* mutations lead to RNA or protein instability *in vivo*. Collectively, these results suggest that a direct correlation exists between human Noonan associated mutations and cardiac defects in *Xenopus*.

Phenotypic analysis of Noonan associated cardiac defects

Phenotypic analysis of embryos derived from multiple rounds of injection show hearts from *Shp-2* N308D-derived stage 37 embryos to be smaller in size and morphologically abnormal compared to uninjected controls or embryos injected with a full-length *Shp-2* or *Shp-2* E76A. By stage 37 the *Shp-2* N308D-derived embryos have a range of defects with the least severely affected hearts displaying developmental delays, failure to undergo cardiac looping, and a failure to undergo chamber formation (Fig. 3.1F) while the more severely affected hearts show a substantially reduced formation of differentiated cardiac tissue (Fig. 3.1G). Thus, in *Xenopus* the affect of Noonan mutations is much more severe than that reported in humans or mice.

To examine the cardiac defects in more detail, we carried out histochemistry on control and *Shp-2* N308D hearts at stage 33 and stage 37. By stage 33, we can detect a single class of heart defects in the *Shp-2* N308D hearts relative to controls. In control hearts, by stage 33 the myocardium has fused along the ventral midline to form a bilaminar heart tube, while *Shp-2* N308D-derived hearts are delayed in dorsal closure and remain as an open cardiac trough (Fig. 3.1 H,I). We note that, as with controls, by stage 33 the *Shp-2* N308D hearts have defined myocardial and endocardial layers. By stage 37, the *Shp-2* N308D hearts display a range of severity in phenotype, with the less severe *Shp-2* N308D hearts (approximately 40%; N>500) eventually closing ventrally to form a bilaminar heart tube that begins to kink or jog but do not undergo looping or chamber formation while the more severe *Shp-2* N308D hearts (approximately 60%; N>500) remain as a cardiac trough; it also appears in some cases that cardiac cells fail to incorporate into the myocardium, the endocardium, or the lateral plate mesoderm (Fig. 3.1 K,L).

Shp-2 N308D expression leads to a decrease in cardiac cell number

To determine if *Shp-2* N308D could affect cardiac cell number, we serial sectioned through the cardiac regions of control and *Shp-2* N308D embryos and double stained with DAPI and an antibody against tropomyosin (data not shown). Both myocardial and endocardial cells were counted in all hearts at all stages for each condition. Results from these experiments show no difference between *Shp-2* N308D embryos and control embryos at stage 29 (Fig. 3.2M) however four stages later at stage 33, and continuing to stage 37, the *Shp-2* N308D embryos show a statistically significant decrease in cardiomyocyte cell number relative to controls (p= 0.04, p= 0.01 stage 33 and stage 37, respectively) (Fig. 3.2M).

3D Modeling of *Shp-2* N308D hearts

To further characterize the defects in cardiac development associated with the *Shp-2* N308D Noonan mutation, we carried out 3D modeling of *Xenopus* hearts derived from control or *Shp-2* N308D embryos at early, mid, and late tadpole stages (stages 29, 33, and 37). For these studies, a minimum of three embryos at each stage were serial sectioned through the cardiac region and stained with anti-tropomyosin to mark myocardial tissue and DAPI to mark cell nuclei. Data was then entered into a 3D global software histology program and rendered by a 3D visualization program (Langdon et al., submitted).

3D reconstruction at stage 29 shows control hearts in which the bilateral heart fields have fused across the ventral midline to form a single heart field arranged into a myocardial trough that runs along the anterior-posterior axis. Examination of 3D reconstruction at stage 29 reveals little to no difference between myocardium derived from control or *Shp-2* N308D embryos at this stage (Fig. 3.2A, B, G, H). Although we observe an equal number of cells

85

between control and *Shp-2* N308D hearts (Fig. 3.2M), we note that the *Shp-2* N308D hearts occasionally do not extend as far anteriorly as controls at this stage (Fig. 3.2G, H).

By Stage 33, control hearts have closed dorsally to form a bilaminar heart tube and the dorsal mesocardium elongates in the posterior portion of the heart (Fig. 3.2C, I). In stark contrast *Shp-2* N308D hearts remain as an open trough and fail to close dorsally while they extend along the dorsal-ventral axis (Fig. 3.2D, J also see 3.1I). We note at these stages however, that the *Shp-2* N308D have significantly fewer cardiac cells and there appears to be less growth in the posterior aspects of *Shp-2* N308D hearts relative to controls (Fig. 3.2I, J). In addition, the more anterior portions of the heart are extended and the chamber is wider in the anterior aspects of the heart possibly representing a differential effect of *Shp-2* N308D along the anterior to posterior axis of the heart. We note we are able to only detect a single class of heart defects at this stage.

By stage 37, control heart tubes have begun to undergo cardiac looping, leading to a shortening of the heart along the anterior-posterior axis and an elongation of the heart along the dorsal-ventral axis. In contrast *Shp-2* N308D hearts display a range of severity in cardiac development. We modeled those with the less severe phenotype (Fig. 3.1), which have significantly fewer cardiomyocytes (p= 0.01), and are developmentally delayed- it is only at this stage that they have rounded up and begun to fuse along the dorsal axis, as we observe two ridges of tissue running down the heart in an anterior-posterior direction at the site of fusion (Fig. 3.2E, F, K, L also see 3.1K, 3.5D). Despite the failure to properly fuse, the *Shp-2* N308D hearts have begun some of the cellular movements associated with looping, including a leftward spiral of the cardiac tissue as noted by the relative shift of the inflow tract relative to the outflow tract (Fig. 3.2I, J, K, L). However, the *Shp-2* N308D hearts are more

86

compressed along the anterior-posterior axis versus controls while still being extended fully along the dorsal-ventral axis (comparing Fig. 3.2K to L). Collectively, these studies demonstrate that the introduction of *Shp-2* N308D leads to an abrupt decrease in cardiac cell numbers relative to controls and a delay in cardiac morphogenetic movements between stages 29 and 33, leading to a smaller morphologically abnormal heart by stage 37.

Noonan associated mutation *Shp-2* N308D leads to alterations in the cardiac mitotic index

To determine if the decrease in cardiac cell number in *Shp-2* N308D hearts is associated with changes in cardiomyocyte cell cycle progression, we conducted a series of studies to analyze the mitotic index of cardiomyocytes at defined time points during heart development. For these studies embryos at early, mid, and late tadpole stages were serial sectioned through the cardiac regions and triple-stained with DAPI to mark cell nuclei, anti-tropomyosin to mark cardiomyocytes, and anti-phospho H3 to mark dividing cells (Fig. 3.3A-D). All cardiac cells, as judged by anti-tropomyosin were counted in all hearts at all stages for all conditions with the complete study being performed at least two independent times.

We found a transient increase in the cardiac mitotic index in *Shp-2* N308D embryos compared to control embryos at stage 33 (P= 0.04) (Fig. 3.3E). This increase was stage specific with no significant increase in the cardiomyocyte mitotic index observed either at earlier or later stages (stage 29 and 37; Fig. 3.3E). Since SHP-2 has recently been reported to have a role in cell survival (Langdon et al., 2007; Yang et al., 2006), we next tested if the decrease in cardiomyocyte cell number and increase in mitotic index in *Shp-2* N308D embryos might be associated with increased programmed cell death. Therefore, we repeated the experiments serial sectioning through heart tissue for each condition triple staining with

DAPI to mark cell nuclei, anti-tropomyosin to mark cardiomyocytes, and anti-Caspase 3 to mark cells undergoing program cell death (Fig. 3.3F). At no time point could we detect any significant difference in programmed cell death between *Shp-2* N308D and control embryos. Thus, we find that *Shp-2* N308D leads to a stage specific increase in the cardiomyocyte mitotic index without a concomitant increase in program cell death.

Noonan mutation *Shp-2* N308D transiently disrupts cell cycle progression

The observation that in *Shp-2* N308D derived hearts there is an increase in the mitotic index without an increase in cardiomyocytes cell number, suggests that *Shp-2* N308D leads to either lengthening in M-phase, lengthening of the cardiac cell cycle as a whole or to cardiomyocytes prematurely exiting from the cell cycle. To address these issues, we dissected out heart tissue from control and *Shp-2* N308D embryos at stages 37 and carried out western blot analysis on isolated cardiac tissue with antibodies that recognize the S-phase enriched proteins Stem Loop Binding Protein (SLBP) and proliferating cell nuclear antigen (PCNA) (Fig. 3.3G). These studies show that over-expression of *Shp-2* N308D leads to a dramatic increase in SLBP and PCNA proteins. These results, taken together with our results showing that *Shp-2* N308D leads to a transient increase in the mitotic index, suggest that Noonan associated mutations lead to a stage specific delay or arrest of the embryonic cardiac cell cycle.

Noonan mutation *Shp-2* N308D does not appear to effect cardiac commitment or differentiation

Histological analysis and 3D molecular modeling of hearts derived from *Shp-2* N308D embryos strongly suggest that the N308D mutation leads to smaller and abnormally shaped

hearts by stage 33. We have previously shown that this is not due to a block in the commitment or migration of cardiac precursors to the ventral midline (Langdon et al., 2007). Therefore, to determine if the cardiac defects in *Shp-2* N308D embryos are due to a block in cardiac differentiation, we collected control and *Shp-2* N308D embryos at stage 37, and serial sectioned through the cardiac tissue and stained for the terminal differentiation markers tropomyosin, cardiac actin, or fibrillin (Fig. 3.4A-I). This data demonstrates that *Shp-2* N308D hearts undergo terminal differentiation but are developmentally delayed in morphogenesis.

Microarray analysis of *Shp-2* N308D mis-expression in the developing heart

To determine the molecular pathways that are disrupted in *Shp-2* N308D we conducted microarray analysis with isolated heart tissue from *Shp-2* N308D injected and FL-SHP-2 injected control embryos. Each study was performed on three independent sets of embryos. We observed an alteration in the transcriptional level of 33 genes of which several are involved in regulating the actin cytoskeleton (Table. 1). To support the microarray data we analyzed the cardiomyocyte structural defects associated with the introduction of *Shp-2* N308D by ultrastructure analysis (Fig. 3.4J-M). This analysis reveals that by stage 33 hearts of control embryos have cardiac muscle bundles located throughout the myocardium, positioned in both longitudinal as well as concentric arrays (Fig. 3.4J, L). In stark contrast, *Shp-2* N308D hearts show far fewer sarcomeres than controls, and the sarcomeres and myofibrils that form are arranged solely in concentric arrays (Fig. 3.4K, M). Collectively, our immuno-histochemistry and ultrastructure analysis suggest that *Shp-2* N308D does not block cardiac differentiation but instead leads to an apparent decrease in myofibrils and defects in myofibril polarity in the developing heart.

SHP-2 associates with actin *in vivo*

Our microarray analysis suggests that SHP-2 is involved in regulating actin dynamics and this is supported by the ultrastructure defects observed in *Shp-2* N308D hearts. Consistent with the experiments shown here Xu et al. established that SHP-2 localizes to actin *in vitro* (Xu et al., 2001). Therefore to determine if SHP-2 directly interact with actin *in vivo* we performed mass spectroscopy on six protein bands isolated from embryos injected with FL-SHP-2. The mass spectroscopy data confirmed that SHP-2 associates with actin *in vivo*. Collectively, these studies suggest that one function of SHP-2 during cardiac development is to promote and maintain actin myofibril development and orientation.

SHP-2 phosphatase activity is required for cardiac defects

Based on the SHP-2 crystal structure, biochemistry, and tissue culture assays, it has been implied that Noonan mutations may function as open or constitutive active forms of SHP-2 (Fragale et al., 2004; O'Reilly et al., 2000; Tartaglia et al., 2003). To test if the effect of *Shp-2* N308D on actin organization requires SHP-2 enzymatic activity, a critical amino acid within the protein phosphatase (PTP) domain, amino acid 459, was mutated from a cysteine to a glycine creating a non-functional PTP domain (Bennett et al., 1996) (Fig. 3.1A). Injection of the corresponding RNA gave rise to embryos with hearts that are indistinguishable from uninjected or full-length controls (Fig. 3.5), and have protein levels equivalent to those from cardiac tissue derived from embryos injected of full-length or *Shp-2* N308D parent constructs (data not shown). Thus, *Shp-2* N308D appears to function as a constitutive active form of SHP-2 *in vivo* and its phosphatase activity is required for the cardiac abnormalities associated with *Shp-2* N308D.

Shp-2 N308D leads to an increase of ERK and MEK in heart tissue *in vivo*

It has been shown that *Shp-2* can function within the MAPK pathway in developing cardiac tissue and that MAPK can function to regulate cardiac cell proliferation or survival (Langdon et al., 2007; Neel et al., 2003; Qu, 2000). To determine whether the cardiac abnormalities associated with *Shp-2* N308D are mediated by the MAPK pathway in cardiac tissue *in vivo*, we tested if *Shp-2* N308D derived hearts lead to either an elevation in levels or increase in the number of cells that express activated ERK or MEK (Fig. 3.6). Consistent with *Shp-2* N308D leading to elevated ERK and MEK activity, isolated cardiac tissue from stage 37 *Shp-2* N308D embryos, versus controls, shows an increase in the levels of both total and activated levels of ERK and MEK. However, the relative levels of activated to total ERK and MEK remain the same in controls and *Shp-2* N308D embryos.

To investigate if the elevation in MAPK is due to either a greater level of MAPK per cardiomyocyte or if it is due to a greater number of cells expressing MAPK, control and *Shp-2* N308D derived embryos at stage 37 were serial sectioned and triple immuno-stained with anti-tropomyosin (Tmy) to mark cardiomyocytes, DAPI to mark cell nuclei, and an antibody that recognizes total active MEK (data not shown) or activated MEK (Fig. 3.6A, B). Since we could not detect any significant difference in the percentage of cells expressing active MEK in control verses *Shp-2* N308D derived hearts, these results suggest that the elevation in MEK is due to an increase in the amount of MEK being expressed per cardiomyocyte and not an increase in the number of cardiomyocytes expressing MEK.

Discussion

Studies on Noonan patients have demonstrated an association between Noonan *Shp-2* mutations and cardiac valve defects (Noonan, 1968). Consistent with these clinical features, studies in mouse and chick have shown SHP-2 to be required in the EGF pathway for proper semilunar valvulogenesis (Chen et al., 2000; Krenz et al., 2005). However, approximately one-third of all Noonan patients have heart defects that are not associated with valve abnormalities, raising the possibility that SHP-2 may have additional roles in heart development (Noonan, 1968; Noonan, 1994). Here we report, that a Noonan associated mutation in *Shp-2* leads to cardiac specific defects at time points that greatly precede that of cardiac valve formation. Our results strongly suggest that the cardiac defects we observe from the introduction of *Shp-2* N308D, the most common Noonan associated *Shp-2* mutation, may leads to alterations in the actin cytoskeleton which in turn may leads to a transient delay in the embryonic cardiac cell cycle that is mediated by an increase in ERK/MEK activation.

Shp-2 N308D disrupts actin myofibril development

SHP-2 functions in diverse signaling pathways to regulate a number of developmental process including cell morphology, cell migration, cell adhesion, and actin dynamics. SHP-2 promotes these processes through regulation of the quantity of focal contacts and modulation of actin dynamics and SHP-2 has been found to localize to F-actin (Xu et al., 2001). Consistent with a role for SHP-2 in actin regulation, loss of function studies found that the absence of SHP-2 results in an increase in the number of actin fibers and focal adhesion contacts *in vitro* (Inagaki et al., 2000; Schoenwaelder et al., 2000; Yu et al., 1998). Our current data suggests an *in vivo* role for SHP-2 in proper myofibril development in cardiac

92

tissue as we show that introduction of the Noonan associated mutation, *Shp-2* N308D, appears to leads to decreased numbers of myofibrils and the disruption of myofibril polarity. Our studies imply that a primary function of SHP-2 in the heart is to regulate actin dynamics. The molecular modeling studies showed that at stage 29, a time where there were no differences in total cell number between control and *Shp-2* N308D hearts, there was still an observable defect within the hearts of *Shp-2* N308D embryos. The hearts of embryos injected with *Shp-2* N308D are more compact along the anterior posterior axis suggesting that this defect precedes the transient changes in cell cycle progression. Therefore, myofibril disruption is the first discernible defect in *Shp-2* N308D hearts and occurs at stage 29, followed by the cell cycle defect which is initiated between stage 29 and 33. *Shp-2* N308D may functions downstream of integrin and/or rho signaling pathways in the heart as both integrin and rho signaling are critical for regulation of actin dynamics (integrin signaling reviewed in Brancaccio et al., 2006; rho signaling reviewed in Brown et al., 2006) and SHP-2 has been implicated in signaling downstream of both pathways (Inagaki et al., 2000; Schoenwaelder et al., 2000). We propose that in the heart *Shp-2* N308D is localized to areas of developing concentric myofibrils and rapidly dephosphorylate one or more molecules associated with the formation of actin filaments during myofibril assembly. However the mechanism of *Shp-2* N308D localization, which proteins are dephosphorylated by *Shp-2* N308D, and how actin filament disruption leads to loss of concentric myofibrils remains to be determined.

Shp-2 N308D leads to a delay in the embryonic cardiac cell cycle

Evidence for SHP-2 as a regulator of cell cycle progression suggests that SHP-2 functions to promote the transition from G1 to S phase (Bennett et al., 1996). Similarly, we find that

cardiac cell cycle progression is altered in response to *Shp-2* N308D mis-expression. We demonstrate that the introduction of the Noonan mutation, *Shp-2* N308D, into *Xenopus* leads to a transient delay of the cardiac cell cycle as measured by a transient increase in the mitotic index, an increase in the S-phase enriched proteins SLBP and PCNA, and a decrease in cardiac cell number. The cell cycle defect is first observed at stage 33 suggesting that the defect may be secondary to earlier defects in actin regulation. However, it is possible that the cell cycle defects are independent of the earlier actin defects. At this point it is still unclear if the actin defects in *Shp-2* N308D hearts lead to the alterations in cell cycle progression or if the cell cycle defects represent a second primary function of SHP-2 in the heart.

We note that our observations of decreased cardiac cell number are contrary to those reported for *Shp-2* N308D in tissue culture cells and tissue explants where it has been shown that activating forms of SHP-2, including *Shp-2* N308D, leads to an increase in cell proliferation (Krenz et al., 2005; Oishi et al., 2006; Schubbert et al., 2005). We suspect that SHP-2 plays different roles that depend on the cellular or temporal context. It is well documented that activation of ERK can lead to growth arrest and differentiation of a number of cell types including neurons and megakaryocytes (Kerkhoff and Rapp, 1997; Mansour et al., 1994). Antiproliferative effects have also been reported for upstream activators of ERK. For example, premature cell cycle arrest is observed in response to activated RAS, including JMML associated RAS mutations, in Schwann cells and primary fibroblasts (Clark et al., 2004; Davies et al., 2002; Flotho et al., 1999; Franza et al., 1986; Kalra et al., 1995; Ussar and Voss, 2004). Moreover, these effects of RAS have been found in some instances to be mediated by the activation of the RAF/MEK/ERK pathway. Similarly, over-expression of an

94

activated Raf can also lead to cell cycle arrest in a variety of cell types including Schwann cells and PC12 cells (Bar-Sagi and Feramisco, 1985; Lloyd et al., 1997).

Thus, similar to our findings with SHP-2, there is a fundamental difference between the oncogenic properties of RAS in immortalized cell lines versus its role in growth arrest and promotion of differentiation in some primary vertebrate cells. In the case of RAS, this is in part mediated by the ability of RAS to activate either the p21^{WAF1} pathway or the p16/p15/p19 pathway in embryonic or primary cell types (Crespo and Leon, 2000). It is interesting to speculate that SHP-2 functions within embryonic cardiac tissue either as a upstream component of this pathway or in a RAS independent pathway with similar cellular outcomes.

Cardiac Specificity of *Shp-2* N308D

The crystal structures of SHP-2 (Hof et al., 1998) and mutational analysis (Fragale et al., 2004; O'Reilly et al., 2000; Tartaglia et al., 2003) show that in its basal state SHP-2 folds back upon itself, with the N-terminal SH2 (N-SH2) domain forming an intra-molecular association with the PTP domain and hence rendering SHP-2 in a 'closed conformation' and enzymatically inactive (Fig. 3.7A). Upon interaction of the C- SH2 domains with a phophotyrosyl motif in the cytoplasmic tail of RTKs or scaffolding proteins (Fig. 3.7B) the intra-molecular association of SHP-2 is disrupted, freeing the PTP domain, and placing SHP-2 in its 'open' or active conformation and resulting in a gain of function for SHP-2 phosphatase activity (Neel et al., 2003) (Fig. 3.7C). Noonan associated mutations mainly cluster at the N-SH2:PTP interface and are therefore thought to destabilize the intra-molecular folding of SHP-2 placing SHP-2 in a more active state (Fragale et al., 2004; O'Reilly et al., 2000; Tartaglia et al., 2003) (Fig. 3.7D). Thus, one simple hypothesis for our

95

results is that the cardiac cell cycle is particularly sensitive to changes in SHP-2 enzymatic activity and that prolonged or elevated levels of SHP-2 activity lengthens or arrests the cell cycle. Consistent with this hypothesis we show that a mutation that abolishes PTP activity in *Shp-2* N308D abolishes the effect on cardiac development (Fig. 3.5). However, a number of findings argue against this model. First, there appears to be no direct genotype-phenotype relationship in patients carrying particular Noonan *Shp-2* mutations (Tartaglia et al., 2002; Zenker et al., 2004). Second, the *Shp-2* mutation at position 76 in the JMML mutant has been demonstrated to have elevated phosphatase activity relative to that of *Shp-2* N308D. Since *Shp-2*E76A has no effect on heart development, there does not appear to be any direct relationship between the strength of a *Shp-2* allele and its ability to affect cardiac development (Fragale et al., 2004). Third, neither decreasing (.5ng) nor increasing (4ng) the amount of *Shp-2* N308D introduced into *Xenopus* has an effect on tissue specificity (data not shown).

What then leads to tissue specific effect of the *Shp-2* N308D mutation? The majority of JMML, ALL, and AML mutations occur in the N-SH2 domain while the *Shp-2* N308D mutation lies within the PTP domain (Bentires-Alj et al., 2004; Kratz et al., 2005; Loh et al., 2004; Musante et al., 2003; Tartaglia et al., 2003). In its closed or inactive state SHP-2 folds back upon itself with the N-SH2 domain in contact with the PTP, leaving the C-SH2 domain to have little to no interaction with the PTP domain, and thus the C-SH2 binding pocket is left free by this 'closed' steric conformation (Fig. 3.7A). This has led to a model that proposes that the C-SH2 domain 'searches' for phospho-tyrosine targets (Neel et al., 2003) (Fig. 3.7B). We would propose that the *Shp-2* N308D mutation leads to an open conformation of SHP-2 which unlike JMML (e.g. E76A), ALL, or AML mutations leaves

96

both the N-SH2 domain and the C-SH2 domain intact, leaving both domains to search for

and bind phospho-tyrosine targets (Fig. 3.7D). We predict that the affinity and/or specificity

of the two SH2 domains are not equivalent to that of the C-SH2 domain alone. Therefore, in

the case of the *Shp-2* N308D mutation, unlike the *Shp-2* E76A mutation, the free N-SH2

leads to an alteration in either the duration or specificity of a specific substrate interaction

(Fig. 3.7E). This model is supported by recent studies mapping the binding preferences of the

N-SH2 and C-SH2 domain in SHP-2 that show different sequence preferences for phospho-

substrate and also demonstrate that constructs containing both the N-SH2 and C-SH2

domains, but not the PTP domain, bind with a higher affinity than constructs containing

either SH2 domain alone (Poole and Jones, 2005; Sweeney et al., 2005). This model is also

consistent with studies on the highly related protein phosphatase SHP-1 that demonstrate that

the N-SH2 and C-SH2 domain prefer different phospho-substrates and bind substrates with

different affinities (Beebe et al., 2000; Pluskota et al., 2000). Taken together, we predict that

the availability of both the N-SH2 and the C-SH2 domain leads to an increased or

inappropriate interaction with a cardiac specific substrate which in turn, leads to the heart

specific defects observed with the *Shp-2* N308D mutation.

Figure 3.1. Noonan associated mutation of *Shp-2* lead to heart defects in *Xenopus*.

(A) Schematic representation of human *Shp-2* constructs introduced into *Xenopus* embryos (not to scale). (B) Western blot analysis of embryo lysates from embryos injected with the respective HA-epitope tagged *Shp-2* constructs at stages 10 (gastrula), 16 (early neurula), and 20 (late neurula) probed with an anti-HA antibody, an anti-SHP-2 antibody that recognizes both endogenous and introduced versions of SHP-2, and an anti-EF-2 antibody as a loading control. (C-G) Whole-mount antibody staining of stage 36 embryos with anti-tropomyosin antibody (Tmy). Anterior is to the left, posterior is to the right. Images are of cleared embryos. Hearts of embryos either (C) uninjected, or (D) embryos from injection of *Shp-2* full-length, (E) *Shp-2* mis-sense mutation E76A, (F) *Shp-2* mis-sense mutation N308D, showing an example of a less severe heart defect, (G) *Shp-2* mis-sense mutation N308D embryo, showing an example of a more severe heart defect. (H-L) Transverse histological

sections of *Xenopus* showing cardiac regions from (H) stage 33 control embryos, (I)

corresponding embryos injected with *Shp-2* N308D, (J) stage 37 control embryos, (K)

corresponding embryos injected with *Shp-2* N308D showing an example of a less severe

heart defect, (L) corresponding embryos injected with *Shp-2* N308D, showing an example of

a more severe heart defect (T, open cardiac trough, M, myocardium; E, endocardium; C,

unincorporated cardiac cells).
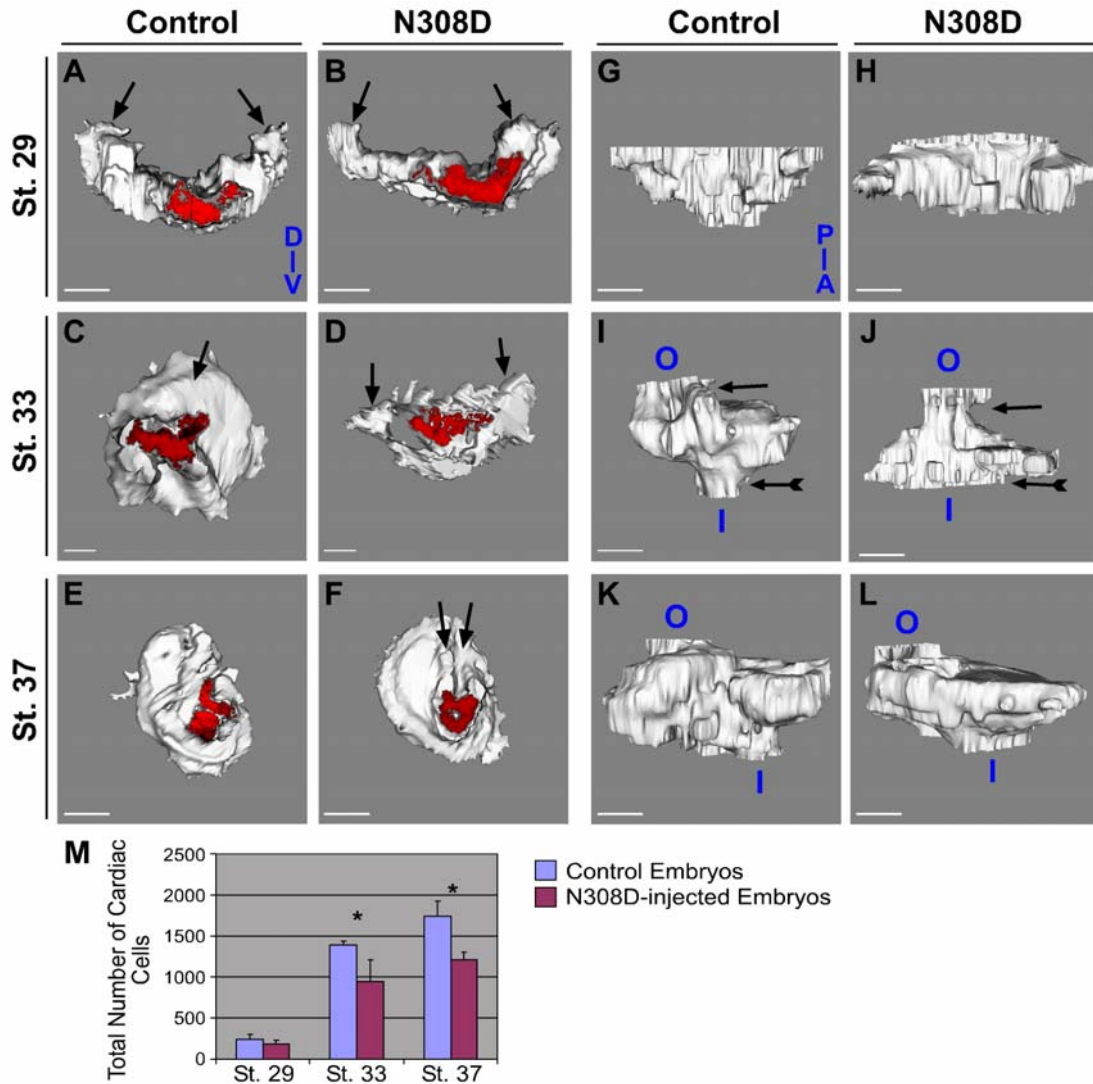
Figure 3.2. 3D Modeling of control and *Shp-2* N308D cardiac tissue shows cardiac abnormalities in *Shp-2* N308D hearts beginning at stage 33.

3D modeling of tropomyosin expression in (A, B, G, H) stage 29 hearts, (C, D, I, J) stage 33 hearts, (E, F, K, L) stage 37 hearts. (A-F) hearts viewed from anterior to posterior, red denoted most anterior section of the heart; lower right corner of panel (A) shows orientation of dorsal (D), ventral (V) axis. (G-L) Lower right corner of panel (G) shows orientation of posterior (P), to anterior (A) axis. In panels (A-F) arrows denote the ends of the cardiac trough. Note in panel (C) that the trough has closed across the dorsal midline in the control

while remaining open in (D) the *Shp-2* N308D heart. The edges of the trough come together

by stage 37 (F) in the *Shp-2* N308D heart but still have not closed across the ventral midline.

Also at stage 33 (J) the *Shp-2* N308D heart is much wider in the anterior portions while much

thinner in the posterior portions (arrows) versus (I) the corresponding control. (O, outflow; I,

inflow). Note, the relative orientation of O to I in panel I verses panel J, indicative of a delay

in looping. (M) Average total number of cells in control and *Shp-2* N308D derived hearts at

stage 29, 33, and 37. Error bars denote the standard deviation and * denotes a statistically

significant difference (at $p < 0.05$) between control and *Shp-2* N308D embryos at a given

stage. (Scale bars = 100 μm, K, L scale bar = 190 μm).
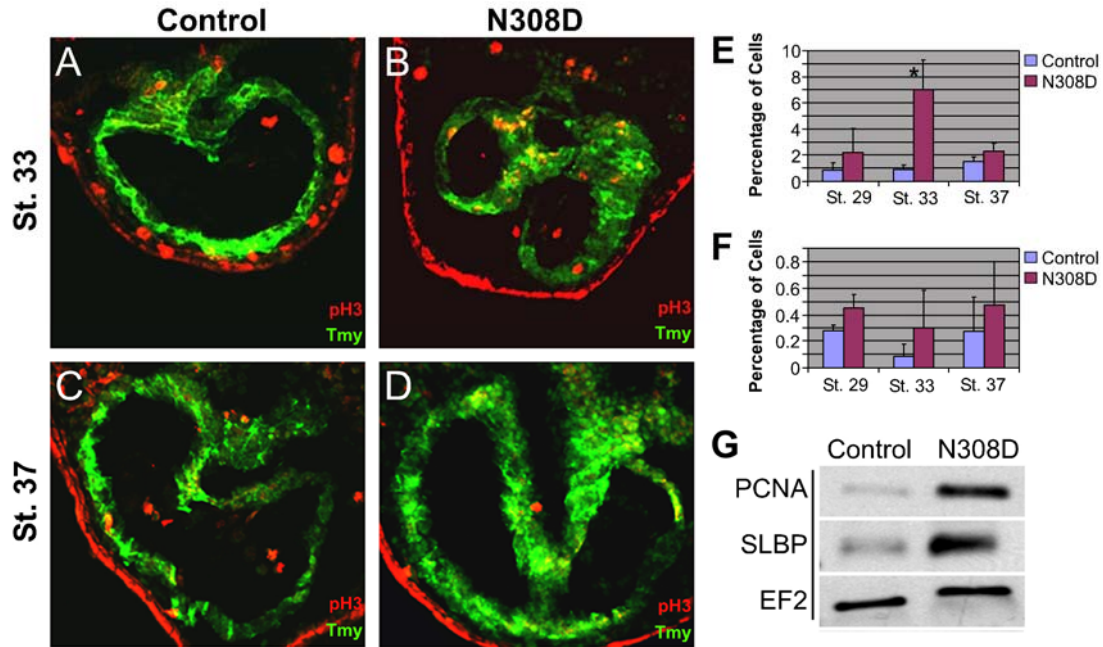
Figure 3.3. *Shp-2* N308D leads to a delay of the cardiac cell cycle.

Transverse heart sections through (A, B) stage 33 and (C, D) stage 37 embryos stained with Tmy, to mark cardiac tissue (green), and anti-histone H3 (red), to mark cells in M-phase (A, C) control embryos (B, D) *Shp-2* N308D derived embryos. Quantification of results from (E) proliferation, and (F) programmed cell death. In all cases, bars represent the average of at least 3 embryos: control = blue bar and *Shp-2* N308D = red bar. Error bars denote the standard deviation and * denotes a statistically significant difference (at $p < 0.05$) between control and *Shp-2* N308D embryos at a given stage. (Scale bars = 100 μm). Results are derived from a single set of experiments, all experiments were repeated at least once with an independent batch of embryos. (G) *Shp-2* N308D leads to a prolonged S-phase. Expression of the S-phase enriched proteins SLBP and PCNA in purified cardiac tissue stage 33 tissues from control uninjected embryos or embryos *Shp-2* N308D as detected by western blot analysis; anti-EF-2 is used as a loading control.
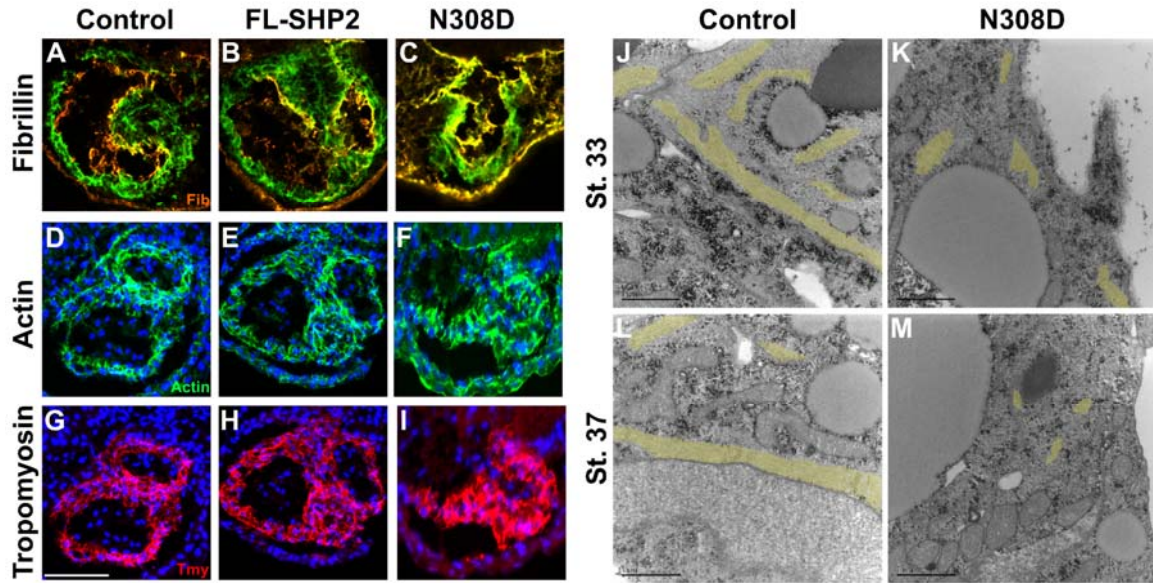
Figure 3.4. *Shp-2* **N308D leads to alterations in cardiac myofibrils but does not disrupt cardiac differentiation.**

Cardiomyocyte structure in transverse sections through the hearts of stage 37 embryos either (A, D, G) control, (B, E, H) injected with full-length *Shp-2* or (C, F, I), injected with *Shp-2* N308D as detected by immunostaining for (A-C) Tmy (green), fibrillin (red), (D-F) cardiac actin as detected by conjugated phalloidin (green), and DAPI (blue) or (G-I) tropomyosin (red) and DAPI (blue) (scale bar = 100 μm). (J-M) Representative transmission electron micrographs of transverse images from (J, K) stage 33 or (L, M) from stage 37 embryos of heart tissue derived from (J, L) control or (L, M) *Shp-2* N308D injections. Cardiac muscle fibrils are shown pseudo-colored in yellow. (Scale bars = 1 μm).

Genes Upregulated 1.5 Fold or More	Genes Downregulated 1.5 Fold or More
Bub3 protein	Liver fatty acid binding protein (FABP)
Trypsin 10	Similar to vomeronasal 2 receptor 600
Ribosomal protein S29	ladybird homeobox 1 transcription factor (Lbx1)
Ras-GTPase activating protein SH3 domain-binding protein 2	
Ndrg2 protein	**Genes Both Upregulated and Downregulated 1.5 Fold or More**[**]
Lingo1 protein– leucine rich repeat and Ig domain containing 1	Zinc finger protein 326
ADP-ribosylation factor like protein 8B (Rab7, ras oncogene family like)	Source of MHC peptide
Immunoglobin like	Vasohibin
Actin interacting protein 1A- WD repeat domain 1	FBJ murine osteosarcoma viral oncogene homolog
Keratin, type I cytoskeletal (keratin XK81B2)	Cell division cycle 42 (GTP binding protein, 25kDa)
Fus protein [fusion, derived from t(12;16) malignant liposarcoma]	Somatostatin precursor
Troponin T type 3 (skeletal, fast)	Intelectin 1 (galactofuranose binding)
Phenylalanyl t-RNA synthetase 1 (mitochondral precursor)	Tubulin, alpha 7
Kelch-like protein 30, similar to Dre1	
TGas040f1 3 wings apart-like homologue	
Glutaminyl-peptide cyclotransferase-like	
Tubulin, alpha 1 (testis specific)	
Profilin 2	
Protein phosphatase 2, regulatory subunit B (PR 52), beta isoform	
TNeu036d08- Titin (Connectin)	
Dynein, cytoplasmic 1, heavy chain 1	
S-Adenosylmethionine decarboxylase 1A (Amd1)	

[**] The genes in this list are both up and downregulated which likely reflects the range of phenotypes of *Shp*-2 N308D hearts. The hearts range in size which could account for the appearance of up regulation in one experiment and downregulation in another.

Table 1. Genes altered at least 1.5 fold in response to expression of *Shp-2* N308D in the heart.
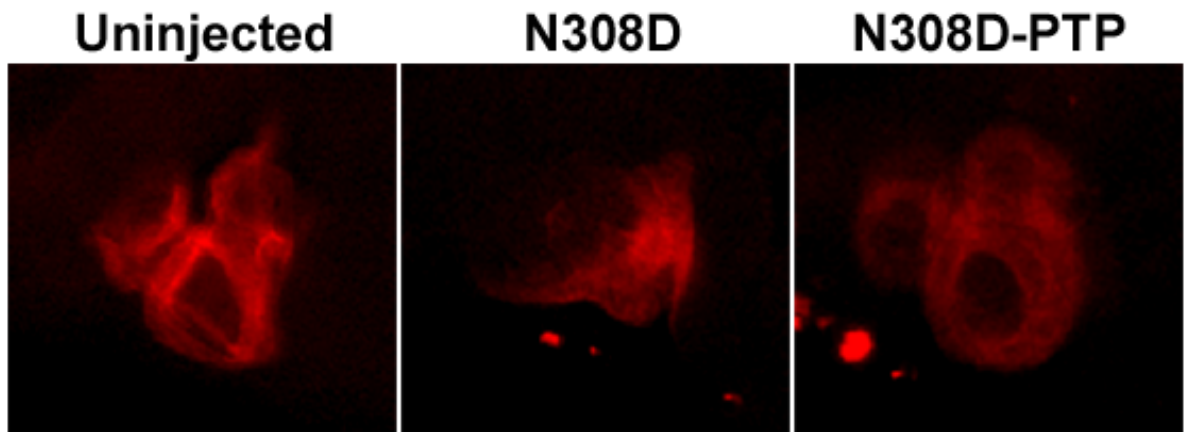
Figure 3.5. Phosphatase activity is required for *Shp-2* N308D function in the heart.

Whole-mount antibody staining of hearts of stage 36 embryos stained with an anti-tropomyosin antibody (Tmy). Anterior is to the left, posterior is to the right. Embryos either uninjected, or injected with *Shp-2* N308D or N308D-PTP.
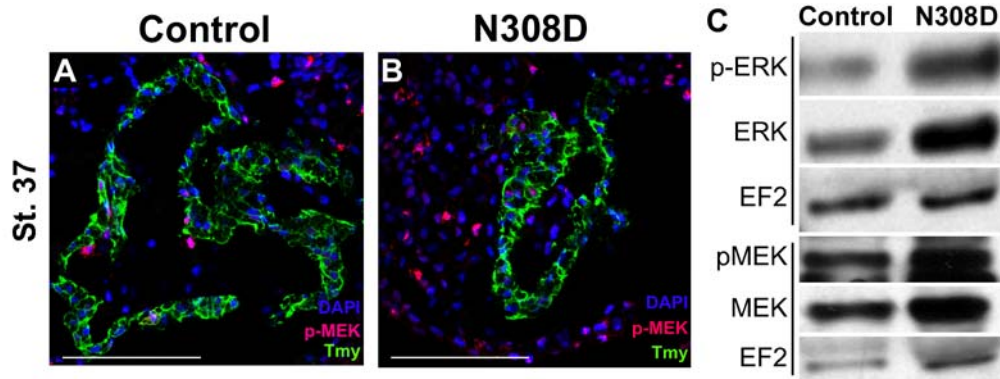
Figure 3.6. *Shp-2* **N308D leads to an increase in phospho-MEK and phospho-ERK in embryonic cardiac tissue.**

(A, B) MAPK positive cells in cardiac tissue in transverse sections of *Xenopus* from stage 37 embryos with (A) uninjected controls or embryos injected with (B) *Shp-2* N308D. Sections are stained with Tmy, to mark cardiac tissue (green), p-MEK (red), and DAPI to mark the cell nuclei (blue). (Scale bars = 100 μm). Phospho-MEK results are derived from a single set of experiments, all experiments being repeated at least once with an independent batch of embryos. (C) *Shp-2* N308D leads to increased ERK and MEK; in cardiac tissue. Expression of ERK, phospho-ERK, MEK, and phospho-MEK in purified cardiac tissue stage 33 tissues from control uninjected embryos or embryos injected with *Shp-2* N308D as detected by western blot analysis; anti-EF-2 is used as a loading control.
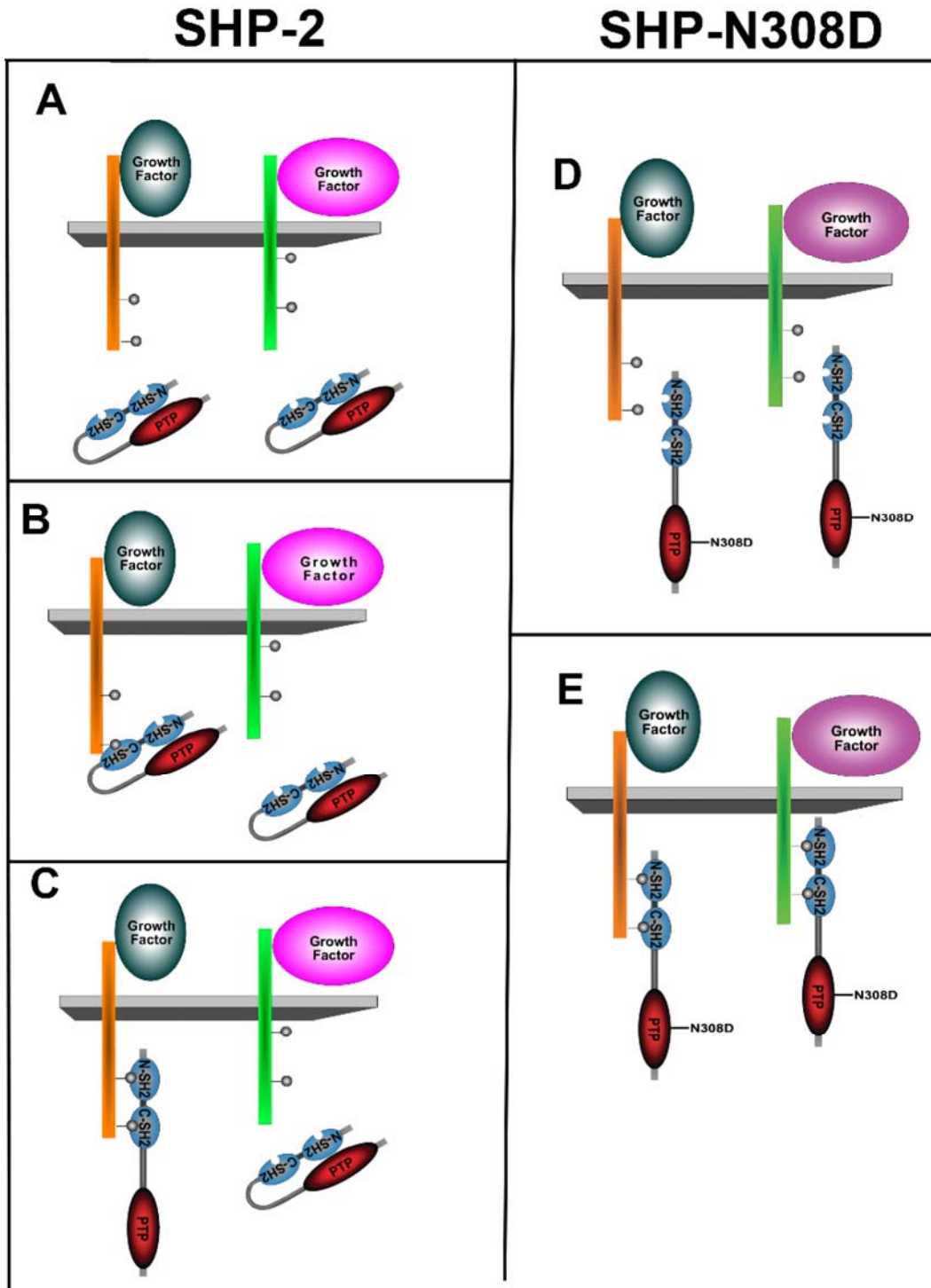
Figure 3.7. Proposed mechanism for *Shp-2* N308D cardiac specific effects.

Schematic depicts growth factor receptors expressed in cardiac tissue (orange and green). (A)

In control embryos, Shp-2 is normally present in a closed or enzymatically inactive state with

a free C-SH2 domain and the N-SH2 domain bound to the PTP domain. Upon interaction with their respective ligands, the growth factor receptors are phosphorylated (grey circles) (B) recruiting SHP-2 to one receptor (orange) through the interaction of the C-SH2 domain however, the C-SH2 domain cannot interact with the other receptor (green). (C) Once the C-SH2 domain interacts with the phospho-residue, SHP-2 undergoes a conformational change to its open or enzymatically active state (Neel et al., 2003). (D, E) In the case of *Shp-2* N308D, SHP-2 is thought to be constitutively active and hence in an open conformation. Thus, unlike the control state the N-SH2 domain is free to interact with phospho-residues leading to an alteration in specificity (depicted as an interaction with the green receptor) which in turns leads to inappropriate signaling in the cardiac tissue.

References

Bar-Sagi, D. and Feramisco, J. R. (1985). Microinjection of the ras oncogene protein into PC12 cells induces morphological differentiation. *Cell* **42**, 841-8.

Barford, D. and Neel, B. G. (1998). Revealing mechanisms for SH2 domain mediated regulation of the protein tyrosine phosphatase SHP-2. *Structure* **6**, 249-54.

Beebe, K. D., Wang, P., Arabaci, G. and Pei, D. (2000). Determination of the binding specificity of the SH2 domains of protein tyrosine phosphatase SHP-1 through the screening of a combinatorial phosphotyrosyl peptide library. *Biochemistry* **39**, 13251-60.

Bennett, A. M., Hausdorff, S. F., O'Reilly, A. M., Freeman, R. M. and Neel, B. G. (1996). Multiple requirements for SHPTP2 in epidermal growth factor-mediated cell cycle progression. *Mol Cell Biol* **16**, 1189-202.

Bentires-Alj, M., Paez, J. G., David, F. S., Keilhack, H., Halmos, B., Naoki, K., Maris, J. M., Richardson, A., Bardelli, A., Sugarbaker, D. J. et al. (2004). Activating mutations of the noonan syndrome-associated SHP2/PTPN11 gene in human solid tumors and adult acute myelogenous leukemia. *Cancer Res* **64**, 8816-20.

Brancaccio, M., Hirsch, E., Notte, A., Selvetella, G., Lembo, G. and Tarone, G. (2006). Integrin signalling: the tug-of-war in heart hypertrophy. *Cardiovasc Res* **70**, 422-33.

Brown, J. H., Del Re, D. P. and Sussman, M. A. (2006). The Rac and Rho hall of fame: a decade of hypertrophic signaling hits. *Circ Res* **98**, 730-42.

Chen, B., Bronson, R. T., Klaman, L. D., Hampton, T. G., Wang, J. F., Green, P. J., Magnuson, T., Douglas, P. S., Morgan, J. P. and Neel, B. G. (2000). Mice mutant for Egfr and Shp2 have defective cardiac semilunar valvulogenesis. *Nat Genet* **24**, 296-9.

Clark, J. A., Black, A. R., Leontieva, O. V., Frey, M. R., Pysz, M. A., Kunneva, L., Woloszynska-Read, A., Roy, D. and Black, J. D. (2004). Involvement of the ERK signaling cascade in protein kinase C-mediated cell cycle arrest in intestinal epithelial cells. *J Biol Chem* **279**, 9233-47.

Crespo, P. and Leon, J. (2000). Ras proteins in the control of the cell cycle and cell differentiation. *Cell Mol Life Sci* **57**, 1613-36.

Davies, H., Bignell, G. R., Cox, C., Stephens, P., Edkins, S., Clegg, S., Teague, J., Woffendin, H., Garnett, M. J., Bottomley, W. et al. (2002). Mutations of the BRAF gene in human cancer. *Nature* **417**, 949-54.

Feng, G. S. (1999). Shp-2 tyrosine phosphatase: signaling one cell or many. *Exp Cell Res* **253**, 47-54.

Feng, G. S., Hui, C. C. and Pawson, T. (1993). SH2-containing phosphotyrosine phosphatase as a target of protein-tyrosine kinases. *Science* **259**, 1607-11.

Flotho, C., Valcamonica, S., Mach-Pascual, S., Schmahl, G., Corral, L., Ritterbach, J., Hasle, H., Arico, M., Biondi, A. and Niemeyer, C. M. (1999). RAS mutations and clonality analysis in children with juvenile myelomonocytic leukemia (JMML). *Leukemia* **13**, 32-7.

Fragale, A., Tartaglia, M., Wu, J. and Gelb, B. D. (2004). Noonan syndrome-associated SHP2/PTPN11 mutants cause EGF-dependent prolonged GAB1 binding and sustained ERK2/MAPK1 activation. *Hum Mutat* **23**, 267-77.

Franza, B. R., Jr., Maruyama, K., Garrels, J. I. and Ruley, H. E. (1986). In vitro establishment is not a sufficient prerequisite for transformation by activated ras oncogenes. *Cell* **44**, 409-18.

Georgescu, M. M., Kirsch, K. H., Kaloudis, P., Yang, H., Pavletich, N. P. and Hanafusa, H. (2000). Stabilization and productive positioning roles of the C2 domain of PTEN tumor suppressor. *Cancer Res* **60**, 7033-8.

Goetz, S. C., Brown, D. D. and Conlon, F. L. (2006). TBX5 is required for embryonic cardiac cell cycle progression. *Development*.

Hanafusa, H., Torii, S., Yasunaga, T., Matsumoto, K. and Nishida, E. (2004). Shp2, an SH2-containing protein-tyrosine phosphatase, positively regulates receptor tyrosine kinase signaling by dephosphorylating and inactivating the inhibitor Sprouty. *J Biol Chem* **279**, 22992-5.

Herbst, R., Zhang, X., Qin, J. and Simon, M. A. (1999). Recruitment of the protein tyrosine phosphatase CSW by DOS is an essential step during signaling by the sevenless receptor tyrosine kinase. *Embo J* **18**, 6950-61.

Hof, P., Pluskey, S., Dhe-Paganon, S., Eck, M. J. and Shoelson, S. E. (1998). Crystal structure of the tyrosine phosphatase SHP-2. *Cell* **92**, 441-50.

Inagaki, K., Noguchi, T., Matozaki, T., Horikawa, T., Fukunaga, K., Tsuda, M., Ichihashi, M. and Kasuga, M. (2000). Roles for the protein tyrosine phosphatase SHP-2 in cytoskeletal organization, cell adhesion and cell migration revealed by overexpression of a dominant negative mutant. *Oncogene* **19**, 75-84.

Jarvis, L. A., Toering, S. J., Simon, M. A., Krasnow, M. A. and Smith-Bolton, R. K. (2006). Sprouty proteins are in vivo targets of Corkscrew/SHP-2 tyrosine phosphatases. *Development* **133**, 1133-42.

Kalra, R., Dale, D., Freedman, M., Bonilla, M. A., Weinblatt, M., Ganser, A., Bowman, P., Abish, S., Priest, J., Oseas, R. S. et al. (1995). Monosomy 7 and activating RAS mutations accompany malignant transformation in patients with congenital neutropenia. *Blood* **86**, 4579-86.

Kerkhoff, E. and Rapp, U. R. (1997). Induction of cell proliferation in quiescent NIH 3T3 cells by oncogenic c-Raf-1. *Mol Cell Biol* **17**, 2576-86.

Kolker, S., Tajchman, U. and Weeks, D. L. (2000). Confocal Imaging of early heat development in Xenopus laevis. *Dev. Biol.* **218**, 64-73.

Kosaki, K., Suzuki, T., Muroya, K., Hasegawa, T., Sato, S., Matsuo, N., Kosaki, R., Nagai, T., Hasegawa, Y. and Ogata, T. (2002). PTPN11 (protein-tyrosine phosphatase, nonreceptor-type 11) mutations in seven Japanese patients with Noonan syndrome. *J Clin Endocrinol Metab* **87**, 3529-33.

Kratz, C. P., Niemeyer, C. M., Castleberry, R. P., Cetin, M., Bergstrasser, E., Emanuel, P. D., Hasle, H., Kardos, G., Klein, C., Kojima, S. et al. (2005). The mutational spectrum of PTPN11 in juvenile myelomonocytic leukemia and Noonan syndrome/myeloproliferative disease. *Blood* **106**, 2183-5.

Krenz, M., Yutzey, K. E. and Robbins, J. (2005). Noonan syndrome mutation Q79R in Shp2 increases proliferation of valve primordia mesenchymal cells via extracellular signal-regulated kinase 1/2 signaling. *Circ Res* **97**, 813-20.

Langdon, Y. G., Goetz, S. C., Berg, A. E., Swanik, J. T. and Conlon, F. L. (2007). SHP-2 is required for the maintenance of cardiac progenitors. *Development* **134**, 4119-30.

Lloyd, A. C., Obermuller, F., Staddon, S., Barth, C. F., McMahon, M. and Land, H. (1997). Cooperating oncogenes converge to regulate cyclin/cdk complexes. *Genes Dev* **11**, 663-77.

Loh, M. L., Reynolds, M. G., Vattikuti, S., Gerbing, R. B., Alonzo, T. A., Carlson, E., Cheng, J. W., Lee, C. M., Lange, B. J. and Meshinchi, S. (2004). PTPN11 mutations in pediatric patients with acute myeloid leukemia: results from the Children's Cancer Group. *Leukemia* **18**, 1831-4.

Maheshwari, M., Belmont, J., Fernbach, S., Ho, T., Molinari, L., Yakub, I., Yu, F., Combes, A., Towbin, J., Craigen, W. J. et al. (2002). PTPN11 mutations in Noonan syndrome type I: detection of recurrent mutations in exons 3 and 13. *Hum Mutat* **20**, 298-304.

Mansour, S. J., Matten, W. T., Hermann, A. S., Candia, J. M., Rong, S., Fukasawa, K., Vande Woude, G. F. and Ahn, N. G. (1994). Transformation of mammalian cells by constitutively active MAP kinase kinase. *Science* **265**, 966-70.

Musante, L., Kehl, H. G., Majewski, F., Meinecke, P., Schweiger, S., Gillessen-Kaesbach, G., Wieczorek, D., Hinkel, G. K., Tinschert, S., Hoeltzenbein, M. et al. (2003). Spectrum of mutations in PTPN11 and genotype-phenotype correlation in 96 patients with Noonan syndrome and five patients with cardio-facio-cutaneous syndrome. *Eur J Hum Genet* **11**, 201-6.

Neel, B. G., Gu, H. and Pao, L. (2003). The 'Shp'ing news: SH2 domain-containing tyrosine phosphatases in cell signaling. *Trends Biochem Sci* **28**, 284-93.

Nieuwkoop, P. D. and Faber, J. (1975). Normal Table of *Xenopus laevis* (Daudin). Amsterdam: North Holland.

Noonan, J. A. (1968). Hypertelorism with Turner phenotype. A new syndrome with associated congenital heart disease. *Am J Dis Child* **116**, 373-80.

Noonan, J. A. (1994). Noonan syndrome. An update and review for the primary pediatrician. *Clin Pediatr (Phila)* **33**, 548-55.

O'Reilly, A. M., Pluskey, S., Shoelson, S. E. and Neel, B. G. (2000). Activated mutants of SHP-2 preferentially induce elongation of Xenopus animal caps. *Mol Cell Biol* **20**, 299-311.

Oishi, K., Gaengel, K., Krishnamoorthy, S., Kamiya, K., Kim, I. K., Ying, H., Weber, U., Perkins, L. A., Tartaglia, M., Mlodzik, M. et al. (2006). Transgenic Drosophila models of Noonan syndrome causing PTPN11 gain-of-function mutations. *Hum Mol Genet* **15**, 543-53.

Pluskota, E., Chen, Y. and D'Souza, S. E. (2000). Src homology domain 2-containing tyrosine phosphatase 2 associates with intercellular adhesion molecule 1 to regulate cell survival. *J Biol Chem* **275**, 30029-36.

Poole, A. W. and Jones, M. L. (2005). A SHPing tale: perspectives on the regulation of SHP-1 and SHP-2 tyrosine phosphatases by the C-terminal tail. *Cell Signal* **17**, 1323-32.

Qu, C. K. (2000). The SHP-2 tyrosine phosphatase: signaling mechanisms and biological functions. *Cell Res* **10**, 279-88.

Saxton, T. M., Henkemeyer, M., Gasca, S., Shen, R., Rossi, D. J., Shalaby, F., Feng, G. S. and Pawson, T. (1997). Abnormal mesoderm patterning in mouse embryos mutant for the SH2 tyrosine phosphatase Shp-2. *Embo J* **16**, 2352-64.

Saxton, T. M. and Pawson, T. (1999). Morphogenetic movements at gastrulation require the SH2 tyrosine phosphatase Shp2. *Proc Natl Acad Sci U S A* **96**, 3790-5.

Schoenwaelder, S. M., Petch, L. A., Williamson, D., Shen, R., Feng, G. S. and Burridge, K. (2000). The protein tyrosine phosphatase Shp-2 regulates RhoA activity. *Curr Biol* **10**, 1523-6.

Schubbert, S., Lieuw, K., Rowe, S. L., Lee, C. M., Li, X., Loh, M. L., Clapp, D. W. and Shannon, K. M. (2005). Functional analysis of leukemia-associated PTPN11 mutations in primary hematopoietic cells. *Blood* **106**, 311-7.

Smith, J. C. and Slack, J. M. W. (1983). Dorsalization and neural induction: properties of the organizer in *Xenopus laevis*. *J. Embryol. Exp. Morph.* **78**, 299-317.

Sweeney, M. C., Wavreille, A. S., Park, J., Butchar, J. P., Tridandapani, S. and Pei, D. (2005). Decoding protein-protein interactions through combinatorial chemistry: sequence specificity of SHP-1, SHP-2, and SHIP SH2 domains. *Biochemistry* **44**, 14932-47.

Tang, T. L., Freeman, R. M., Jr., O'Reilly, A. M., Neel, B. G. and Sokol, S. Y. (1995). The SH2-containing protein-tyrosine phosphatase SH-PTP2 is required upstream of MAP kinase for early Xenopus development. *Cell* **80**, 473-83.

Tartaglia, M., Kalidas, K., Shaw, A., Song, X., Musat, D. L., van der Burgt, I., Brunner, H. G., Bertola, D. R., Crosby, A., Ion, A. et al. (2002). PTPN11 mutations in Noonan syndrome: molecular spectrum, genotype-phenotype correlation, and phenotypic heterogeneity. *Am J Hum Genet* **70**, 1555-63.

Tartaglia, M., Mehler, E. L., Goldberg, R., Zampino, G., Brunner, H. G., Kremer, H., van der Burgt, I., Crosby, A. H., Ion, A., Jeffery, S. et al. (2001). Mutations in PTPN11, encoding the protein tyrosine phosphatase SHP-2, cause Noonan syndrome. *Nat Genet* **29**, 465-8.

Tartaglia, M., Niemeyer, C. M., Fragale, A., Song, X., Buechner, J., Jung, A., Hahlen, K., Hasle, H., Licht, J. D. and Gelb, B. D. (2003). Somatic mutations in PTPN11 in juvenile myelomonocytic leukemia, myelodysplastic syndromes and acute myeloid leukemia. *Nat Genet* **34**, 148-50.

Ussar, S. and Voss, T. (2004). MEK1 and MEK2, different regulators of the G1/S transition. *J Biol Chem* **279**, 43861-9.

Van Vactor, D., O'Reilly, A. M. and Neel, B. G. (1998). Genetic analysis of protein tyrosine phosphatases. *Curr Opin Genet Dev* **8**, 112-26.

Vogel, W., Lammers, R., Huang, J. and Ullrich, A. (1993). Activation of a phosphotyrosine phosphatase by tyrosine phosphorylation. *Science* **259**, 1611-4.

Wang, Z. F., Ingledue, T. C., Dominski, Z., Sanchez, R. and Marzluff, W. F. (1999). Two Xenopus proteins that bind the 3' end of histone mRNA: implications for translational control of histone synthesis during oogenesis. *Mol Cell Biol* **19**, 835-45.

Wilson, P. A. and Hemmati-Brivanlou, A. (1995). Induction of epidermis and inhibition of neural fate by Bmp-4. *Nature* **376**, 331-3.

Xu, F., Zhao, R., Peng, Y., Guerrah, A. and Zhao, Z. J. (2001). Association of tyrosine phosphatase SHP-2 with F-actin at low cell densities. *J Biol Chem* **276**, 29479-84.

Yang, W., Klaman, L. D., Chen, B., Araki, T., Harada, H., Thomas, S. M., George, E. L. and Neel, B. G. (2006). An Shp2/SFK/Ras/Erk signaling pathway controls trophoblast stem cell survival. *Dev Cell* **10**, 317-27.

Yu, D. H., Qu, C. K., Henegariu, O., Lu, X. and Feng, G. S. (1998). Protein-tyrosine phosphatase Shp-2 regulates cell spreading, migration, and focal adhesion. *J Biol Chem* **273**, 21125-31.

Zenker, M., Buheitel, G., Rauch, R., Koenig, R., Bosse, K., Kress, W., Tietze, H. U., Doerr, H. G., Hofbeck, M., Singer, H. et al. (2004). Genotype-phenotype correlations in Noonan syndrome. *J Pediatr* **144**, 368-74.

CHAPTER 4

A **3D Modeling Program to Rapidly Assess Cardiac Morphological Abnormalities: 3D Analysis of TBX5 Depleted Heart Tissue**

PREFACE TO CHAPTER 4

Chapter 4 describes a 3D molecular modeling program designed to rapidly reconstruct serial sectioned vertebrate hearts. The 3D models allow for analysis of the overall morphology of the heart, thus allowing visual access to surfaces and regions of the heart previously unseen by techniques such as whole mount tissue analysis. Here we reconstruct hearts from embryos depleted of TBX5, a T-box protein know to regulate the cardiac cell cycle (Goetz et al., 2006).

This work was done in collaboration with two students in the lab of Dr. Stephen Aylward, Remi Charrier and Cedric Caron, who designed the modeling program. Additional collaborators on the project include Dr. Sarah C. Goetz, Tamaryn Kelley, Ashley Hayes, and Jennifer Duddy. I initiated this project in our lab and I was intimately involved in the testing and optimization of the modeling program for *Xenopus* hearts. In addition, I performed the majority of the modeling and reconstruction of TBX5 depleted and control hearts.

Summary

Characterizing the cellular and molecular basis of heart development largely depends on the ability to describe normal heart development, as well as cardiac phenotypes arising from the disruption of specific molecular pathways. To build upon existing techniques for the examination of cardiac morphology during development, we have devised a 3-D modeling program known as HistologicalImageReconstruction. This program provides an inexpensive and rapid method for characterizing the morphology of the heart or other tissue of interest at a high level of detail. As a test of the 3D modeling system, we have developed 3D images of *Xenopus* hearts using 2 different antibodies at 3 different developmental stages. This analysis shows both the utility of the program and also demonstrates a detailed temporal and spatial comparison of the cardiac cells expressing cardiac myosin heavy chain and tropomyosin. As a further test of the utility of the program we have conducted a detailed 3D analysis of *Xenopus* embryos depleted of TBX5, the gene mutated in the human congenital heart disease Holt Oram syndrome. We show that the HistologicalImageReconstruction is able to detect morphological and cellular abnormalities not previously described from 2D analysis which collectively suggest a role for TBX5 in dorsal tube closure and cardiac looping.

Introduction

Congenital heart defects are among the most common forms of birth defects in humans, comprising approximately 1% of all live births (Hoffman, 1995a; Hoffman, 1995b). In recent years, numerous studies have elucidated many of the basic processes of heart

development, employing both embryological and molecular approaches (Bruneau, 2002; Kolker et al., 2000; Mohun, 2000; Olson and Srivastava, 1996) . However, in spite of this, our understanding of the molecular mechanisms underlying normal heart development, as well as the mechanisms of human disease states remains incomplete.

Understanding the molecular mechanisms of heart development relies upon the ability to accurately describe both normal heart development and abnormalities resulting from the disruption of certain gene products or molecular pathways. Existing tools for visualizing cardiac phenotypes consist primarily of whole-mount immunostaining, and immunostaining of histological sections. Whole-mount immunostaining allows for the visualization of overall cardiac morphology, but is somewhat limited in ability to detect more subtle defects. In contrast, histological sections provide a greater degree of detail and more easily allow for quantitative analysis of a cardiac phenotype, such as determination of cell number. However, visualization of the overall morphology of the heart is often not possible using this technique. To address the limitations of these methods, we have devised an inexpensive, high-throughput 3-dimensional (3D) modeling program, known as HistologicalImageReconstruction, that combines the detail of histological sections with the ability to easily observe the overall morphology of the heart. Using this system we have conducted a detailed analysis of heart developmental in *Xenopus* during the early stages of heart tube formation.

As further demonstration of this technique, we generated 3D images of heart tissue depleted of *Tbx5*, the gene mutated in the human congenital disease Holt Oram syndrome. *Tbx5*, like *Tbx1*, *Tbx2* and *Tbx3*, was first reported from studies of a mouse library screened with the PCR primers derived from Brachyury and *omb* (Bollag et al., 1994), and

homologues were identified in a wide variety of vertebrate species including chicken

(Gibson-Brown et al., 1998a; Ohuchi et al., 1998), zebrafish (Begemann et al., 2002;

Ruvinsky et al., 2000), *Xenopus* (Horb and Thomsen, 1999; Showell et al., 2006), and human

(Basson et al., 1997; Li et al., 1997). Sequence comparison of the vertebrate homologues

show that TBX5 has an extremely high degree of conservation through evolution: 99% in the

T-box domain, and 57% overall between *Xenopus* and human (Horb and Thomsen, 1999).

Similar to other individual T-box containing genes, *Tbx5* homologues share not

only sequence similarity but also a high degree of conservation in their temporal and

spatial pattern of expression. Initial studies in the mouse showed *Tbx5* expression is

restricted to a subset of cells in the developing heart, eye, and limb; it persists throughout

all later stages of development except in the dorsal eye (Chapman et al., 1996). *Tbx5*

homologues display a very similar pattern of expression (Begemann et al., 2002; Gibson-

Brown et al., 1998b; Horb and Thomsen, 1999; Li et al., 1997). In the developing heart

Tbx5 initially appears to be expressed throughout the heart field with relatively high levels

in the inflow tract and atrium, and low to undetectable levels observed in the ventricle. No

staining is ever observed in the outflow tract or major arteries but in some species *Tbx5*

has been reported to be expressed at relatively high levels in the veins including the

common cardinal vein and the anterior aspects of the hepatic vein (Brown et al., 2005). In

the atrium *Tbx5* is expressed both in the endocardial and myocardial layers. Thus, *Tbx5* is

expressed in a posterior to anterior gradient and along with *Nkx2.5* and *Tbx20*, *Tbx5* is

among the first genes expressed in cardiogenic precursor cells (Begemann and Ingham,

2000; Bimber et al., 2007; Brown et al., 2005; Bruneau et al., 1999; Chapman et al., 1996;

Gibson-Brown et al., 1998a; Griffin et al., 2000; Horb and Thomsen, 1999; Showell et al.,

2006; Tonissen et al., 1994).

The first indication of a function for TBX5 in heart development came from studies of the human congenital heart disease Holt-Oram Syndrome (HOS), a relatively rare highly penetrant autosomal dominant condition that is associated with skeletal and cardiac malformations. The cardiac developmental abnormalities include atrial and ventricular defects, aberrant chamber formation, and conductivity abnormalities (Newbury-Ecob et al., 1996). Patients with HOS often carry mutations within the coding region of TBX5 (Basson et al., 1997; Basson et al., 1999; Basson et al., 1995; Benson et al., 1996; Li et al., 1997). The role of TBX5 in heart development, and in the HOS disease state, are supported by gene targeting experiments in mouse, that demonstrate mice heterozygous for mutations in *Tbx5* display many of the phenotypic abnormalities of HOS patients (Bruneau et al., 2001; Hiroi et al., 2001) specifically, mice lacking a copy of *Tbx5* display atrial septal defects (ASDs), including secundum and primum ASDs. In line with these cardiac abnormalities, the *Tbx5* heterozygous mutant mice show a dramatic reduction in the expression of ventricle contractile specific genes *MLC2v*, *Irx4* and *Hey2* as well as two markers associated with early cardiac commitment *Nkx2*.5 and *Gata4*. (Moskowitz et al., 2004).

Distinct from its role in chamber specification and differentiation, TBX5 is also required for correct development of the cardiac conduction system. In newborn mice, *Tbx5* is expressed in the atrioventricular bundle and in the left and right bundle branch where it continues to be expressed to adulthood. In *Tbx5* heterozygous mutant newborn mice *Tbx5* expression is initiated in the proper time within the tissue of the conductivition system, but the mutant mice display conductivity patterning defects in the bundle branches

and the atrioventricular bundle and fail to under go the morphological changes in the conduction system observed in wildtype mice. These defects in conductivity maturation are manifested in altered ECGs; *Tbx5* mutant heterozygous and wildtype mice have an indistinguishable ECG at birth but as the mice mature, the *Tbx5* heterozygous mutant mice fail to undergo a shortening of the time required for electrical propagation from the sinoatrial node to the ventricular myocardium, leading to a prolonged PQ interval. Thus, it appears that *Tbx5* loss results in maturation failure in the atrioventricular node or the atrioventricular bundle and further implies that *Tbx5* is required for the normal function of the ventricular conduction system, the atrioventricular bundle and the left and right bundle branches (Moskowitz et al., 2004).

Analysis in *Xenopus* and zebrafish where *Tbx5* is the gene mutated in the *heartstrings* mutation, has suggested an additional role for TBX5 in heart development prior to chamber formation or development of the conduction system. Loss of TBX5 leads to morphological defects in the heart including pericardial edema and loss of circulation. In *Xenopus* these defects are concomitant with a decrease in cardiac cell number, which results from a G1/S phase delay or arrest (see below) (Brown et al., 2005; Goetz et al., 2006). Although these studies provide insight into the precise role for TBX5 in heart development, the studies fail to demonstrate the overall morphological consequences of depleting TBX5 on the early steps of heart development. To address this issue we have used HistologicalImageReconstruction to generate 3D models of TBX5 depleted heart tissue at distinct stages of cardiac development. Results from these studies confirm previous studies on the size of TBX5 depleted hearts but also reveal new phenotypic abnormalities and critically, show defects in dorsal tube closure and cardiac looping.

Materials and Methods

Cryosectioning and Immunostaining of Heart Tissue

For immunostaining of histological sections, embryos were collected at the indicated stages, fixed for 2 hours in 4% paraformaldehyde, and embedded in OCT cryosectioning medium (Tissue Tek). Serial cryostat sections (14μm) corresponding to the entire heart region were collected and rinsed with wash buffer (PBS with 1% Triton and 1% heat inactivated calf serum), and incubated at 4 ºC overnight as indicated with mouse anti-tropomyosin 1:50 or (Developmental Studies Hybridoma Bank); mouse anti-myosin heavy chain (Zymed). The sections were rinsed with wash buffer and the fluorescent conjugated secondary antibody, anti-mouse-Cy3 (Sigma), was applied to the samples, diluted in wash buffer at 1:100. The slides were incubated with secondary antibody for 30 minutes at room temperature and rinsed with wash buffer. Samples were then incubated 30 minutes at room temperature with DAPI (Sigma) to stain nuclei. The samples were imaged on a Nikon E800 epiflourescent microscope. Images were captured using the Metamorph software package.

3D Molecular Modeling

The 3D reconstruction software HistologyImageReconstruction was designed to reconstruct Mouse and *Xenopus* hearts. The program consists of four steps: segmentation, stitching, stacking, and reconstruction. For the current 3D reconstructions only 3 steps of the program are used segmentation, stacking, and reconstruction. Briefly, the program utilizes tiff files of fluorescent heart histological sections which must be copied and placed in individual folders under a main folder i.e. 3D Model *Xenopus*. Copies of the original tiff files are necessary as

the program overwrites the tiff data in the files. Load the folder containing the 2D

representations of the histological images into the histology program and begin the

segmentation step. Segmentation involves selecting the area of the heart to be reconstructed

as marked by tropomyosin and excludes other areas of the sectioned embryo. When a point

on the heart is clicked the program selects all pixels of the same intensity and highlights the

selected pixels in red. To remove or add additional areas to the highlighted tissue the hand

tracer tool can be used to erase tissue or add to the highlighted area. Following segmentation

of each image is the stacking step. Stacking allows the user to pick corresponding points on

consecutive sections and align the points together. Initially the user is prompted to choose

the best section of all of the sections as this is the section on which the stacking will be

based. For the current 3D models the section chosen contained the fewest tears and is the

most morphologically distinct section. The stacking step involves choosing a landmark on

the starter section and then choosing the corresponding landmark on the subsequent section.

A minimum of four landmarks must be selected for each section, but it is best to select as

many landmarks as possible. In addition to, landmark selection the transformation method

should be selected. For the current 3D models Rigid+Warp was selected. It allows rotation,

shifting, and deformation based on the images. Once landmarks have been selected the

transformed image can be calculated and a new window opens with the option to compare

consecutive V sections. This button shows the two sections overlaid on each other with the

left image in green and the right image in red allowing for visualization of the combined

sections. If the sections are properly aligned then the transformation is accepted by pushing

the rescale button, otherwise new landmarks can be selected by hitting the redo button.

Following stacking all of the sections in the heart is the final reconstruction step. The final

reconstruction step consists of the computer generating the 3D model of the stacked images into one final model which can be resized and displayed as a 3D image. The program asks for several parameters gap size, height, multiplier, and spacing. For the current models the gap size, height, and multiplier are 10, 25 and 1 respectively and the spacing is 1 for x and y and 25 for z. The sections must then be transformed. Following transformation the sections are then stacked. The program will ask if folder size should be respected and no should be selected. Subsequently the program will ask if the final image should be smaller; click yes and set a ratio of 0.5. The program then writes a mhd file that can be visualized using VisualizeHistologyImage program.

Results

Xenopus is an especially valuable tool for the study of cardiovascular development because, unlike mammalian embryos, amphibian embryos can survive to late developmental stages without functional circulation. *Xenopus* embryos are highly amenable to embryological manipulations and, with the advent of antisense morpholino technology, it has been possible to generate highly specific loss-of-function phenotypes for many genes of interest. Amphibian embryos also possess pulmonary circulation, making the physiology of their circulatory system more closely related to that of the mammals than is that of the zebrafish.

Briefly, the modeling program consists of four steps: segmentation, stitching, stacking and the three dimensional reconstruction. Utilizing sections through the *Xenopus* heart that have been stained with a cardiac muscle-specific antibody such as myosin heavy chain, a 3-dimensional model of the heart can be rendered. The heart in each serial section is selected during segmentation and the images are stacked together based on reference points

124

provided by the previous image. The stacked images are then converted to a 3D model that can be visualized using the VisualizeHistologyImage program, which is a companion program to HistologicalImageReconstruction.

3D imaging of MHC expression during early Xenopus heart development

To demonstrate the utility of the modeling program as a tool for analyzing normal heart development, we initially reconstructed 3D models of *Xenopus* hearts at three developmental stages, determined according to Nieuwkoop and Faber (Nieuwkoop and Faber, 1975); stage 29, which corresponds to the folding of the cardiac field into the bilaminar heart tube; stage 33, which corresponds to the onset of cardiac looping; and stage 37, corresponding to early cardiac remodeling and chamber formation. At each of these stages hearts were serial section and immunostained with an antibody against cardiac myosin heavy chain (MHC) or tropomyosin. Representative sections from the anterior, middle, and posterior regions of the heart for each stage are shown in Fig. 4.1. The series of sections were then used to reconstruct a 3D model of the heart for each stage and visualized by VisualizeHistologyImage (Fig. 4.2). These models reveal the overall morphology as detected by staining with cardiac specific antibodies of the heart at each stage as well as cataloging the expression of genes/ proteins at each of these developmental stages. Through the visualization program, the rendered surface of the heart can be made transparent and each individual section of the heart viewed providing internal details of the heart relative to overall heart morphology.

The model based on MHC expression of un-manipulated embryos at stage 29 shows that the bilateral *Xenopus* heart primordia have joined across the ventral midline to form a

single heart field. The heart field has begun to round up to form a trough that is open at the dorsal-most aspect (Fig. 4.2A-C). At this stage the heart and MHC expression are in a linear configuration, with the presumptive inflow and outflow of the heart aligned along the anterior-posterior axis (Fig. 4.2B-arrows).

By stage 33, the heart tube is fully closed for much of its length (Fig. 4.2D-F), with the exception of the anterior-most portion of the heart, near the future outflow tract, where it remains open at the dorsal aspect (Fig. 4.2E-arrowhead). By this stage, the heart has begun the morphogenetic process of rightward looping, as seen by the visible offsetting of the inflow to the right of the outflow (Fig. 4.2E-arrows). At this stage the MHC expression domain has also increased in size due to high levels of cell proliferation within the *Xenopus* heart (Goetz et al., 2006), and has increased in length along the anterior-posterior axis (Fig. 4.2- compare F with C).

Finally, at stage 37, a greater degree of morphological complexity is evident as the heart continues to undergo cardiac looping and begins cardiac remodeling (Fig. 4.2G-I). At this stage, the heart elongates along the left-right axis (Fig. 4.2H), and the chamber primordia become more distinct (Fig. 4.2G, I-arrow heads). As was the case at stage 33, the hearts of the stage 37 embryos have fully closed with the exception of the anterior-most sections, although the dorsal opening in these anterior sections is more narrow than that of the stage 33 embryos (Fig. 4.2-compare D with G), suggesting that the anterior portion of the heart at stage 37 is continuing to complete dorsal closure to form a fully enclosed tube. By this point in development, our HistologicalImageReconstruction-generated model reveals that the outflow tract of the heart is still shifted to the right with respect to the inflow (Fig. 4.2H-arrows).

126

3D imaging of TBX5 depleted heart tissue

To show the utility of the HistologicalImageReconstruction modeling program in characterizing morphological abnormalities arising from loss or mis-expression of a particular gene product, we conducted further 3D modeling of Xenopus hearts with a second cardiac marker tropomyosin and compared these models to those of TBX5 depleted heart tissue(Brown et al., 2005; Goetz et al., 2006). In control hearts at stage 29, similar to MHC tropomyosin positive cells ventrally-fuse across the midline and round up dorsally to form the linear heart tube by stage 33 (Fig. 4.3A, C). In TBX5-depleted hearts, tropomyosin positive cells fuse at the ventral midline, in stark contrast to controls the cell fail or are delayed in migration towards the dorsal side of the embryo to initiate heart tube formation (Fig. 4.3B, D). In addition, the number of cells expressing tropomyosin is reduced compared to controls.

At stage 33, control and TBX5-depleted embryos contain approximately equal numbers of tropomyosin positive cells; however, several morphological abnormalities become apparent in the expression of tropomyosin in TBX5-depleted embryos (Fig. 4.3G-L). In control embryos, consistent with what we observed for the models based on MHC staining, we observe in tropomyosin 3D models that the heart tube is fully closed for much of its length with the exception of the most anterior portions of the heart (Fig. 4.3G,I) and cardiac tissue has begun the process of cardiac looping (note: the inflow tract is noticeably offset to the right from the outflow tract; Fig. 4.3I- arrows). In comparison, hearts of the TBX5-depleted embryos at stage 33 still form a trough opening dorsally for all but a small, central portion of the heart tube (Fig. 4.3H-blue arrow) giving the appearance in Fig. 4.3H of a hole through the center of the heart. The hearts derived from TBX5-depleted embryos have

also failed to initiated cardiac looping as the inflow tract is aligned with the outflow along the anterior-posterior axis, rather than offset to the right (Fig. 4.3J-arrows).

By stage 37, control embryo tropomyosin staining marks the chamber primordia (Fig. 4.3M, O-arrowheads). In contrast, the hearts of TBX5- depleted embryos show fewer tropomyosin-positive cells (Fig. 4.3N, P, R). In addition, the inflow and outflow tracts are aligned along the anterior-posterior axis, indicating that the heart has failed to undergo cardiac looping (Fig. 4.3P-arrows) (Goetz et al., 2006). We also observe that the central portion of the dorsal aspect of the heart tube remains as an open trough (denoted by the blue arrow; Fig. 4.3P). Interestingly, it appears that blood flow into the heart tube of the TBX5-depleted embryos may be offset dorsally, as the anterior most portions of the heart tube are occluded (Fig. 4.3N-blue arrow). This observation indicates that the defects seen in the TBX5-depleted embryos are not simply due to a delay in heart development, as the morphological abnormalities are more severe than those seen in earlier stage control hearts.

Discussion

While other modeling programs to examine heart development in *Xenopus* have been described (Mohun, 2000), the program we have developed offers several advantages and thus complements existing modeling programs. First, in HistologicalImageReconstruction, the 3D model can be reconstructed solely from corresponding points on adjacent sections through the heart without requiring the use of reference points outside the heart upon which to align the 3D model. As a result, HistologicalImageReconstruction requires the use of less tissue and allows for a rapid reconstruction of 3D images. In addition, HistologicalImageReconstruction utilizes the expression of cardiac muscle proteins to define

the cardiac tissue to be imaged. In this way, we are able to distinguish cardiac tissue from surrounding mesoderm more easily at earlier developmental stages or in regions of the heart that are not morphologically well defined. Thirdly, this program can reconstruct hearts from fluorescent immunostaining or from *in situ* hybridization without necessitating expensive software. Thus, this method also allows us to catalog and compare the expression patterns of various heart proteins throughout development.
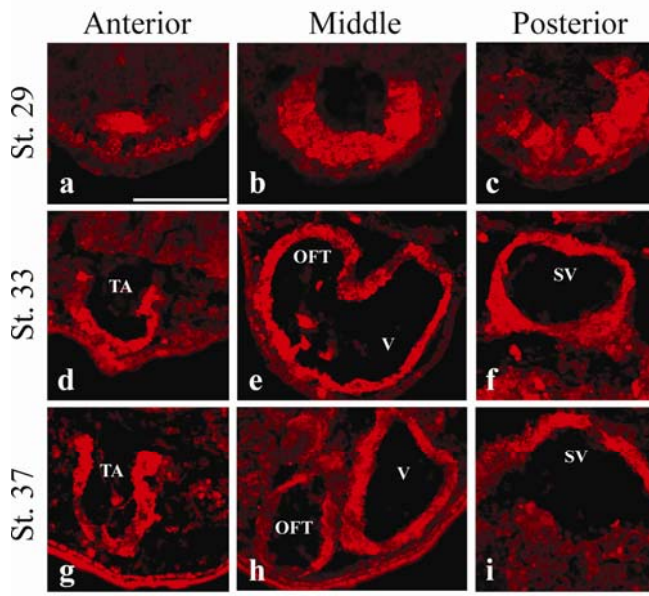
3D Imaging of TBX5 depleted heart tissue

Our HistologicalImageReconstruction- generated 3D models of hearts from embryos lacking TBX5, shown in Fig. 4.3, are consistent with previous analysis, while also revealing differences in morphology between control and TBX5-depleted embryos that were not previously described (Brown et al., 2005; Goetz et al., 2006).   Specifically, the HistologicalImageReconstruction-generated 3D models accurately recapitulate both antibody expression patterns and morphological defects in TBX5-depleted cardiac tissue. These include the failure of the heart to properly form a linear heart tube, defects in the relative positioning of the heart, and a general decrease in cardiac mass. In addition to these defects the 3D images reveal additional morphological abnormalities not previously reported. Critically, we observe a misalignment of the inflow tract relative to the outflow tract even before the onset of cardiac looping. Collectively, suggesting a role for TBX5 in dorsal tube closure and cardiac looping.

Although the software has allowed a rapid evaluation of molecular expression patterns and cardiac defects in *Xenopus*, the program can be easily adapted or other tissues, organs, or model organisms. A considerable advantage offered by our 3D modeling is its use of immunostaining to label the tissue of interest to be modeled. Thus, this program offers

129

inexpensive, high-throughput 3D imaging to investigators wishing to study alterations in tissues that may not be morphologically distinct from the surrounding tissue during the developmental window of interest.

Figure 4.1. Histological sections of *Xenopus* hearts showing expression of myosin heavy chain.

Wild-type embryos were transversely serial sectioned at stages 29 (a-c), 33 (d-f), or 37 (g-i). Shown are representative sections from the anterior-most, middle, and posterior regions of the heart tube, as indicated, at each stage. Cardiac myosin heavy chain expression is shown in red. Scale= 100μM. TA= truncus arteriosis, OFT= outflow tract, V= Ventricle, SV= sinus venosus.
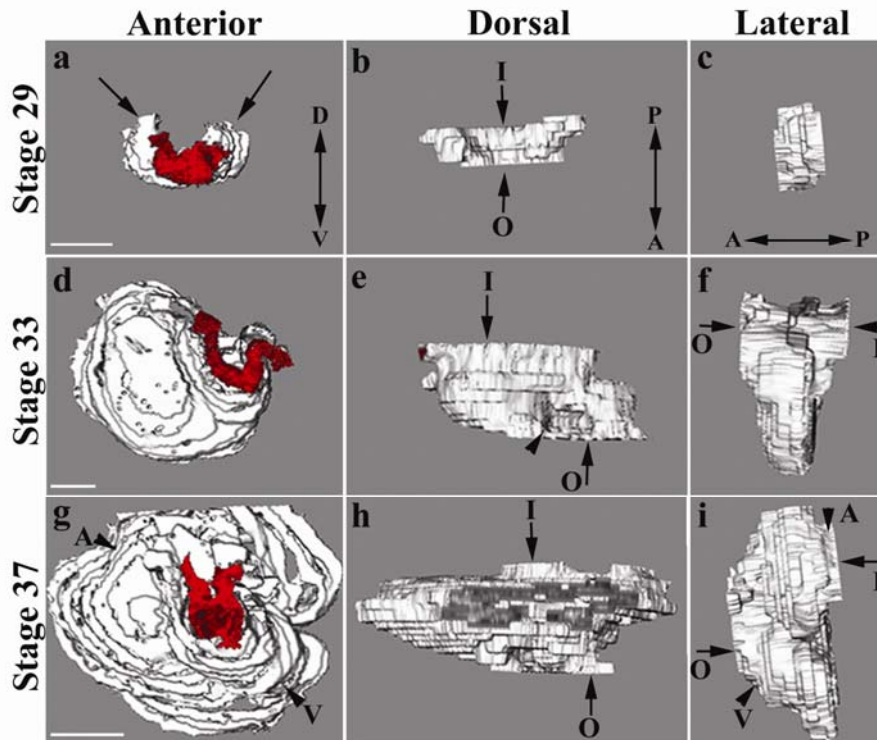
Figure 4.2. 3D models of *Xenopus* hearts based on myosin heavy chain expression reveal dynamic MHC expression in the developing heart.

VisualizeHistologyImage program was used to generate 3D models of *Xenopus* hearts at stages 29 (a-c), 33 (d-f) or 37 (g-i) based on sections immunostained with myosin heavy chain. The models are shown in anterior (a,d,g), dorsal (b,e,h), and lateral (c,f,i) views, with orientation of axes is shown for each series at stage 29. A section corresponding to the most anterior region of the heart is shown in red for each stage. Arrowheads mark cardiac chambers. A= atrium, V= ventricle. Arrows in panels b-i mark the outflow (O) and inflow (I) tracts. Orientation axis is shown for each series at stage 29 in the bottom right corner of the panel. A= anterior, P= posterior, D= dorsal, V= ventral. Scale= 50μM.
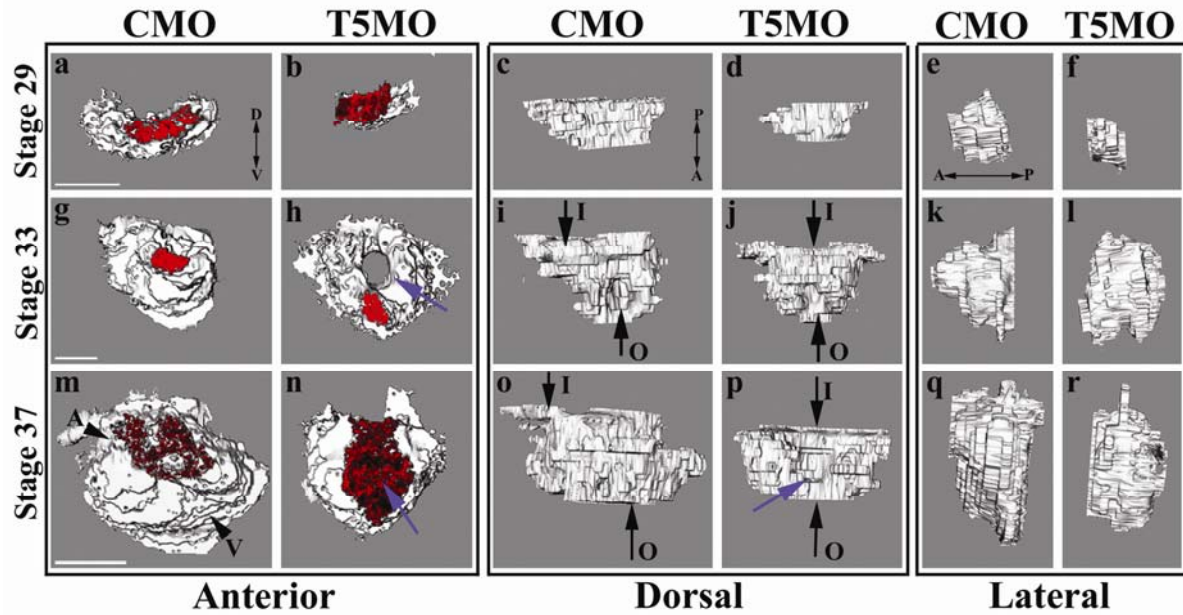
Figure 4.3. 3D modeling of tropomyosin expression in TBX5-depleted hearts reveals dynamic aspects of the cardiac phenotype.

VisualizeHistologyImage program generated 3D models of *Xenopus* hearts from embryos at stages 29 (a-f), 33 (g-l), or 37 (m-r) injected with either control (CMO) or TBX5 morpholinos (T5MO) as indicated. 3D models are shown in anterior (a,b,g,h,m,n), dorsal (c,d,i,j,o,p), or lateral (e,f,k,l,q,r) views, with orientation of axes shown for each series at stage 29. Arrowheads mark cardiac chambers. A= atrium, V= ventricle. Black arrows in panels i-j,o-p mark the outflow (O) and inflow (I) tracts. Blue arrows indicate special features of the T5MO phenotype. Axes are indicated in the top left panel of each grouping. A= anterior, P= posterior, D= dorsal, V= ventral. Scale= 50μM.

References

Basson, C. T., Bachinsky, D. R., Lin, R. C., Levi, T., Elkins, J. A., Soults, J., Grayzel, D., Kroumpouzou, E., Traill, T. A., Leblanc Straceski, J. et al. (1997). Mutations in human cause limb and cardiac malformation in Holt-Oram syndrome. *Nat. Genet.* **15**, 30-35.

Basson, C. T., Huang, T., Lin, R. C., Bachinsky, D. R., Weremowicz, S., Vaglio, A., Bruzzone, R., Quadrelli, R., Lerone, M., Romeo, G. et al. (1999). Different TBX5 interactions in heart and limb defined by Holt-Oram syndrome mutations. *Proc Natl Acad Sci U S A* **96**, 2919-2924.

Basson, C. T., Solomon, S. D., Weissman, B., MacRae, C. A., Poznanski, A. K., Prieto, F., Ruiz de la Fuente, S., Pease, W. E., Levin, S. E. and Holmes, L. B. (1995). Genetic heterogeneity of heart-hand syndrome. *Circulation* **91**, 1326-1329.

Begemann, G., Gibert, Y., Meyer, A. and Ingham, P. W. (2002). Cloning of zebrafish T-box genes tbx15 and tbx18 and their expression during embryonic development. *Mech Dev* **114**, 137-41.

Begemann, G. and Ingham, P. W. (2000). Developmental regulatoin of Tbx5 in zebrafish embryogenesis. *Mech Dev.* **90**, 299-304.

Benson, D. W., Basson, C. T. and MacRae, C. A. (1996). New understandings in the genetics of congenital heart disease. *Curr. Opin. Pediatr.* **8**, 505-511.

Bimber, B., Dettman, R. W. and Simon, H. G. (2007). Differential regulation of Tbx5 protein expression and sub-cellular localization during heart development. *Dev Biol* **302**, 230-42.

Bollag, R. J., Siegfried, Z., Cebra-Thomas, J. A., Garvey, N., Davison, E. M. and Silver, L. M. (1994). An ancient family of embryonically expressed mouse genes sharing a conserved protein motif with the T locus. *Nature Genetics* **7**, 383-389.

Brown, D. D., Martz, S. N., Binder, O., Goetz, S. C., Price, B. M. J., Smith, J. C. and Conlon, F. L. (2005). Tbx5 and Tbx20 act synergistically to control vertebrate heart morphogenesis. *Development* **132**, 553-563.

Bruneau, B. G. (2002). Transcriptional regulation of vertebrate cardiac morphogenesis. *Circ Res* **90**, 509-19.

Bruneau, B. G., Logan, M., Davis, N., Levi, T., Tabin, C. J., Seidman, J. G. and Seidman, C. E. (1999). Chamber-specific cardiac expression of Tbx5 and heart defects in Holt-Oram syndrome. *Dev Biol* **211**, 100-8.

Bruneau, B. G., Nemer, G., Schmitt, J. P., Charron, F., Robitaille, L., Caron, S., Conner, D. A., Gessler, M., Nemer, M., Seidman, C. E. et al. (2001). A Murine Model of Holt-Oram Syndrome Defines Roles of the T-Box Transcription Factor Tbx5 in Cardiogenesis and Disease. *Cell* **106**, 709-721.

Chapman, D. L., Garvey, N., Hancock, S., Alexiou, M., Agulnik, S. I., Gibson-Brown, J., Cebra-Thomas, J., Bollag, R., Silver, L. M. and Papaionnou, V. E. (1996). Expression of the T-box family genes, *Tbx1-Tbx5*, during early mouse development. *Dev. Dynam.* **206**, 379-390.

Gibson-Brown, J. J., Agulnik, S., Silver, L. M. and Papaioannou, V. E. (1998a). Expression of T-box genes Tbx2-Tbx5 during Chick Organogenesis. *Mech Dev.* **74**, 165-169.

Gibson-Brown, J. J., Agulnik, S. I., Silver, L. M., Niswander, L. and Papaioannou, V. E. (1998b). Involvement of T-box genes Tbx2-Tbx5 in vertebrate limb specification and development. *Development* **125**, 2499-509.

Goetz, S. C., Brown, D. D. and Conlon, F. L. (2006). TBX5 is required for embryonic cardiac cell cycle progression. *Development* **133**, 2575-84.

Griffin, K. J., Stoller, J., Gibson, M., Chen, S., Yelon, D., Stainier, D. Y. and Kimelman, D. (2000). A conserved role for H15-related T-box transcription factors in zebrafish and Drosophila heart formation. *Dev Biol* **218**, 235-47.

Hiroi, Y., Kudoh, S., Monzen, K., Ikeda, Y., Yazaki, Y., Nagai, R. and Komuro, I. (2001). Tbx5 associates with Nkx2-5 and synergisticallly promotes cardiomyocyte differentiation. *Nature Genetics* **28**, 276-280.

Hoffman, J. I. (1995a). Incidence of Congenital Heart Disease: I. Postnantal Incidence. **16**, 103-113.

Hoffman, J. I. (1995b). Incidence of Congenital Heart Disease: II Prenatal Incidence. *Pediatr. Cardiol* **16**, 155-165.

Horb, M. E. and Thomsen, G. H. (1999). Tbx5 is essential for heart development. *Development* **126**, 1739-1751.

Kolker, S., Tajchman, U. and Weeks, D. L. (2000). Confocal Imaging of early heat development in Xenopus laevis. *Dev. Biol.* **218**, 64-73.

Li, Q. Y., Newbury Ecob, R. A., Terrett, J. A., Wilson, D. I., Curtis, A. R., Yi, C. H., Gebuhr, T., Bullen, P. J., Robson, S. C., Strachan, T. et al. (1997). Holt-Oram syndrome is caused by mutations in TBX5, a member of the Brachyury (T) gene family. *Nat. Genet.* **15**, 21-29.

Mohun, T. J., Leong, L.M., Weninger, W. J., and Sparrow, D. B. (2000). The Morphology of Heart Development in Xenopus laevis. *Dev Biol* **218**, 74-88.

Moskowitz, I. P., Pizard, A., Patel, V. V., Bruneau, B. G., Kim, J. B., Kupershmidt, S., Roden, D., Berul, C. I., Seidman, C. E. and Seidman, J. G. (2004). The T-Box transcription factor Tbx5 is required for the patterning and maturation of the murine cardiac conduction system. *Development* **131**, 4107-16.

Newbury-Ecob, R., Leanage, R., Raeburn, J. A. and Young, I. D. (1996). The Holt-Oram Syndrome: a clinical genetic study. *J. Med. Genet.* **33**, 300-307.

Nieuwkoop, P. D. and Faber, J. (1975). Normal Table of *Xenopus laevis* (Daudin). Amsterdam: North Holland.

Ohuchi, H., Takeuchi, J., Yoshioka, H., Ishimaru, Y., Ogura, K., Takahashi, N., Ogura, T. and Noji, S. (1998). Correlation of wing-leg identity in ectopic FGF-induced chimeric limbs with the differential expression of chick Tbx5 and Tbx4. *Development* **125**, 51-60.

Olson, E. N. and Srivastava, D. (1996). Molecular pathways controlling heart development. *Science* **272**, 671-676.

Ruvinsky, I., Oates, A. C., Silver, L. M. and Ho, R. K. (2000). The evolution of paired appendages in vertebrates: T-box genes in the zebrafish. *Dev Genes Evol.* **210**, 82-91.

Showell, C., Christine, K. S., Mandel, E. M. and Conlon, F. L. (2006). Developmental expression patterns of Tb x 1, Tb x 2, Tb x 5, and Tb x 20 in Xenopus tropicalis. *Dev Dyn* **235**, 1623-30.

Tonissen, K. F., Drysdale, T. A., Lints, T. J., Harvey, R. P. and Krieg, P. A. (1994). XNkx-2.5, a Xenopus gene related to Nkx-2.5 and tinman: evidence for a conserved role in cardiac development. *Dev. Biol.* **162**, 325-328.

CHAPTER 5

Conclusion and Future Directions

Protein tyrosine phosphates are critical for the regulation of a diverse set of developmental processes and consequently disruption of their activities can result in a number of developmental abnormalities. The work presented in this dissertation begins to address the precise role for the non-receptor protein tyrosine phosphatase SHP-2 in cardiac development. The function of SHP-2 in cardiac development was addressed by 1) characterizing the requirement for SHP-2 in the maintenance of cardiac progenitor cells and 2) determining the effect of the Noonan associated SHP-2 mutation, SHP-2 N308D on cardiac development.

Cardiac cell survival

SHP-2 is a protein tyrosine phosphatase that is be required for the development of terminal structures in *Drosophila*, required for mesoderm patterning, morphogenetic movements at gastrulation and survival of trophoblast stem cells in the mouse, and required for posterior mesoderm patterning in *Xenopus* (Cleghon et al., 1998; Perkins et al., 1992; Saxton et al., 1997; Saxton and Pawson, 1999; Tang et al., 1995; Yang et al., 2006). Due to the early developmental requirement for SHP-2 it has not been possible to ascertain the precise role of SHP-2 in cardiac development. In Chapter 2 we circumvented the early requirements for SHP-2 signaling through elaboration of an explant assay first reported by Tim Mohun and Mark Mercola (Raffin et al., 2000). Prior to excision of the cardiac

explants, *Xenopus* embryos were allowed to develop to neurula stage at which point we isolated cardiac explants and inhibited SHP-2 signaling with a pharmacological inhibitor of SHP-2. From these studies we showed that in the absence of SHP-2 signaling there is a rapid and progressive loss of early cardiac marker expression and inhibition of cardiac differentiation. In addition we determined that in the absence of SHP-2 signaling cardiac cells undergo programmed cell death thus, demonstrating a role for SHP-2 in cardiac cell survival.

SHP-2 has been demonstrated to function downstream of a number of growth factor signaling pathways including FGF, EGF, and PDGF growth factor signaling pathways (Hanafusa et al., 2004; Neel et al., 2003; Schaeper et al., 2007; Wu et al., 2006). Since a number of studies demonstrate a role for FGF signaling in the maintenance of cardiac cells or cardiac cell identity (Abu-Issa et al., 2002; Cohen et al., 2007; Davidson et al., 2006) we hypothesized that the SHP-2 functions downstream of FGF signaling to maintain proliferating cardiac progenitor cells. In Chapter 2, we provide the first evidence that SHP-2 interacts directly *in vivo* with a downstream component of the FGF signaling pathway, FRS and demonstrate that inhibition of FGF signaling has the same effect on cardiac development as the inhibition of SHP-2 signaling. Critically, we found that an activated form of SHP-2 can rescue the cardiac lineage defects resulting from loss of FGF signaling.

Cardiac abnormalities associated with SHP-2 N308D mis-expression

Chapter 3 analyzes the cellular and molecular effects of SHP-2 N308D, the most common Noonan associated mutation, on heart development. Mis-sense mutations in SHP-2 are frequently associated with the human congenital syndrome Noonan syndrome, an autosomal dominant disorder that occurs in 1 to 1000-2500 live births (Tartaglia et al., 2001). Patients

with Noonan syndrome have proportionate short stature, cranial-facial abnormalities, mental retardation, and cardiac disease which is manifested by atrial septal defects, ventricular septal defects, atrial-ventricular septal defects, pulmonary stenosis and hypertrophic cardiomyopathy to name a few (reviewed in Tartaglia and Gelb, 2005). The most common Noonan syndrome associated SHP-2 mutation is a mis-sense mutation occurring at position 308 in which an asparagine is substituted for aspartic acid (N308D). This mutation accounts for one third of all Noonan affected individuals.

In Chapter 3 we show that introduction of human *Shp-2* N308D into *Xenopus* results in cardiac abnormalities. To characterize the cardiac defects in *Shp-2* N308D embryos, we performed 3-dimensional (3D) molecular modeling of control and *Shp-2* N308D hearts. The development and application of the 3D molecular modeling process was used in a pilot study in Chapter 4, to model control and *Tbx5* morphant hearts. When applied to *Shp-2* N308D the 3D models illustrate a delay with respect to morphological movements of the heart and a reduction in the size of the heart. This result is consistent with previously described roles for SHP-2 in cell migration (Manes et al., 1999; O'Reilly et al., 2000; Saxton and Pawson, 1999; Tang et al., 1995) and our microarray experiments which identified changes in expression of a number of genes involved in actin dynamics. Additionally, we performed TEM of control and *Shp-2* N308D hearts and found that while control hearts contained both longitudinal and concentric muscle fibers, *Shp-2* N308D hearts lacked concentric muscle fibers suggesting that *Shp-2* N308D hearts may have a muscle polarity defect or be deficient for a subset of cardiac muscle. By conducting immunoprecipitations of SHP-2 from whole embryos and analyzing the proteins associated with SHP-2 by mass spectroscopy we showed that SHP-2 associates with actin *in vivo*. Collectively these studies suggest that *Shp-2* N308D cardiac

cells may have an impaired ability to migrate and maybe deficient for a subset of cardiac muscle.

Shp-2 N308D and the cardiac cell cycle

In addition, to a potential role for *Shp-2* N308D in the actin cytoskeleton, our studies also reveal a role for SHP-2 in mediating cell cycle progression (Bennett et al., 1996; Guillemot et al., 2000).   Importantly, *Shp-2* N308D hearts were found to have an increase in the expression of S-phase associated proteins suggesting the reduced number of cardiac cells may result from a block or delay (lengthening) in the cardiac cell cycle. At the present time, it remains unclear if this occurs in response to *Shp-2* N308D or if this is a secondary response to alterations in the actin cytoskeleton.

Future Directions

Tyrosine kinase signaling, SHP-2 and cardiac survival

Our current work demonstrates that SHP-2 is required downstream of FGF signaling to maintain cell survival of cardiac progenitor cells in the heart. However, it is well established that SHP-2 functions in additional growth factor signaling pathways (Chen et al., 2000; Van Obberghen et al., 2001; Wu et al., 2006). Therefore an immediate goal of this project is to determine if additional signaling pathways are involved in SHP-2 mediated cardiac cell survival. Cell survival can be mediated through the EGF/PI3K/AKT pathway. However; in this pathway SHP-2 negatively regulates cell survival by dephosphorylating Gab1 thus inhibiting the ability of Gab1 to activate PI3K. In contrast in the MAPK pathway SHP-2 has been found to promote cell survival (D'Alessio et al., 2007; Ren et al., 2007). In particular,

Shp2 E76K, an activated mutant, leads to an increase in pro-survival factors in response to constitutive ERK activation (Ren et al., 2007).

Taken together these studies suggest additional mechanism by which SHP-2 may function to maintain cardiac cell survival. To test the hypothesis that SHP-2 functions downstream of additional growth factors in the heart for the maintenance of cardiac cells we will isolate cardiac explants and treat the explants with specific inhibitors of EGF, PDGF, NGF, or IGF signaling. The tissue will then be analyzed by methods identical to those in Chapter 2. If we identify additional signaling pathways for cardiac cell survival these studies will be further extended to determine whether the additional pathways act in parallel or converge on the FGF signaling pathway.

Downstream Pathways

Ultimately, it is essential is to determine what genes act downstream of SHP-2 to maintain cardiac cell survival. To approach this objective, we will perform subtractive hybridization screens of cardiac explants treated with the SHP-2 inhibitor at specific stages of cardiac development. In Chapter 2, we demonstrate that treatment of our cardiac explants with the SHP-2 specific inhibitor at stage 22 results in the initiation of cardiac cell death at stage 26. Therefore, there is a six hour window between SHP-2 inhibition (stage 22) and cardiac cell death (stage 26). Since we know the window of time in which the cell death phenotype is observed, we can initiate inhibitor treatment at early stages of cardiac development and collect the explants at stages and times prior to when we would expect to observe any cell death. We will then compare the results from each screen. In this manner we will determine a subset of genes which may function to promote cardiac cell survival. Once identified, candidate genes will be assayed for the ability to rescue the loss of

differentiated cardiac tissue in response to SHP-2 inhibition. Thus we will gain a better understanding of the molecular mechanisms used to promote cell survival of cardiac cells *in vivo*.

Shp-2 N308D and actin cytoskeleton

Our work on *Shp-2* N308D has defined several potential cellular pathways by which *Shp-2* N308D may affects cardiac development. Having identified actin dynamics and cell cycle progression as candidate SHP-2 regulated processes, an immediate goal of the project is to precisely define the role of *Shp-2* N308D in these pathways. Since SHP-2 has been shown to function downstream of integrin and Rho signaling for the regulation of actin stress fiber formation (Inagaki et al., 2000; Schoenwaelder et al., 2000) and we show that SHP-2 associates with actin, we anticipate that cardiac cells in *Shp-2* N308D hearts contain fewer actin fibers which in turn leads to alteration in the orientation of the remaining fibers or leads to the loss of a subset of actin fibers. To test this hypothesis we will perform a detailed analysis of actin fiber orientation, distribution, and size by serial section confocal microscopy on *Shp-2* N308D hearts stained for F-actin. To identify whether integrin signaling, Rho signaling, or a combination of the two pathways result in the cardiac phenotypes observed in *Shp-2* N308D embryos, the signaling pathways will be activated via expression of constitutively active molecules in the respective pathways. Hearts of injected embryos will be serial sectioned and stained to mark actin fibers and confocal microscopy used to determine if activation of either pathway phenocopies the effects of *Shp-2* N308D on heart development. Finally, we will determine if inhibition of either pathway can rescue the defects in actin muscle fiber orientation and/or the defects in the numbers of actin muscle fibers. Understanding the molecular pathway by which *Shp-2* N308D alters actin fiber

orientation in the heart can give clues to the range of defects observed in Noonan syndrome patients.

SHP-2 N308D and the cardiac cell cycle

In Chapter 3 we observed that *Shp-2* N308D leads to an alteration in cell cycle progression and hypothesize that this alteration results in lengthening of the cardiac cell cycle. Therefore to further characterize the role of *Shp-2* N308D in cell cycle progression, I will assay *Shp-2* N308D derived hearts by western blot analysis, for expression of a panel of phase specific cell cycle markers that we have previously shown to be expressed in the embryonic heart (Goetz et al., 2006). This data will identify the precise point *Shp-2* N308D alters the cardiac cell cycle. In addition, we propose that lengthening of the cardiac cell cycle occur cell autonomously. To test this proposal we will co-inject *Shp-2* N308D and a lineage tracer into one cell of the two-cell stage embryo allowing us to determine if only the cardiac cells receiving *Shp-2* N308D have an increased rate of proliferation or whether proliferation is also increased in cells not expressing *Shp-2* N308D. If the effect is cell autonomous this would imply that activation of SHP-2 directly leads to modulation of genes required for the regulation of cell cycle progression.

Ultimately a goal of this project is to identify direct endogenous SHP-2 and SHP-2 N308D binding partners in the heart. We hypothesize that the altered conformation of *Shp-2* N308D allows for promiscuous binding and subsequent dephosphorylation of molecules upstream of diverse pathways in the heart (Chen et al., 2006; Fragale et al., 2004; Hof et al., 1998). Initiation or inhibition of these signaling pathways eventually results in mis-regulation of the pathways leading to altered muscle fiber development and cell cycle progression in *Shp-2* N308D hearts. To address this hypothesis, we will inject substrate

trapping mutants of *Shp-2* N308D into the one cell stage *Xenopus* embryo. Similar to wild-type SHP-2 these mutants bind to SHP-2 interacting proteins however, the target proteins are unable to disengage from the substrate trapping mutants. We will then identify the substrate trapped proteins through biochemical and molecular methods including immuno-precipitation, mass spectroscopy, and mapping of binding domains. Identification of endogenous and *Shp-2* N308D binding proteins is critical as the list of known SHP-2 binding partners is relatively short and can not account for all of SHP-2/ *Shp-2* N308D function in the heart.

Finally, we are interested in investigating the precise timing of the effect of *Shp-2* N308D on the cardiac cell cycle and cardiac morphogenesis. We suspect temporal requirements for *Shp-2* N308D as preliminary results in Chapter 3 suggest that *Shp-2* N308D may have more than one function in regards to the cardiac cell cycle. Thus it is necessary to regulate *Shp-2* N308D expression in a temporal fashion through the use of inducible N308D-GR constructs. From these studies we will determine discrete windows of *Shp-2* N308D activity in the heart for cell cycle progression, actin regulation, as well as any of the other pathways found from the studies mentioned above. Once we have identified the independent and overlapping requirement for *Shp-2* N308D we can develop a signaling network of *Shp-2* N308D in the heart and begin to develop the same type of network for endogenous SHP-2.

References

Abu-Issa, R., Smyth, G., Smoak, I., Yamamura, K. and Meyers, E. N. (2002). Fgf8 is required for pharyngeal arch and cardiovascular development in the mouse. *Development* **129**, 4613-25.

Bennett, A. M., Hausdorff, S. F., O'Reilly, A. M., Freeman, R. M. and Neel, B. G. (1996). Multiple requirements for SHPTP2 in epidermal growth factor-mediated cell cycle progression. *Mol Cell Biol* **16**, 1189-202.

Chen, B., Bronson, R. T., Klaman, L. D., Hampton, T. G., Wang, J. F., Green, P. J., Magnuson, T., Douglas, P. S., Morgan, J. P. and Neel, B. G. (2000). Mice mutant for Egfr and Shp2 have defective cardiac semilunar valvulogenesis. *Nat Genet* **24**, 296-9.

Chen, L., Sung, S. S., Yip, M. L., Lawrence, H. R., Ren, Y., Guida, W. C., Sebti, S. M., Lawrence, N. J. and Wu, J. (2006). Discovery of a novel shp2 protein tyrosine phosphatase inhibitor. *Mol Pharmacol* **70**, 562-70.

Cleghon, V., Feldmann, P., Ghiglione, C., Copeland, T. D., Perrimon, N., Hughes, D. A. and Morrison, D. K. (1998). Opposing actions of CSW and RasGAP modulate the strength of Torso RTK signaling in the Drosophila terminal pathway. *Mol Cell* **2**, 719-27.

Cohen, E. D., Wang, Z., Lepore, J. J., Lu, M. M., Taketo, M. M., Epstein, D. J. and Morrisey, E. E. (2007). Wnt/beta-catenin signaling promotes expansion of Isl-1-positive cardiac progenitor cells through regulation of FGF signaling. *J Clin Invest* **117**, 1794-804.

D'Alessio, A., Cerchia, L., Amelio, I., Incoronato, M., Condorelli, G. and de Franciscis, V. (2007). Shp2 in PC12 cells: NGF versus EGF signalling. *Cell Signal* **19**, 1193-200.

Davidson, B., Shi, W., Beh, J., Christiaen, L. and Levine, M. (2006). FGF signaling delineates the cardiac progenitor field in the simple chordate, Ciona intestinalis. *Genes Dev* **20**, 2728-38.

Fragale, A., Tartaglia, M., Wu, J. and Gelb, B. D. (2004). Noonan syndrome-associated SHP2/PTPN11 mutants cause EGF-dependent prolonged GAB1 binding and sustained ERK2/MAPK1 activation. *Hum Mutat* **23**, 267-77.

Goetz, S. C., Brown, D. D. and Conlon, F. L. (2006). TBX5 is required for embryonic cardiac cell cycle progression. *Development* **133**, 2575-84.

Guillemot, L., Levy, A., Zhao, Z. J., Bereziat, G. and Rothhut, B. (2000). The protein-tyrosine phosphatase SHP-2 is required during angiotensin II-mediated activation of cyclin D1 promoter in CHO-AT1A cells. *J Biol Chem* **275**, 26349-58.

Hanafusa, H., Torii, S., Yasunaga, T., Matsumoto, K. and Nishida, E. (2004). Shp2, an SH2-containing protein-tyrosine phosphatase, positively regulates receptor tyrosine kinase signaling by dephosphorylating and inactivating the inhibitor Sprouty. *J Biol Chem* **279**, 22992-5.

Hof, P., Pluskey, S., Dhe-Paganon, S., Eck, M. J. and Shoelson, S. E. (1998). Crystal structure of the tyrosine phosphatase SHP-2. *Cell* **92**, 441-50.

Inagaki, K., Noguchi, T., Matozaki, T., Horikawa, T., Fukunaga, K., Tsuda, M., Ichihashi, M. and Kasuga, M. (2000). Roles for the protein tyrosine phosphatase SHP-2 in cytoskeletal organization, cell adhesion and cell migration revealed by overexpression of a dominant negative mutant. *Oncogene* **19**, 75-84.

Manes, S., Mira, E., Gomez-Mouton, C., Zhao, Z. J., Lacalle, R. A. and Martinez, A. C. (1999). Concerted activity of tyrosine phosphatase SHP-2 and focal adhesion kinase in regulation of cell motility. *Mol Cell Biol* **19**, 3125-35.

Neel, B. G., Gu, H. and Pao, L. (2003). The 'Shp'ing news: SH2 domain-containing tyrosine phosphatases in cell signaling. *Trends Biochem Sci* **28**, 284-93.

O'Reilly, A. M., Pluskey, S., Shoelson, S. E. and Neel, B. G. (2000). Activated mutants of SHP-2 preferentially induce elongation of Xenopus animal caps. *Mol Cell Biol* **20**, 299-311.

Perkins, L. A., Larsen, I. and Perrimon, N. (1992). corkscrew encodes a putative protein tyrosine phosphatase that functions to transduce the terminal signal from the receptor tyrosine kinase torso. *Cell* **70**, 225-36.

Raffin, M., Leong, L. M., Rones, M. S., Sparrow, D., Mohun, T. and Mercola, M. (2000). Subdivision of the cardiac Nkx2.5 expression domain into myogenic and nonmyogenic compartments. *Dev Biol* **218**, 326-40.

Ren, Y., Chen, Z., Chen, L., Woods, N. T., Reuther, G. W., Cheng, J. Q., Wang, H. G. and Wu, J. (2007). Shp2E76K mutant confers cytokine-independent survival of TF-1 myeloid cells by up-regulating Bcl-XL. *J Biol Chem* **282**, 36463-73.

Saxton, T. M., Henkemeyer, M., Gasca, S., Shen, R., Rossi, D. J., Shalaby, F., Feng, G. S. and Pawson, T. (1997). Abnormal mesoderm patterning in mouse embryos mutant for the SH2 tyrosine phosphatase Shp-2. *Embo J* **16**, 2352-64.

Saxton, T. M. and Pawson, T. (1999). Morphogenetic movements at gastrulation require the SH2 tyrosine phosphatase Shp2. *Proc Natl Acad Sci U S A* **96**, 3790-5.

Schaeper, U., Vogel, R., Chmielowiec, J., Huelsken, J., Rosario, M. and Birchmeier, W. (2007). Distinct requirements for Gab1 in Met and EGF receptor signaling in vivo. *Proc Natl Acad Sci U S A* **104**, 15376-81.

Schoenwaelder, S. M., Petch, L. A., Williamson, D., Shen, R., Feng, G. S. and Burridge, K. (2000). The protein tyrosine phosphatase Shp-2 regulates RhoA activity. *Curr Biol* **10**, 1523-6.

Tang, T. L., Freeman, R. M., Jr., O'Reilly, A. M., Neel, B. G. and Sokol, S. Y. (1995). The SH2-containing protein-tyrosine phosphatase SH-PTP2 is required upstream of MAP kinase for early Xenopus development. *Cell* **80**, 473-83.

Tartaglia, M. and Gelb, B. D. (2005). Noonan syndrome and related disorders: genetics and pathogenesis. *Annu Rev Genomics Hum Genet* **6**, 45-68.

Tartaglia, M., Mehler, E. L., Goldberg, R., Zampino, G., Brunner, H. G., Kremer, H., van der Burgt, I., Crosby, A. H., Ion, A., Jeffery, S. et al. (2001). Mutations in PTPN11, encoding the protein tyrosine phosphatase SHP-2, cause Noonan syndrome. *Nat Genet* **29**, 465-8.

Van Obberghen, E., Baron, V., Delahaye, L., Emanuelli, B., Filippa, N., Giorgetti-Peraldi, S., Lebrun, P., Mothe-Satney, I., Peraldi, P., Rocchi, S. et al. (2001). Surfing the insulin signaling web. *Eur J Clin Invest* **31**, 966-77.

Wu, J. H., Goswami, R., Cai, X., Exum, S. T., Huang, X., Zhang, L., Brian, L., Premont, R. T., Peppel, K. and Freedman, N. J. (2006). Regulation of the platelet-derived growth factor receptor-beta by G protein-coupled receptor kinase-5 in vascular smooth muscle cells involves the phosphatase Shp2. *J Biol Chem* **281**, 37758-72.

Yang, W., Klaman, L. D., Chen, B., Araki, T., Harada, H., Thomas, S. M., George, E. L. and Neel, B. G. (2006). An Shp2/SFK/Ras/Erk signaling pathway controls trophoblast stem cell survival. *Dev Cell* **10**, 317-27.